Statistical Evaluation of Particle-Tracking Models Predicting Proportional Entrainment Loss for Adult Delta Smelt in the Sacramento-San Joaquin Delta

Josh Korman, Ecometric Research, 3560 W 22nd Ave., Vancouver, BC, V6S 1J3

Edward S. Gross, Resource Management Associates, 1840 San Miguel Dr., Suite 102, Walnut Creek, CA 94596, and Center for Watershed Sciences, University of California Davis One Shields Avenue, Davis, CA 95616

Peter E. Smith (retired), US Geological Survey, California Water Science Center, California State University, 6000 J Street, Placer Hall, Sacrament, CA 95819

Benjamin Saenz, Resource Management Associates, 1840 San Miguel Dr., Suite 102, Walnut Creek, CA 94596

Lenny F. Grimaldo, ICF, 650 Folsom St., Suite 200, San Francisco, CA. 94107

April-11-2018

Abstract

Entrainment of fish at dam and water intake structures results in directly-observed mortality that can trigger protective management actions. The impact of entrainment on the viability of fish populations has been challenging to determine and has led to considerable debate and litigation about the efficacy of protection actions. There has been particularly intense debate regarding the population-level effects of the entrainment of endangered fish at water export facilities located in the Sacramento-San Joaquin River Delta. Water from the Sacramento and San Joaquin Rivers flows into the Delta and is diverted through large export pumping facilities to supply water to millions of Californians and a very large agricultural industry. These water export facilities can entrain substantial numbers of fish, including Delta Smelt (*Hypomesus transpacificus*), a small pelagic fish endemic to the San Francisco Estuary that is listed as endangered and threatened under California and federal Endangered Species Acts, respectively. In some years, some Delta Smelt disperse into the less saline water in the eastern Delta in winter prior to spawning in spring, and this movement brings a proportion of the adult population in closer proximity to pumping facilities which puts them at greater risk to entrainment. In this paper we use a particle-tracking model (PTM) in conjunction with a population dynamics model to estimate the proportion of the adult population that is lost to entrainment (proportional entrainment loss, PEL). We use a two-stage modelling procedure. In the first stage, a computationally-intensive PTM simulates a variety of potential behaviors of Delta Smelt to predict movement of particles among regions in the Delta as well as the proportion of particles from each region that are entrained. These predictions are based on behavioral rules that represent different hypotheses about how Delta Smelt movement is related to hydrodynamics (depth, velocity, and flow direction), salinity, and turbidity. In the second stage, we use a population dynamics model, driven by unscaled movement and entrainment rates from the PTM, to predict abundance over time in each region as well as the number of fish from each region that are entrained, which are in turn used to compute proportional entrainment loss. Parameters of the population model are estimated by non-linear search by statistically comparing predictions to data from Fall Midwater Trawl and Spring Kodiak Trawl surveys as well as observed daily salvage records. Our objectives are to evaluate the reliability of different movement hypotheses to rank estimates of PEL based on how well each combined PTM and population dynamic model

fits the data, and to sharpen our understanding of the data for making future research and monitoring decisions.

We found that PTMs that simulated more complex fish movement behaviors that included lagged responses to multiple cues fit the data much better than simpler models based solely on behavioural rules like tidal surfing, or movement towards more turbid or saline water. Estimates of proportional entrainment loss varied considerably among PTMs and among water years, but were similar across alternate population model structures. Estimates of PEL of adult Delta Smelt from PTMs that were most consistent with the data were approximately 35% in water year 2002, 50% in 2004, 15% in 2005, and 3% in 2011. The 2002, 2004, and 2005 estimates were more than double those from Kimmerer (2008) which were 15%, 19% and 7%, respectively. Our estimates of PEL were higher because movement predictions from the PTM resulted in greater entrainment.

Fits of our model to data from 2002 and 2004 were greatly improved by allowing salvage efficiency (proportion of entrained fish that are observed as salvage) to vary with turbidity. The improved fit could indicate that peak salvage events during periods of high turbidity are caused by reduced predation loss rather than the prevailing hypothesis that movement towards the pumps increase with turbidity. Alternatively, turbidity-related changes in activity or micro-habitat could affect the vulnerability of Delta Smelt to entrainment. Lack of support for a turbidity-salvage efficiency relationship in 2005, and inconsistencies in the relationship between 2002 and 2004, suggest it may be spurious and is instead compensating for temporal or spatial error in predictions of entrainment from the PTMs. This in turn could lead to overestimates of PEL. Best fits in each water year were often obtained by either different PTMs or different assumptions about population and observation dynamics. This suggests our PEL estimates may be unreliable, and makes it challenging to determine which PTM to apply in more recent and future years where SKT catch and salvage is too low to evaluate model fit. Further refinement and evaluation of the combined PTM and population dynamics models is required before they can be used to guide flow management decisions.

Mark-recapture experiments to estimate salvage expansion directly from field data are critical to resolve uncertainties in predictions of movement towards export facilities and estimates of PEL. Ideally, these experiments would be conducted over a number of years and across varying turbidity levels to provide adequate replication and contrasting conditions which would affect mortality between release and salvage locations. Improved estimates of salvage expansion factors from these experiments could be used to evaluate PTMs in earlier years (e.g., 2002, 2004, 2005) when there was better information on abundance and entrainment. This in turn would identify the PTMs that are most consistent with historical data, and determine the set of PTMs which could be used to guide future decisions on export regimes. It seems likely that many years of field effort would be required to provide sufficient information on expansion factors to better resolve which PTMs are more reliable.

Introduction

Worldwide over 58,000 dams and diversion structures (>15 m height) have been constructed to provide water supply, flood control, and hydroelectric power generation (ICOLD 2015). The presence and operations of these facilities can create a number of challenges for fish populations, including habitat fragmentation, reductions in habitat quantity and quality, promotion of non-native species, and direct mortality resulting from entrainment (Rytwinski et al. 2017). The latter effect is one of the most obvious impacts because it is often easily observed through tagging or collection of dead fish on screens and louvers. Directly-observed mortality can trigger protective managements actions intended to eliminate or minimize destruction of fish or 'take' as specified in the Canadian Fisheries Act and the US Endangered Species Act (ESA), respectively. Significant efforts to quantify and reduce mortality associated with entrainment have been undertaken in a number of large river systems in the US including the Hudson River, Columbia River, and the Sacramento-San Joaquin River Delta. The net effect of entrainment on the viability of fish populations in these systems has been challenging to determine, often because the proportion of the population that is lost to entrainment is not known. Uncertainty in the proportion of the population lost to entrainment hampers affective decision-making about the cost effectiveness of entrainment reduction measures versus other protective actions.

Entrainment of Delta Smelt (*Hypomesus transpacificus*) and other fish at water export facilities located in the Sacramento-San Joaquin River Delta, and associated export constraining regulatory measures have led to intensive study and debate regarding entrainment effects on fish population viability. Delta Smelt is a small pelagic fish endemic to the San Francisco Estuary. Abundance of this species declined in the 1980s, and it was listed as a threatened under both California and federal ESA in 1993 (Feyrer et al. 2007). A rapid and sustained drop in Delta Smelt abundance beginning in ca. 2002, coincident with the decline of other pelagic species (the Pelagic Organism Decline, Sommer et al. 2007, Mac Nally et al. 2010) resulted in a revision of the listing to endangered under the California ESA in 2009. Over their annual life cycle, juvenile Delta Smelt typically spend the summer and fall in brackish (1-6 practical salinity units) regions of Suisun Bay and the western and norther portions of the Sacramento-San Joaquin Delta (hereafter referred to as the "Delta"). In anticipation of spring spawning, there is commonly a landward migration into less saline water (Grimaldo et al. 2009, Sommer et al. 2011, Fig. 1). This spawning migration is believed to be triggered by higher inflows and turbidity caused by the first large precipitation event in winter, which is referred to as the "first flush" (Grimaldo et al. 2009).

The Delta is a key part of the water supply for California. Water from the Sacramento and San Joaquin river drainages flow into the Delta, and approximately 30-60% of this inflow is diverted through massive state (State Water Project; SWP) and federal (Central Valley Project; CVP) export pumping facilities to supply water for about 25 million Californians and a multi-billion dollar agricultural industry (Kimmerer 2004, Thomson et al. 2010). These pumping facilities, located in the south-eastern portion of the Delta (Fig. 1), substantially alter seasonal patterns in flow and can entrain large numbers of Delta Smelt and other fish species under certain hydrodynamic, physical, and biological conditions (Kimmerer 2008, Grimaldo et al. 2009). The landward spawning migration of Delta Smelt results in some of the population moving closer to pumping facilities which makes them more vulnerable to entrainment. Fish screening facilities located upstream of the pumping plants collect some of the fish that would otherwise be entrained into the pumps. These collections, known as "salvage", provide an imperfect index of seasonal and annual variation in entrainment.

Entrainment of Delta Smelt has been suggested as one of the potential causes for its decline (Sommer et al. 2007; Brown et al. 2009). Concern over effects of entrainment losses prompted the USFWS to issue a Biological Opinion on the SWP and CVP with targeted Reasonable and Prudent Alternative (RPA) actions designed to minimize Delta Smelt entrainment (USFWS 2008). These include including prescriptive and conditions-based constraints on the magnitude of reverse flows towards the pumps in Old and Middle rivers (OMR flows). OMR reverse flow restrictions can require reductions in water export rates, which have been the subject of considerable litigation (Wanger 2007 and 2010). A better understanding of the migratory dynamics of Delta Smelt is warranted to evaluate the effectiveness of current and future flow and export management options. Moreover, improved estimates of Delta Smelt entrainment losses are also needed to understand how water exports may impact population viability and recovery (Maunder and Deriso 2011; Rose et al 2013). Kimmerer (2008) provided the first estimates of the proportion of the population lost to entrainment, most commonly referred to as Proportional Entrainment Loss (PEL). His estimates, which were as high as 40%, indicate that entrainment could be having substantive population-level effects in some years. These initial estimates have been the subject of debate (Miller 2011, Kimmerer 2011), and there is continued interest in reducing scientific uncertainty associated with Delta Smelt entrainment dynamics and improving PEL estimates.

Proportional entrainment loss for adult Delta Smelt has been calculated based on the ratio of entrainment to population size (Kimmerer 2008 and 2011, Miller 2011). In these studies, entrainment was calculated by expanding the observed salvage, and population size was calculated by expanding catches from a Delta-wide scientific survey used to index abundance. There are two limitations to this ‘ratio approach’ for estimating PEL. First, it relies very heavily on uncertain expansion assumptions used to calculate entrainment and population size. Second, the method cannot be used to predict how future operations will affect PEL, since historical estimates depend on the magnitude and timing of inflow and export rates in each year. Particle-tracking models (PTMs) provide an alternative way of predicting entrainment losses that can be used to evaluate future operations. These models simulate movement of particles as determined by hydrodynamic predictions and other factors thought to control the distribution of fish such as salinity, water temperature, and turbidity. PTMs have been used to predict entrainment in the Delta, especially for zooplankton and eggs and larval stages of Delta Smelt and other fishes that are assumed to behave as passively drifting particles (Culberson et al. 2004, RMA 2014). The advantage of using PTMs to predict proportional entrainment loss is that they can be used to evaluate population-level effects of different operating strategies. However, it is uncertain whether this approach can be used to model movement and entrainment vulnerability for older life stages of fish which exhibit a variety of complex behaviors in response to changes in abiotic and biotic conditions.

The central objective of the work presented here is to evaluate whether particle-tracking models can be used to simulate movement and estimate proportional entrainment loss for adult Delta Smelt. Our approach differs from past efforts (e.g. Rose et al. 2013) because we test predictions by comparing them directly to data. We use a two-stage modelling procedure. A computationally-intensive PTM simulates a variety of potential behaviors of Delta Smelt to predict movement of particles among regions in the Delta as well as the proportion of particles from each region that are entrained. These predictions are based on behavioral rules that represent different hypotheses about how Delta Smelt respond to hydrodynamics (depth, velocity, and flow direction), salinity, and turbidity. A key advantage of this approach is that it allowed us to test hypotheses about factors that affect Delta Smelt migration which are not well-understood and represent a key management issue for this species (Sommer et al. 2011, Bennet and Burau 2014). Proportional entrainment predictions from the PTM are unscaled or naïve in the sense that they do not account for variation in abundance among regions at the start of the simulation, or losses due to natural mortality prior to and during entrainment. The initial distribution of the population would have an important effect on proportional entrainment loss owing to differences in vulnerability to entrainment among regions, and proportional entrainment loss will be underestimated if natural mortality is not accounted for (Kimmerer 2008). In the second stage of our modelling procedure, we use a population dynamics model, driven by unscaled movement and entrainment rates from the PTM, to estimate initial regional abundance, natural mortality rate, and salvage expansion factors. The population model predicts abundance over time in each region as well as the number of fish from each region that are entrained, which are in turn used to compute proportional entrainment loss. Parameters of the population model are estimated by non-linear search by statistically comparing predictions of initial distribution, abundance, and entrainment to field observations.

There are three main objectives of our modelling effort:

1. To evaluate behavioral rules predicting movement and entrainment vulnerability of adult Delta Smelt. We do this by comparing the fit of predictions from the population dynamics model to observed spatial and temporal changes in catch from historical fish field surveys (Fall Midwater Trawl and Spring Kodiak Trawl), and daily salvage estimates at the state and federal fish collection facilities.
2. To translate unscaled estimates of proportional entrainment loss generated from the PTMs into a metric that quantifies the proportion of the population lost due to entrainment via the population model. PEL estimates from models that fit the data better would be considered more reliable than PEL estimates from models that don’t fit the data as well. Model evaluation can be used to determine if best-fit models are good enough to be used for quantifying impacts of future export regimes.
3. To better understand the strengths and limitations of available information for estimating PEL. The process of formulating hypotheses as mathematical models and fitting them to observations leads to a sharper understanding of the data which can be invaluable for making future research and monitoring decisions.

The long-term goal of the work presented here is to support a more confident assessment of Delta Smelt entrainment and, stemming from that greater understanding, to assess the efficacy of management actions used to operate the water projects in a manner consistent with the ESA.

Methods

Model Description

Our population dynamic model predicts the abundance, distribution, survival, and entrainment of adult Delta Smelt on a daily time step over an approximate period of 4 months between early- to mid-December to mid- to late-April (Table 1). This simulation window was selected to begin just prior to the first flush and extend through most of the spawning period and include all Spring Kodiak Trawl surveys through April. The model was applied separately in water years 2002, 2004, 2005, and 2011. These years were selected to provide a contrast in flow conditions and seasonal salvage patterns. Two-dimensional (2D) PTMs were applied in each of these water years, and 3D PTMs were applied in 2002 only. A comparison of 2D- and 3D-based results in 2002 allows us to partially evaluate whether the higher resolution and more accurate hydrodynamics and turbidity fields produced by the 3D model effects predictions of movement and proportional entrainment loss.

The population dynamics model consists of process, observation, and likelihood (fitting) components (Fig. 2). The process component predicts the abundance of the population in each of 15 regions for each day of the simulation (Fig. 1). The model uses estimates of abundance in each region and the proportion of particles in that region that are entrained, as determined by a PTM, to predict the number entrained each day (Fig. 2). The observation component of the model translates predictions into catches from Fall Midwater Trawl (FMWT) and Spring Kodiak Trawl surveys (SKT), and daily salvage at each fish collection facility. The likelihood component compares predictions and observations to estimate process and observation parameters by maximizing the likelihood using a gradient search method. The model was fit to each water year using all combinations of ten alternate behaviours (PTMs) and 10 alternate versions of the population dynamic model. Thus a total of 100 different models were fit to each water year (and for both 2D and 3D PTMs for water year 2002).

Predictions of movement and entrainment from the PTM have a strong effect on the population dynamics model. Details of the PTM are provided in RMA (2018) and only a very brief summary is provided here. The PTM is initialized by placing a large number of uniformly distributed particles in each of the 15 regions. Each PTM run (a single behavior) requires 3-7 hours to simulate the movement of approximately 200,000 particles over 120-140 days even with threading the application over 24 XEON cores (2.5-3.0 GHz). Rules that specify the movement behaviour of each particle in response to hydrodynamic, salinity, and turbidity fields influence the location of each particle through the simulation. There is no stochastic variation in behavioural rules for individual particles; each particle will have the same response when exposed to the same stimuli. As noted previously, Delta Smelt behavior during migration is poorly understood (Sommer et al. 2011; Bennett and Burau 2014), so it was important to test several potential behaviors in the modeling process. Only ten of the many PTM behaviors developed by RMA (2018) are analyzed here. They were selected to represent a range of behaviours and fit, and include simple behaviours such as passive drift or movement towards more turbid or less saline water, to more complex behaviours based on multiple physical cues with different thresholds or acclimatization periods (Table 2). Simulation results from the PTM are summarized in an exchange or movement matrix $\mathbf{m_{j,i,d}}$, which is the cumulative proportion of the original particles released in region j that are present in region i on day d, or are entrained at each pumping facility ($i=k$). This exchange matrix is treated as a large set of fixed parameters by the population dynamics model (Fig. 2). Predictions of abundance and entrainment from the population model are translated into relative differences in FMWT catch at the start of the simulation, trends in SKT catch over space and time, and trends in salvage at each facility. These predictions are compared to data, and parameters are estimated by nonlinear search using a maximum likelihood approach. In the description of the population dynamics model which follows, Greek letters denote parameters that are estimated, upper case letters denote predicted state variables, and lower case letters denote indices (not bold), or data (bold) or fixed parameters (bold).

Process Model

The process component of the population dynamics model predicts the abundance of Delta Smelt adults by model day and region. Initial abundance is calculated from,

1) $$N_{i,d=0} = e^{\gamma} \cdot \theta_{I_i}$$

where $N_{i,d=0}$ is initial abundance in each region *i* prior to the first day of the simulation (*d*=0) , γ is the estimated initial total abundance across all 15 regions in log-space, and θ_I is the proportion of the total population in each region at the start of the simulation. Regional abundance on subsequent days depends on cumulative survival and movement, and is calculated from,

2) $$N_{i,d} = \left[\sum_j N_{j,d=0}\right] \cdot \prod_d \phi_d \cdot \mathbf{m}_{j,i,d}$$

where ϕ is the estimated survival rate on day *d*, with the product of those rates up to day *d* (denoted by the $\prod$ symbol) being the cumulative survival from the start of the simulation to the end of day *d*, and $\mathbf{m}_{j,i,d}$ is the cumulative proportion of fish that move from one region to another or are entrained (the exchange matrix from the PTM). Note that abundance in region *i* is the sum of surviving fish from source regions *j* that move to region *i* as well as surviving fish that remain in that region between time steps. We do not allow survival rate to vary across regions owing to the way PTM particle tracks were summarized in $\mathbf{m}_{j,i,d}$ (see RMA 2018). This matrix does not track the history of locations for each particle or group of particles, and therefore does not allow us to apply spatially varying survival rates. However, as discussed below, additional mortality for particles that are entrained is captured in the estimate of the salvage expansion factor.

The natural survival rate of Delta Smelt is modeled in one of four ways to account for potential temporal variation:

2a) $\phi_d = \text{logit}(\alpha_o)$ constant survival over time (hereafter referred to as survival model S_c). logit() denotes that the value inside the parentheses is logit-transformed so $0 \le \phi \le 1$.

2b) $\phi_d = \text{logit}(\alpha_{1:N_{skt}})$ Survival rate is constant over days between each SKT survey, but can vary among each of the N_{SKT} intervals, but with the same survival rate for the interval before and after last survey (survival model S_{skt}).

2c) $\phi_d = \text{logit}(\alpha_o + \alpha_1 \cdot d)$ variable survival over time modelled as a logit-linear function of model day (survival model S_d). A negative value of α_1 will lead to declining survival rate over time.

2d) $\phi_d = \text{logit}(\alpha_o + \alpha_1 \cdot W_d)$ variable survival over time modelled as a logit-linear function of water temperature (W_d, survival model S_w).

Model 2a assumes that survival is constant over time, while 2b allows it to vary among SKT surveys but makes no assumptions about the timing or factors causing variable survival rates. Model 2c allows survival to potentially decline over time which may occur due to spawning-related mortality. Model 2d allows survival rate to vary with water temperature which may affect spawn-timing and therefore spawning-related mortality.

The cumulative number of fish entrained is calculated from,

3) $$N\_Ent_{k,d} = \sum_i N_{i,d=0} \cdot \prod_d \phi_d \cdot \mathbf{m}_{i,k,d}$$

where N_Ent is the number entrained from the start of the simulation through day *d* at pumping location *k*, and $\mathbf{m}_{i,k,d}$ is the cumulative proportion of fish from source region *i* that are entrained at pumping location *k*, as determined by the PTM. Equation 3 scales the proportional entrainment rates from the PTM ($\mathbf{m}_{i,k,d}$) by accounting for differences in initial abundance among regions and losses due to natural mortality. The proportion of the initial population that is entrained at each pumping location up to and including day *d* is calculated from,

4) $$p\_Ent_{k,d} = 1 - \prod_d 1 - \frac{N\_Ent_{k,d} - N\_Ent_{k,d-1}}{\sum_i N_{i,d-1}}$$

Equation 4 follows the same logic as Kimmerer (2008) and assumes natural and entrainment mortality are continuous processes over the duration of the model simulation. As a result, proportional entrainment on each day depends on the abundance at the end of the previous day, where that abundance in turn depends on the initial abundances, and cumulative natural and entrainment losses. The ratio in eqn. 4 is the proportion of fish entrained on day *d* from all regions relative to the total abundance (across all regions) at the end of the previous day. The term inside the product symbol (∏) is therefore the proportion of the population surviving entrainment on day *d*, and that product over days is the cumulative proportion surviving from the start of the simulation through day *d*. Thus 1- this product is the proportion of the population that is lost due to entrainment. Entrainment losses include both pre-screen losses and direct losses to the pumps.

We provide three proportional entrainment metrics in this analysis. We refer to the output from eqn. 4 as proportional entrainment loss (PEL). We also compute the ratio of total entrainment over the simulation ($N\_Ent_{k,d=D}$, where D is the last day of the simulation) to the initial abundance ($\sum_i N_{i,d=0}$) and refer to this as the 'discrete proportional entrainment rate'. This value will be lower than PEL (eqn. 4) because it does not account for fish that would have died of natural causes prior to entrainment (hence the denominator is too large), but it is simpler to understand and closely tracks PEL (because both the numerator and denominator decline with decreases in the natural survival rate). We also refer to an 'unscaled proportional entrainment rate', which is just the output from the PTM for any region for the last simulation day *D* ($\mathbf{m_{i,k,D}}$). This value is the proportion of the initial particles from each region that are entrained by the end of the simulation. They describe relative differences in vulnerability to entrainment among our 15 regions. The contribution of each region to the total entrainment depends on these values but also on the initial abundance estimated for each region at the start of the simulation, and on the natural survival rate. Unscaled proportional entrainment provides a simple summary statistic to compare PTMs.

Observation Model

The observation model predicts SKT catch for each station and survey period from,

5a) $$\hat{C}_{SKT_{s,d}} = N_{i(s),d} \cdot \theta_{SKT_{s,d}}$$

where, $\hat{C}_{SKT_{s,d}}$ is the predicted SKT catch at station *s* on day *d*, $N_{i(s),d}$ is the abundance in region *i* where station *s* is located (*i(s)*), and $\theta_{SKT_{s,d}}$ is the proportion of the population in region *i* sampled at station *s* on day *d*. This SKT sampling efficiency term is calculated from, 5b) $$\theta_{SKT_{s,d}} = \theta_{c_{s,d}} \frac{\mathbf{vtow}_{s,d}}{\mathbf{vreg}_i}$$

where $\theta_{c_{s,d}}$ is an estimate of the proportion of smelt within the volume towed at a station that are captured (sampling efficiency), **vreg** is the volume of region *i* that Delta Smelt are distributed in, and **vtow** is the volume for the tow at station *s* sampled on day *d*. We assumed that Delta Smelt were evenly distributed to a maximum depth of 4 m (as in Kimmerer 2008) but alternate distributions (upper 2 m, entire water column) are easily explored. Assumptions about the depth distribution of Delta Smelt have no effect on our estimates of PEL because they are accounted for in the estimates of salvage expansion factors. For example, if the maximum depth is set to 2 m, the abundance of the population will be lower than the estimated based on a maximum depth of 4 m. However to match the observed salvage data, the salvage expansion under the 2 m depth distribution will be higher than at 4 m. This dynamic is reviewed in more detail in the discussion section. The proportion of smelt within the volume towed that are captured can either be set to 1 or calculated from,

5c) $$\theta_{c_{s,d}} = \text{logit}(\beta_0 + \beta_1 \cdot \text{secchi}_{\text{s,d}})$$

where β_0 and β_1 are parameters predicting SKT sampling efficiency as function of Secchi disc depth recorded at each station on each SKT survey. The logit() term indicates that the prediction is logit-transformed so the efficiency estimates is limited to values ranging from 0 to 1. Delta Smelt may be able to avoid capture to a greater extent when the water is clear which would result in a negative estimate for β_1 (Latour 2015). Increased water clarity may also result in a change in the vertical or lateral distribution of Delta Smelt which could also impact sampling efficiency. Other factors that could affect sampling efficiency could also be modelled using the format in eqn. 5c, but were not explored in this paper for brevity. Catchability, the proportion of the population in a region captured at a station, is the product of θ_c and **vtow/vreg** (eqn. 5b). Station-specific effects on catchability (θ_c) are easily excluded by not estimating parameters defining $\theta_{c_{s,d}}$ and instead fixing this value at 1. In this case, catchability for any region is simply the ratio of the volume sampled in that region across stations on a particular survey to the volume over which smelt are assumed to be distributed over. Owing to the very large volumes of each region, the proportion of the population sampled is very small (Table 3).

Salvage in the population dynamics model is calculated from,

7) $$\hat{C}_{SAL_{k,d}} = (N\_Ent_{k,d} - N\_Ent_{k,d-1}) \cdot \theta_{S_{k,d}} \cdot \mathbf{p}_{S_k}$$

where $\hat{C}_{SAL_{k,d}}$ is the predicted salvage on model day *d* at salvage location *k*, $\theta_{S_{k,d}}$ is the proportion of entrained fish that enter the salvage facility, and $\mathbf{p}_{S_k}$ is the proportion of the flow in the salvage facility that is sampled per day. For consistency with past efforts, we often refer to the inverse of salvage efficiency (θ_S^{-1}) as the salvage expansion factor. Time-specific values for $\mathbf{p}_S$ for each facility were not available for all relevant time periods (Table 1). The 'observed' daily salvage data available to us was already expanded to account for the proportion of volume sampled each day. By using expanded salvage observations one is assuming that $\mathbf{p}_S$=1. However, when fitting the model, using expanded salvage data would overweight the importance of the salvage data relative to other data sources (FMWT, SKT). To correct for this, $\mathbf{p}_s$ was set to values that reflects the typical proportion of fish at each salvage facility that are sampled. We set $\mathbf{p}_s$ to 0.08 (sampling 10 minutes out of every two hours) for the federal facility (CVP) and 0.18 (sampling 21.6 minutes every two hours) at the state facility (SWP). These values were very close to the average sampling proportions across all days during the modelled periods in water years 2002 (CVP=0.084, SWP=0.188) and 2004 (CVP=0.083 SWP=0.175). We do not add the predicted number of Delta Smelt that are salvaged at the facilities to the populations in the region where the salvage is released. The contribution of these releases is negligible because the number of fish released is small relative to the population size in release regions, and because the survival rate of these fish is assumed to be very low (Bennett 2005, Miller 2011, Newman et al. 2014).

The simplest model of salvage efficiency ($\theta_{S_{k,d}}$) assumes it can vary across facilities but does not vary over time,

8a) $$\theta_{S_{k,s}} = \text{logit}(\lambda_{0k})$$

where λ_0 is the proportion of entrained fish that enter the salvage facility *k* on day *d* and are counted, in logit space. Alternate models allow salvage efficiency to vary over time as a function of covariates using, 8b) $$\theta_{S_{k,d}} = \text{logit}(\lambda_{0_k} + \lambda_{1k} \cdot \mathbf{X_{k,d}})$$

where λ_0 is the proportion of entrained fish entering the facility when the covariate **X** is 0, and λ_1 is a linear effect of the covariate $\mathbf{X_{k,d}}$, which varies over time and can vary across facilities. We explored effects of export rates from each salvage facility (as calculated by the DAYFLOW model) water clarity, as indexed by turbidity measured at Clifton Court Forebay (CCF), and water temperature as measured at Mallard. Salvage efficiency could change with export rate due to changes in the efficiency of the louvers to screen fish and changes in the time fish are exposed to predators during the entrainment process (pre-screen losses). Turbidity could also affect the efficiency of the louvers to screen fish and the ability of visual sight predators like striped bass or largemouth bass to detect and capture Delta Smelt. If higher turbidity reduces predation and hence pre-screen losses, salvage efficiency should increase (thus λ_1 should be positive). Water temperature could affect pre-screen loss through changes in predator behavior, their energetic requirements, or the behaviour of Delta Smelt. For brevity, we only show results based on turbidity, which led to the greatest improvements in fit to the salvage data.

Model Fit (Likelihood)

The model is fit to the data by minimizing a negative log likelihood (NLL_{TOT}) that quantifies the combined fit of the model to FMWT catch (NLL_{FMWT}), SKT catch (NLL_{SKT}), and salvage data (NLL_{SAL}). The total negative log likelihood (NLL_{TOT}) is computed from,

9) $$NLL_{TOT} = NLL_{FMWT} + NLL_{SKT} + NLL_{SAL}$$

Each likelihood component is described below. Note that the total negative log likelihood only quantifies the discrepancy between predictions and observations (observation error). There is no component that penalizes process variation in population dynamics because that variation is not modelled. For example, we could have allowed daily survival rates to be drawn from a distribution where we estimated both the mean and the extent of variation across days. In data-limited situations it is not possible to separate process error from observation error. Including both would increase computational time considerably and would require informative priors on the extent of process or observation error, with total variance estimates conditional on those priors. We therefore use an ‘observation error only’ model (see Ahrestani et al. 2013).

It is widely acknowledged that the FMWT program does not provide a sensitive index of Delta Smelt abundance, and that the survey has an unknown capture probability (Newman et al. 2015). In this modelling effort, we assume only that the FMWT catch provides a reliable index of relative differences in abundance across the 15 regions at the start of the simulation in early winter. Correcting for differences in sampling effort in each region in terms of the proportion of the volume that is sampled relative to the volume over which Delta Smelt are distributed, the total FMWT catch of Delta Smelt in each region summed across the four surveys between September and December can be thought of as a random variable drawn from a multinomial distribution,

10) $$NLL_{FMWT} = -\sum_i \log(multinom(\mathbf{c}_{\mathbf{FMWT}_i}, \theta_{I_i}))$$

where NLL_{FMWT} is the sum of negative log likelihood values from a multinomial distribution[1] across the 15 regions, with observed catches $\mathbf{c}_{\mathbf{FMWT}}$, and initial regional proportions defined by model-estimated θ_I values in eqn. 1 (the proportion of the initial population in each CAMT region at the start of the simulation). In the absence of any other information, this error structure will result in a set of estimated initial proportions equivalent to the ratio of each regions catch relative to the total catch. The certainty in those proportion estimates will increase with the total catch. Values of $\mathbf{c}_{\mathbf{FMWT}}$ used in the computation were adjusted to reflect differences in relative sampling effort while conserving the total catch across regions[2].

We assume that the SKT surveys provide a reliable index of abundance over both space (across regions) and time (over SKT survey periods in a year). Unlike the FMWT likelihood, we

[1] A multinomial distribution is used to model the probabilities associated with more than two outcomes. As an example, a multinomial distribution can be used to model the probability of obtaining values of 1 through 6 on a six-sided dice based on a total of N rolls. If the dice is balanced, the probability for each of the six possible outcomes is 1/6. This probability can be precisely estimated if many trials are conducted (say 1000 dice rolls). However, uncertainty in estimates of the probability of obtaining any outcome (say rolling a one) will be much greater when fewer trials are conducted. In the application of the multinomial distribution in this model, the total FMWT catch across all regions on the December survey represents the number of trials, the catch in each region represents the number of dice rolls for each outcome, and θ_{I_i} represents the estimated probability of each outcome.

[2] Adjusted c_{FMWT} values were computed by expanding the sum of catches across all stations in a region by the proportion of the useable volume of the region sampled by the sum of tow volumes. These sample volume-adjusted catch values for each region were then standardized by dividing them by their sum across regions. The sum of the standardized values across regions is identical to the sum of original catches across regions, preserving the total sample size.

assume that the capture probability of the SKT survey is known and is accurately determined by the scaling factors in eqn. 5a. SKT catch at each station and SKT survey period is assumed to be a random variable drawn from a negative binomial distribution (negbin),

11) $$NLL_{SKT} = -\sum_{s,d} \log(negbin(\mathbf{c}_{\mathbf{SKT_{s,d}}}, \hat{C}_{SKT_{s,d}}, \tau))$$

where, NLL_{SKT} is the sum of negative log likelihoods across all sampling days (*d*) and stations (*s*), $\mathbf{c}_{\mathbf{SKT_{s,d}}}$ is the observed SKT catch by station and day, $\hat{C}_{SKT_{s,d}}$ is the predicted catch from eqn. 5, and τ represents the extent of overdispersion in the data. In the form of the negative binomial we use, this latter parameter is the variance-to-mean ratio and reflects the average extent of variation in catches across stations averaged over all regions and surveys. We estimated its value for each modelled water year by fixing the density on each SKT survey and region at its conditional maximum likelihood value (sum of catches across stations divided by sum of tow volumes). For each region and SKT survey, we multiplied this density by the tow volume at each station to compute $\hat{C}_{SKT_{s,d}}$. We then used non-linear search to find the value of τ that returned the lowest value of the NLL from the negative binomial distribution. τ therefore represents the average extent of overdispersion in the SKT catch data across stations and surveys if the mean density could be perfectly predicted. τ estimates were 11 (water year 2002), 16 (2004), 8 (2005), and 30 (2011), which are very high levels of overdispersion. We selected a value of τ=10 to use for all years as higher values result in very poor fits to the SKT data because they imply that there is little information about mean density (by region and SKT survey). To simulate greater belief in the SKT data, we also examined fits of the population dynamic model where τ was set to 1. In this case the negative binomial distribution is equivalent to the Poisson, where the variance is equal to the mean[3]. Our approach to modelling error in the SKT data is rather ad-hoc, but as we discuss in the conclusions section, there is insufficient information to accurately model the error.

[3] The poisson distribution can be used to predict the probability of obtaining X events based on sampling for a fixed period of time or over a fixed area or volume. In this example, X would be the catch of Delta Smelt at a station based on sampling the typical volume of water swept by an SKT tow. The poisson distribution has only one parameter which is the mean rate (e.g. typical catch per volume) across stations within a region. The variance of a poisson distribution is assumed equal to the mean rate. Due to random processes there will be some variation in catches across stations even if the densities (mean rate) are the same across stations, and the extent of this variation in a relative sense depends on the sample size (catch in each tow). The poisson variance assumption (variance=mean rate) may not be sufficient to explain the variation in catches across stations in a region. A negative binomial

The observed salvage at each salvage location is assumed to be poisson-distributed (pois) random variable[4],

12) $$NLL_{SAL} = -\sum_{k,d} \log(pois(\mathbf{c}_{\mathrm{SAL}_{k,d}} \cdot \mathbf{p}_{\mathrm{s}_k}, \hat{C}_{SAL_{k,d}}))$$

where, NLL_{SAL} is the sum of the negative log likelihoods across all days, $\mathbf{c}_{\mathrm{SAL}_{k,d}}$ is the reported expanded daily salvage at facility *k* on day *d*, $\mathbf{p}_{\mathrm{S}_k}$ is the average proportion of water that is sampled for fish at the salvage facility, and $\hat{C}_{SAL_{k,d}}$ is the predicted salvage computed from eqn. 7. By including the proportion of water sampled for fish at the salvage facility for both observations (eqn. 12) and predictions (eqn. 7), approximately correct samples sizes are used in the likelihood.

Parameters of the model were estimated by maximum likelihood using nonlinear search in AD model-builder (ADMB, Fournier et al. 2011). We ensure convergence had occurred based on the gradients of change in parameter values relative to changes in the log likelihood and the condition of the Hessian matrix returned by ADMB. Asymptotic estimates of the standard error of parameter estimates at their maximum likelihood values were computed from the Hessian matrix within ADMB.

Model Comparison

We used the Akaike Information Criteria (AIC) to compare PTMs and alternate versions of the population model. AIC measures the trade-off between model complexity and fit and is calculated from,

---

distribution can be used to model the probability distribution for the rate parameter across stations in a region, with the overdispersion term describing how much variance there is in this mean rate across stations. Under the formulation used here, the negative binomial distribution is equivalent to the poisson distribution when τ=1. During estimation, τ increases to reflect the degree of extra-poisson variation in the catches across stations.

[4] Theoretically, the number of Delta Smelt that are salvaged should be a binomially distributed random variable that depends on the total number entrained (the number of trials) and the probability of salvaging a fish (proportion of entrained water sampled * proportion of fish salvaged from sampled water). However, the binomial probability distribution cannot be calculated when the observed number of salvaged fish exceeds the predict number that are entrained. This situation can occur in the model during the non-linear search since (depending on estimates of initial abundance, survival, etc.). Unlike the binomial distribution, the probability from a poisson distribution is calculable in such circumstances. For a given dataset, the expected values and variance returned a poisson distribution will be indistinguishable from a binomial distribution except when the sample size is very small or probability of success is very large (with the latter being quite unlikely).

13) AIC = 2·K - 2·LL

where K is the number of estimated parameters and LL is the log likelihood calculated as $-NLL_{Tot}$ in eqn. 9. More complex models with more parameters (higher K) may fit the data better (higher LL) than simpler models, but parameter estimates will be less precise. Models with lower AIC (i.e., higher LL and lower K) are considered to have better predictive performance when applied to replicate data sets. Models within 0-2 AIC units of the most parsimonious model (the one with the lowest AIC) are considered to have strong support and cannot be distinguished; models within 2-7 units are considered to have moderate support, and models that had AIC values > 7 units relative to the best model are considered to have weak support (Burnham and Anderson 2002).

Our main analysis consists of comparing 10 different versions of the population dynamics model for each of the 10 PTM behaviours. The different population dynamics models are intended to span the range of potential process and observation dynamics. The simplest population model we examined estimates 19 parameters which include the total initial abundance, 15 initial abundance proportions, 2 constant salvage efficiencies (one for each facility), and one constant survival rate. The most complex model we examined estimates 26 parameters, which includes two additional parameters to model salvage efficiency as a function of turbidity, 3 extra parameters to allow survival to vary between SKT surveys, and two extra parameters to model the effect of Secchi depth on SKT sampling efficiency.

The ten population models we fit include all four methods for estimating the daily survival rate (eqn.'s 2a-2d) and two methods for estimating salvage efficiency (eqn.'s 8a and 8b (X=turbidity) for a total of 8 different versions of the population dynamics model with constant SKT sampling efficiency (θ_c=1 in eqn. 5b). We also fit the Secchi-SKT efficiency model (eqn. 5c) with the time-based survival model (eqn. 2c) under constant and turbidity-based salvage efficiency. Thus we estimated 10 alternate population dynamics models for each of the 10 PTM behaviours (10x10=100). These models were fit using both high overdispersion in SKT catch data (variance-to-mean ratio τ=10, see eqn. 11), and assuming error in SKT catch data was poisson-distributed (variance-to-mean ratio τ=1). Thus we fit 200 models for each of the five scenarios (3D for water year 2002, 2D for water years 2002, 2004, 2005, and 2011) for a total of

1000 models. Best models identified by AIC may still fit the data poorly or exhibit obvious biases. In addition, because we could not model all variance components (e.g. process error in survival, uncertainty in movement), we definitely underestimate the extent of variance in predictions. As a result, AIC differences overestimate differences in information loss among models. We therefore use the AIC analysis as a screening tool to identify a manageable number of models whose fit we then examine in detail, but do not adhere strictly to the Burnham and Anderson (2002) AIC difference criteria in identifying the best models.

Results and Discussion

Owing to the large number of models that were evaluated, we begin by ranking the models for each water year based on the AIC analysis, and then examine the predictions and fit for some of the better models. Four general patterns are evident in the AIC analysis.

1. More complex PTMs result in much better fits compared to simpler PTMs. This is seen by lower ΔAIC values and higher rank order for more complex PTMs under the same population model structure (moving down rows within columns in Table 4). As more complex PTM behaviours do not increase the number of parameters estimated in the population model (recall the PTM movement matrix are treated as fixed parameters in the population model), the improved fits result in higher log likelihoods with no parameter penalty, and hence lower AIC values and higher model ranks. This pattern occurred in all water years except 2011 which was challenging year to fit owing to a very limited number of salvage observations. The AIC model selection approach correctly identifies simpler models as better in this more data-limited situation.
2. The ranking of PTMs was generally very consistent across alternate population model structures (no or small change in rank moving across columns within rows in Table 4). Within PTMs, increasing the complexity of the population model (moving from left to right in Table 4) resulted in substantially lower AIC values. The addition of only one extra parameter to predict daily salvage efficiency as a function of turbidity (λ_1 in eqn. 8b, population models 5-8 and 10) reduced AIC values by hundreds of points in water years 2002 and 2004 due to the improved fit to the salvage data. This indicates very strong statistical support for turbidity-based variation in salvage efficiency in these years. Allowing

daily variation in natural survival rates also lowered AIC values relative to the constant survival model (e.g. population model 1 vs. 3-4 in Table 4), but the improvement was much less than the AIC reduction associated with using turbidity to predict salvage efficiency. Allowing SKT sampling efficiency to vary with Secchi disc depth generally resulted in smaller or no reductions in AIC compared to models that assumed SKT sampling efficiency was constant (thus only varying with the ratio of tow and regional 4 m volumes).

3. There was substantial variation in proportional entrainment loss estimates across PTMs and negligible variation across population models for a given PTM (Table 4). This indicates that movement predictions from the PTM (the **m** exchange matrix in eqn. 3) dominate PEL estimates in the population model. Variation in the magnitude of initial abundances across regions has the potential to influence PEL estimates, but the extent of this variation was limited through fitting to FMWT and SKT data.
4. AIC differences between models (both across and within population model structures) were large and indicated very strong statistical support for more complex PTM behavioural rules and more complex population model structures. However, these differences likely overestimate the extent of model separation because we do not model important sources of variation, such as uncertainty in movement dynamics. As expected, AIC differences were generally smaller when we assumed greater error in the SKT data (τ=10 vs τ=1).

Water Year 2002 (3D)

Particle-tracking model 6 and population model 10 applied in water year 2002 had the lowest AIC value of all 100 models that were fit (Table 4a). It provided a good fit to the adjusted FMWT catch data (r^2=0.98, see Table A1a) and predicted an initial abundance of about 2.4 million fish (Fig. 3a top panels). This combination of models (hereafter referred to as ‘the model’) predicted a substantial decrease in daily survival rates starting in March, consistent with the hypothesis that mortality rates are higher during and following spawning (lower-left panel). The predicted total abundance of the population across regions was reasonably close to values calculated from expanding the SKT catch data (by the ratio of regional 4 m volume/tow volume) on the last two surveys, but the model substantially overpredicted abundance on the January survey (lower-right panel). The model predicted peak entrainment in mid-December through early January and more entrainment at the state facility (Fig. 3b, left panels). These patterns were largely driven by the PTM-based unscaled entrainment rates (top-right panel in Fig. 3b). Proportional entrainment loss predicted from the population model was about 35% when summed across facilities, and was higher at the state facility. Discrete proportional entrainment values (entrainment/initial abundance) were lower owing to the fact that this metric does not account for losses from natural mortality that occurs over the simulation period (thus denominator in eqn. 4 is too large and hence entrainment proportion too low), but differences were relatively modest. The model predicted some highly variable and perhaps unlikely patterns in abundance over time in some regions (Fig. 3c). Of particular concern are large abundance estimates in some of the southern and eastern regions (sjr_ant, cdelta, sdelta) early in the simulation. As these regions have relatively high values of unscaled proportional entrainment (as determined by **m** from the PTM, Fig. 3b), these potential overestimates of abundance would lead to overestimates of entrainment. The population model provided a reasonable fit to most of the SKT catch data as predictions of mean catch rate by region and trip (red dots, Fig. 3d) were generally within the range of observed values and close to the observed means (large open dots, Fig. 3d). The model explained 80% of the variation in SKT catch across survey trips and regions when the data were averaged across stations (Table A1a). The model predicted that SKT catch efficiency declined with increases in water clarity (Fig. 3e), a similar finding to Latour (2015) based on his analysis of FMWT data for Delta Smelt and other species. This relationship lowered AIC by 28 units compared to assuming capture efficiency was constant under poisson error (Table 4a, models 7 vs. 10), but there was no AIC difference between these models under negative binomial error which assumes there is less information in the SKT data (Table 4b). The population model provided a very good fit to temporal patterns in salvage at both facilities and explained 63% and 91% of the variation in observed daily salvage at federal and state facilities, respectively. (Fig. 3e, Table A1a). It predicted that salvage expansion factors were very sensitive to turbidity changes, with much higher expansions at lower turbidity (Fig.'s 3f and g). Expansion factor at SWP were higher and more sensitive to turbidity compared to those at CVP. This could be driven by higher pre-screen loss at SWP as fish move through the Clifton Court Forebay (CCF), or because the model overpredicts the relative amount of entrainment at SWP (requiring a greater expansion factor to compensate for that overprediciton).

In our model, salvage efficiency (inverse of the expansion factor) is estimated to maximize the fit to the salvage data. As the salvage observations are fixed (data), the salvage expansion factor will increase with the predicted level of entrainment. Estimates of the salvage expansion, whether constant of varying with turbidity (Table 4), are larger than previously published values derived from the ratio of predicted entrainment to salvage, but are within ranges from mark-recapture based estimates (Table 5). Kimmerer (2008) calculated an expansion factor for both facilities of 29, where entrainment was calculated as the product of abundance in the south Delta (determined from SKT surveys) and the proportion of passively drifting particles in that area that were entrained as determined by a hydrodynamic model. Kimmerer (2011) later revised his expansion factor to 22 (95% confidence interval of 13-33). More recently Smith et al. (in prep.) calculated PEL from the ratio of calculated entrainment to observed salvage using improved hydrodynamic predictions and passive particle movement from the same 3D model used here. Their expansion factors ranged from 35 (CVP) to 50 (SWP). In comparison, our estimates of the salvage expansion at the state facility for the top-ranked PTMs for some of the better population models (PTM models 6, 7 and 10 for population model 3 in Table 4a) ranged from about 45-115. Castillo et al. (2012) estimated salvage expansion at the state facility empirically by releasing known numbers of marked cultured adult Delta Smelt immediately in front of the louvers as well as at the CCF gates They estimated salvage expansions of 32 and 250 from two separate release experiments conducted in February and March, 2009 (Table 5). These values span the range of time-averaged salvage expansion (blue line in Fig. 3f), however predicted expansion factors on some dates exceeded Castillo et al.'s maximum value (dashed line in Fig. 3e).

In water years 2002, population models that did not allow salvage expansion to vary over time (models 1-4 and 9 in Table 4), overpredicted salvage early in the simulation at the state facility prior to the first flush when the water was clear, and underpredicted peak salvage, especially at the state facility when the water was more turbid (Fig. 4). These models explained much less of the variation in observed salvage relative to models where salvage efficiency could vary over time (Table 1Aa). The salvage efficiency-turbidity function predicts low salvage efficiency in clear water (Fig. 3g) and hence leads to lower salvage predictions early in the simulation (Fig. 4 blue line) which are more consistent with the data (leading to better fit to the salvage data and lower AIC values). In this example, the turbidity-salvage efficiency relationship improved the fit to the salvage data by hundreds of AIC units compared to the model which assumed salvage efficiency was constant over time. The turbidity-based model implies that peak salvages are the result of reduced pre-screen loss due to high turbidity, rather than the prevailing interpretation that greater entrainment rates occur when there is a turbidity bridge between the south Delta and the pumps. Higher levels of turbidity have the potential to lower predation rates and hence reduce pre-screen loss and the magnitude of the salvage expansion factor. However, we suspect the magnitude of the turbidity effect estimated by the model (in this and other water years) may be too high. Turbidity, as measured at CCF, ranged from about 15-35 NTUs during the period when salvage was observed in water year 2002. This resulted in salvage expansion factors ranging from about 200 (at 15 NTUs) to 75 (at 35 NTUs) at CVP, and 350-25 at SWP. Castillo et al. (2012) estimated salvage expansions of 32 at an average turbidity of 11.5 NTUs (February 2009), and 250 at an average turbidity of 13.5 NTUs (March 2009, Table 5). While the range in salvage expansion factors estimated by the turbidity model were typically within the range estimated by Castillo et al., their study does not provide any empirical support for a negative relationship between the salvage expansion factor and turbidity. However, Castillo et al. estimated pre-screen loss from the CCF gates, while the expansion factor used in our model applies to all fish that are entrained. As the majority of fish entering the south Delta and other southern-eastern regions will be entrained (Fig. 3b), our salvage expansion therefore applies to an area well upstream of CCF where turbidity effects would have more time to effect survival and hence salvage expansion factors. To some extent our model accounts for reduced survival in southern-eastern regions that are more vulnerable to entrainment by increasing the salvage expansion factor.

To examine this issue in more detail, we estimated the potential additional mortality in southern-eastern regions and CCF by combining our estimate of salvage efficiencies with field-based estimates of total facility efficiency at SWP. All fish that are entrained must pass through our south Delta region. The proportion of Delta Smelt surviving from their location of entrainment (say the center of the sdelta region) to salvage at the state facility is the product of survival from the entrainment point to the CCF gates and the total facility efficiency (louver efficiency and pre-screen loss in CCF). Thus, given a total salvage efficiency estimated by the model and the total facility efficiency estimated by Castillo et al. (2012) for SWP in 2009 (which we assume here applies in 2002), the proportion lost between the entrainment point and the CCF gates can be back-calculated (Table 5). For example, given a relatively low salvage efficiency of 0.0025 predicted by the model (expansion of 1/0.0025 = 400, Fig. 3e), about 90% and 40% of Delta Smelt must be lost to predation between the entrainment point and the CCF gates. Such high loss rates in southern-eastern Delta regions may not be that unrealistic (e.g. Fig. 3b top-right panel).

Water Year 2002 (2D)

Particle-tracking model 8 fit the data best in water year 2002 using the 2D simulation framework (Table 4c, Fig. 5). This model produced similar estimates of PEL of ~35% (Fig. 5b) to the best 3D model (PTM 6). It also overpredicted abundance on the January SKT survey (Fig. 5a), largely due to overestimating abundance in cache_dwsc and sac_sherm regions (Fig. 5c and d). The model estimated a steep negative relationship between Secchi depth and SKT sampling efficiency (Fig. 5e) as it did for the 3D simulation in 2002. The model fit the salvage data very well (Fig. 5f), and like the 3D model in 2002, also predicted a very steep positive relationship between turbidity and salvage efficiency (Fig. 5g). The 2D model explained a similar amount of variation in FMWT, SKT, and salvage data (Tables A1c and d) as the 3D model (Tables A1a and b).

Water Year 2004

Particle-tracking model 10 fit the data best in water year 2004 (Table 4e and f). As in 2002 (both 2D and 3D models), there was strong support for models that used turbidity to predict salvage efficiency (e.g. population model 1 vs 5). There was less support for population models that allowed survival to vary as a smooth function of model day compared to 2002. For example the AIC for population model 3 was only one unit lower than model 1 (Table 4e). However, models that allowed survival to vary freely among SKT surveys or as a function of water temperature provided better fits and predicted a large decrease in survival beginning in early March. The best-fit model in water year 2004 explained less variation in FMWT data (r^2=0.69) and especially salvage data (r^2=0.20 and 0.17 for CVP and SWP respectively. Tables A1e and f)) compared to 2002 (Tables A1 a-d). Using Secchi depth to predict salvage efficiency led to large reductions in AIC, but the slope of the relationship was positive which makes the unlikely prediction that sampling efficiency increases with water clarity (results not shown for brevity). This is a good example where the lowest AIC model may be misleading relative to a model with a higher AIC value. We therefore examined the fit of population model 8, which allows survival to vary as a function of water temperature and salvage efficiency to vary as a function of turbidity, but without a Secchi depth effect on SKT sampling efficiency (Fig. 6). This model produced a reasonable estimate of the initial abundance and feasible pattern in daily survival rate (Fig. 6a). To provide better fits to the SKT and salvage data, the model estimated a higher proportion of the initial population in the smarsh region and a lower proportion in cache_dwsc relative to what the FMWT data indicate. The model estimates that PEL was 49% with considerable entrainment over an extended period between late December and early March (Fig. 6d). However, PEL may have been overestimated as the model substantially overpredicted abundance in sjr_stk and sdelta regions (Fig. 6c) where unscaled proportional entrainment values were large (Fig. 6b). The fit to the SKT catch data in 2004 was poor in some regions but explained a similar amount of variation (r^2=0.8) compared to 2002 (Fig. 6d, Tables A1e and f). The model did not fit the salvage data as well compared to other years (r^2=0.20 and 0.17 for CVP and SWP, respectively), perhaps because the two separate salvage peaks in 2004 provide a more rigorous test for the model. The model predicted that the first peak salvage event occurred too early in the year, but predicted the timing and magnitude of the second peak salvage event relatively well (Fig. 6e), The turbidity-salvage efficiency relationship at SWP was similar to the one estimated in 2002 (Fig. 6f). The CVP relationship in 2004 was steeper compare to one in 2002. This could indicate that the PTM is underpredicting the amount of entrainment at CVP relative to SWP.

Water Year 2005

Particle-tracking model 8 fit the data best in water year 2005 assuming poisson error in SKT data (Table 4g) and PTM 8 or 9 fit the data best assuming negative binomial error (Table 4h). There was some evidence for daily variation in survival rate, but unlike water years 2002 and 2004, there was no evidence for a turbidity effect on salvage efficiency. The lowest AIC model included a negative effect of Secchi depth on SKT efficiency. However, it predicted that SKT efficiency was very low even when Secchi depth was low, leading to very large estimates of abundance which in turn led to unrealistically high salvage expansion factors (plots not shown for brevity but see Table 4g). This is another example where the lowest AIC model is likely misleading. The next lowest AIC models which allowed survival rate to vary between SKT surveys had unrealistic survival patterns (near 1 except between the 3rd and 4th survey). We therefore examined the fit of population model 4, which was the lowest AIC model that did not exhibit unrealistic abundance or survival patterns. This model allows for time-varying survival rate as a function of water temperature but no effects of turbidity on salvage efficiency or Secchi depth on SKT efficiency. This model provided good fits to the FMWT catch data (r^2=0.93, Table A1g) and expanded SKT population estimates (r^2=0.73, Table A1g), and predicted a reasonable initial abundance and declining survival rate over time (Fig. 7a). Proportional entrainment estimates were relatively low (~15%) even though the unscaled rates in southern and eastern regions were large (Fig. 7b). This occurred because the model estimated that the majority of the population at the start of the simulation was located in regions with relatively low vulnerability to entrainment. Lower levels of entrainment resulted in lower estimates of salvage expansion factors (Table 4g and h) compared to other years. As in other water years, the model appears to overpredict abundance in some regions (sjr_ant, sdelta) with high unscaled entrainment rates (Fig. 7c and d). The model did not fit the daily salvage very well (r^2=0.17 and 0.37 for CVP and SWP, respectively, Table A1g), which is perhaps not surprising since salvage expansion factors for population model 4 did not vary over time (Fig. 7e).

Observed salvage of adult Delta Smelt in winter peaked during the “first flush” when turbidity was higher in all our study years except 2011 (Fig. 8). Recall there was strong support for a turbidity-salvage efficiency relationship in 2002 and 2004, but not in 2005. PTM 8 in 2005 correctly predicted the timing of the initial increase in salvage in mid-January at both facilities when turbidity reached maximum values (Fig.’s 7e, 8). However, the observed peak in salvage occurred after the peak in turbidity. Thus a positive turbidity-salvage efficiency relationship would have led to a poorer fit to the salvage data since it would have overestimated salvage in mid-January and underestimated it during peak salvage in late-January. Peak salvage also lagged behind peak turbidity during the first peak salvage event in 2004, and this led to an overprediction of salvage in early January (Fig. 6e). These patterns suggest that the turbidity-salvage efficiency relationship may be an artefact that is compensating for slightly mistimed entrainment predictions from the PTM. Similarly, inconsistencies in how these relationships differ between CVP and SWP among years may be an artefact that is compensating for error in the relative difference in entrainment between these locations.

Water Year 2011

Water year 2011 was challenging to fit as few Delta Smelt were salvaged and SKT catch was low. 2011 was selected because outflows during the winter were high, providing a unique condition to evaluate PTM predictions. Water year 2011 is also representative of challenges in fitting the model to the current situation of very low Delta Smelt abundance which leads to virtually no salvage observations and highly uncertain and low abundance estimates. PTM model 6 fit the data best assuming poisson error in SKT catch data (Table 4i), while PTM 10 was best assuming negative binomial error (Table 4j). Model selection was more sensitive to assumptions about SKT error in 2011 because there was very little information about the initial distribution from FMWT data or the timing of entrainment from the salvage data due to low sample size. Concerning aspects of fitting to 2011 data include ranking the PTM 1 as the 2nd-best model (Table 4i) and estimation of very large salvage expansion factors. The latter result is not surprising as there was such limited observed salvage that salvage expansion factors were essentially not estimable. Given limitations in the 2011 data, we examined the fit of the simplest population model (1) which estimated a low initial abundance and fit the expanded SKT catch data (across regions) relatively well (Fig. 9a). It estimated a lower survival rate compared to other years and did not fit the FMWT data very well (r^2=0.63, Table A1i) compared to water years 2002 and 2005 (r^2=0.93-0.98). This occurred because the total FWMT catch in 2011 (summed across Sep, Oct, Nov, and Dec surveys) was only 49 fish, so there was little penalty in predicting initial across-region population proportions that did not match these limited data. Unscaled proportional entrainment rates were essentially zero for most regions which is a sensible prediction from the PTM due to the very large outflows (Fig. 9b). The model estimated that the majority of the population was located in the cache_dwsc region which had a near-zero unscaled entrainment rate in 2011 owing to the high flows. As a result, the PEL estimated by the model was very low (3%). Fits to the expanded abundance (Fig. 9c) estimates and SKT catches (Fig. 9d) were poor (r^2=0.33, Table A1i) compared to other years (Fig. 9a).

Comparison of Models Across Water Years

The PTM which fit the data best varied across water years and even across 2D and 3D versions in water year 2002 (Table 6). However, PTMs 8 and 9 were ranked as either the 1st- or 2nd-best model in 2002, 2004, and 2005 (2D, 2011 excluded due to limitations in data). The differences in AIC among the top-ranked models in any year were large relative to the 0-10 unit scale typically used to differentiate among competing models, suggesting strong support for the PELs associated with the best model. However these differences should be interpreted cautiously owing to our inability to model important components of the variance. Fortunately, from a policy perspective, distinguishing among alternate PTMs does not always matter. For example, the 1^{st} and 2^{nd} ranked models in water years 2002 (2D), 2005, and 2011 produce very similar estimates of proportional entrainment loss. However the 1^{st}- and 2^{nd}-ranked models for the 3D PTMs in water year 2002, and the 2D PTMs in water year 2004, have substantively different PEL estimates. We therefore compare the graphical fit of these PTMs in each of these water years to provide a clearer sense of whether these models are as distinguishable as the AIC analysis suggests. In water year 2002, the fits of the 3D 1^{st}- (PTM 6) and 2^{nd}- (PTM 10) ranked PTMs to the salvage and FMWT data were almost indistinguishable (Fig. 10a). The pattern between predicted and observed SKT catches from PTM 6 and 10 were also similar (Fig. 9b). The log likelihood values indicate that PTM 10 actually fit the FMWT and SKT data slightly better than PTM 6 (higher log likelihood) but provided a worse fit to the salvage data (lower log likelihood), which led to a lower value for the total log likelihood (Table 7). This results in an AIC difference between models of 91 units. It is hard to rationalize such strong statistical support for PTM 6 compared to PTM 10 given the very modest differences seen in the graphical comparison. In our view, the data do not allow us to differentiate among these two alternate PTMs which is disappointing as they have such different PELs (0.35 vs 0.46, respectively). In water year 2004, the AIC difference between the 1^{st}- (PTM 10) and 2^{nd} (PTM 9) -ranked models was 306 units. In this case the better fit to the second observed salvage peak of the top-ranked model is apparent in the graphical comparison, as is the better fit to the FMWT data (Fig. 11a). As for 2002, the difference in fit to the SKT data between models is not distinguishable from the plots (Fig. 11b). The log likelihoods for PTM 10 from all three data sources were higher than for PTM 9. Relative to the 3D 2002 example, it is perhaps easier to rationalize the strong statistical support for the top-ranked model in water year 2004, which has a considerably higher PEL estimate (0.50) compared to the 2^{nd}-ranked model (0.37).

Conclusions

The objectives of our analysis were to: 1) evaluate particle-tracking models predicting the movement of adult Delta Smelt and their vulnerability to entrainment by comparing predictions to data; 2) provide proportional entrainment loss estimates from the more reliable models; and to 3) better understand the strengths and weaknesses of available information with respect to quantifying PEL to inform future research and monitoring decisions. We found that PTMs that simulated more complex behaviors fit the data much better than simpler models. Simple behavioural rules like tidal surfing (Sommer et al. 2011), movement towards more turbid water (Bennett and Burau 2015), or movement towards less saline water (Rose et al. 2013) did not on their own do well at explaining the seasonal and spatial variability in adult Delta Smelt catch rates and salvage. More complex models that combined some of these behaviours and included lagged responses fit the data much better. Estimates of proportional entrainment loss could vary considerably among PTMs and among water years, but were similar across alternate population model structures. PEL estimates from the models that provided good fits to the data were much higher than previously reported values. Our statistical analysis suggests that PEL estimates are relatively well defined, but this result is an artefact of the strong assumptions made in our modelling approach which were required due to limitations in the data. Better definition of salvage expansion factors through field experiments would improve our ability to distinguish among PTMs based on comparisons of fit to historical data with sufficient information in fish surveys and salvage trends. This in turn would increase the reliability of PTMs to predict how future alternate export regimes affect PEL.

We estimated that proportional entrainment loss of adult Delta Smelt from PTMs that were most consistent with the data was approximately 35% in water year 2002, 50% in 2004, 15% in 2005, and 3% in 2011 (values varied slightly across alternate population models). These estimates are more than double those from Kimmerer (2008) which were 15% (5-24% confidence limit) in water year 2002, 19% (6-31%) in 2004, and 7% (2-12%) in 2005. Our estimates of PEL were higher because movement predictions from the PTM resulted in greater entrainment. In order to fit the scale of the observed salvage, our models needed to estimate much larger salvage expansion factors than those of Kimmerer (2008 and 2011) and Miller (2011). In our view, estimates of salvage expansion factors and PEL from earlier studies, which rely on estimates of abundance in the southern Delta regions, are highly uncertain owing to uncertainty in both the abundance and entrainment components of the calculation. The abundance estimates are based on expanding catches from a very limited number of samples. There are no data to support the assumption that Delta Smelt are distributed evenly to a depth of

4 m in both deep and shallower water habitats, or that this distribution does not vary with abundance or other conditions. To our knowledge there are no studies that indicate that individual fish within a population are uniformly distributed, justifying the use of a volumetric population expansion. These strong assumptions were unavoidable, and Kimmerer (2008, 2011) and Miller (2011) acknowledge the uncertainty in their PEL and salvage expansion factor estimates. Their work has been very helpful in advancing discussions on entrainment on Delta Smelt and other species. Our point here is only that their estimates do not provide a reliable baseline from which to judge PEL and salvage expansion factors estimated by our PTM-population modelling approach. Field-based estimates of salvage expansion factors, such as Castillo et al. (2012), are much more reliable because they avoid these highly uncertain assumptions. Unfortunately, only two estimates for Delta Smelt are available (and only for SWP) and they range by almost an order of magnitude (Table 5). The salvage expansions estimated in this modelling exercise for all years except 2011 fall within this range (2011 not reliably estimated due to very limited salvage). Thus, additional mark-recapture experiments upstream of both state and federal fish collection facilities to estimate salvage expansions (and relationships with covariates) are critical to resolve uncertainties about whether our estimates of high proportional entrainment loss are reasonable or are too high. Ideally, these experiments would be conducted over a number of years to provide adequate replication and contrasting conditions which would affect mortality between release salvage locations. In the long run, releasing fish at greater distances from screening facilities (e.g. compared to CCF gate release points of Castillo et al.) should be considered to estimate the total loss between fish collection facilities and locations where Delta Smelt are unlikely to escape entrainment (e.g. head of Old and Middle Rivers). These efforts should only be conducted if we can assume that pre-screen loss estimates, or relationships between pre-screen loss and covariates like turbidity, are exchangeable among years. In this case they could be used in modelling efforts like this one to better distinguish among PTMs that are applied to historical data where there is more information on abundance and entrainment to evaluate the models. We also recommend that additional PTM modelling and statistical evaluation be conducted with the objective of determining whether similar or better fits to the data could be achieved from behaviours that result in lower PEL estimates more in-line with previously published values. Much of the effort in the current project has gone to

development of simulation and statistical evaluation frameworks, and costs for conducting additional runs would be relatively low.

Fits of our model to data from 2002 and 2004 were greatly improved by allowing salvage efficiency to vary with turbidity. The improved fit could indicate that peak salvage events during periods of high turbidity are caused by reduced predation loss (turbidity-predation loss hypothesis) rather than the prevailing hypothesis that movement towards the pumps increase with turbidity (turbidity-movement hypothesis, Grimaldo et al. 2009). However, the lack of support for this relationship in 2005, and inconsistencies in relationships across years within locations, suggests it may be artefact that compensates for temporal or spatial error in predictions of entrainment from the PTM. It is important to distinguish among these competing interpretations. The remarkable fit to the salvage data based on models that include a turbidity-salvage efficiency suggest that PEL estimates may be reliable, however this conclusion is wrong if these relationships are spurious. There is certainly lots of evidence from other systems that support the turbidity-predation hypothesis (Ginetz and Larking 1976, Gregory and Levings 1998, Johnson and Hines 1999, Yard et al. 2011). But there are also many studies that document increased movement or vulnerability to sampling during periods of higher turbidity supporting the turbidity-movement hypothesis (Gradall and Swenson 1982, Guthrie and Muntz 1993, Miner and Stein 1996, Korman et al 2016, Korman and Yard 2017). Turbidity-predation and – movement hypotheses are almost certainly related because reduced predation risk associated with higher turbidity would reduce concealment behaviours and lead to increased movement (Yackulic et al. 2017), which in turn would increase vulnerability to entrainment. There is no empirical support of a turbidity-salvage efficiency relationship at the state facility where whole facility efficiency for Delta Smelt has been estimated, but only two estimates are available to date. Conducting mark recapture-based salvage efficiency estimates over contrasting turbidity conditions would help resolve this uncertainty.

Differences in AIC among PTMs were very large, which implies a high degree of certainty in identifying the best PTM of the ones that were examined, and hence the most reliable PEL estimate. This result is largely an artefact of our two-step modelling procedure where the PTM is used to calculate a movement exchange values, which are then treated as fixed parameters with no uncertainty in the population model. This strategy was necessary because the PTM simulation is much too slow to run in an optimization environment where thousands if not millions of iterations would be needed to jointly fit movement and population parameters. If PTM parameters were estimated there would likely be many alternate combinations that fit the data well, some of which could have very different PELs. This approach would lead to much larger PEL variance estimates and much smaller differences in AIC among alternate PTM structures. Limitations in data did not allow us to include process error in population model predictions which would also lead to underestimates of variance and AIC differences among models. Owing to these issues, the AIC results presented here should not be used to quantify the degree of statistical support for various levels of proportional entrainment loss. Instead they should be used as a tool to order alternative PTMs and population model structures and to understand sensitivities (e.g., limited effects of population model structure). This is a disappointing result as there can be large differences in PEL among some PTMs. The more complex and integrated structure in the Delta Smelt life cycle modelling work (Newman et al. 2014) addresses many of these limitations, but fitting this life cycle model has been problematic. Future modelling work could explore options for directly estimating movement parameters in an optimization environment. This could be achieved by limiting the number of spatial regions (Newman et al 2014), use of cloud computing, and developing more efficient ways of drawing parameters during optimization (Noble et al. 2017).

Estimating proportional entrainment loss of Delta Smelt is extremely challenging, and shares many of the problems in commercial fisheries stock assessments. There has been considerable work identifying limitations in stock assessments which therefore apply to understanding limitations in estimating PEL. Stock assessments largely rely on catch data from fisheries and sometimes fishery-independent surveys. These measures are equivalent to the observed salvage at fish collection facilities and SKT survey data, respectively. A central objective of stock assessments is to estimate an exploitation rate in a single year or an exploitation rate history. This is equivalent to the Delta science objectives of estimating PEL in particular years as we do here, or a historical time series of PEL as in Kimmerer (2008) or Smith et al., in prep.). One of the equations central to almost all stock assessments is:

$$C=q\cdot N$$

where C is the catch from a survey or fishery, N is the abundance, and q is the catchability. Rearranging this equation to solve for q it is easy to see that catchability represents the proportion of the population that is sampled. In other words, if q were known, then abundance can be estimated from catch. In the vast majority of stock assessment cases, q is not known, even for statistically designed fisheries-independent surveys (like the SKT survey). Thus catch data alone provides no information on abundance (Maunder and Piner 2014), though it may provide a useful index of relative changes in abundance over time and space if q doesn't vary too much. Historical PEL estimates (e.g., Kimmerer 2008) are based on a volumetric expansion of catch data from SKT surveys combined with a similar expansion of salvage,

$$PEL \approx \frac{salvage \cdot \theta_S^{-1}}{SKT\_catch \cdot \theta_{SKT}^{-1}}$$

In other words, PEL estimates assume that q (θ^{-1}) for both salvage and SKT surveys is known. Such catchability assumptions are not used in stock assessments, a field which is at times infamous for making assumptions that have led to some unfortunate collapses of major fisheries (Hilborn and Walters 1982). In our model, we use the same volumetric assumption to convert abundance to catch densities for fitting to the SKT data, but we allow the salvage expansions to freely vary to accommodate this assumption (similar to estimating q in stock assessments). If we decrease the volumetric expansion (e.g. assume Delta Smelt are distributed to 2 m rather than 4 m depth), the abundance estimated by the model will decline which will in turn lead to lower estimates for salvage expansion factor so that the scale of observed salvage is correctly predicted. Our PEL estimates therefore do not depend and are not sensitive to population expansion assumption directly. However, predictions of SKT catch are sensitive to the differences in volumetric expansions across regions, and our approach requires a perhaps equally uncertain assumption that some PTMs provide reliable estimates of the vulnerability to entrainment over space and time. So both ratio- and PTM-based PEL methods have issues. The two main advantages of the PTM approach are that: 1) predictions of movement and entrainment vulnerability can be checked against observations so we do not have to blindly trust the behavioral rules and movement predictions; and 2) it can be used to evaluate alternate future export and flow release strategies and other flow-related management actions. PTMs 8 and 9 were ranked as either the 1st- or 2nd-best model in 2002, 2004, and 2005 (2D simulations, 2011 excluded due to limitations in data). At this point, these are the best models to use to evaluate the relative benefits of alternate export regimes for reducing PEL of Delta Smelt.

A concerning aspect of our results is that different PTMs and population dynamic model structures fit the data best in different water years. For example PTM 8 fit the data best in water years 2002 and 2005 but PTM 10 fit the data best in water years 2004. There was strong evidence for turbidity effects on salvage efficiency in water years 2002 and 2004, but not in water year 2005. These differences could be driven by a number of factors including error in hydrodynamic and turbidity predictions, and error in movement behaviours. They suggest that the ability of existing PTMs to estimate proportional entrainment should be considered relatively poor. In the absence of identifying a model structure that fits the data well in different data years, it is impossible to identify the correct model to apply in future years for evaluating pumping alternatives.

Additional field work on expansion factors used for salvage and SKT data would increase certainty in identifying the best PTM and predictions of PEL. In our view, estimation of salvage efficiency from mark-recapture using cultured Delta Smelt should be an annual activity once the genetic plan for Delta Smelt is approved. A multi-year effort is required to provide ‘pre-screen’ loss estimates under contrasting environmental conditions, and in some cases using release locations further upstream from salvage facilities relative to experiments conducted to date. Note estimates of salvage expansions from these experiments would contribute to the evaluation of models applied in earlier years when there are sufficient numbers of Delta Smelt to evaluate the fit the model (e.g. some salvage and sufficient catch in SKT surveys). Determining the SKT population expansion factor and how it varies across regions and over time will remain a challenge. The Enhanced Delta Smelt Survey (EDSM) will improve the precision of the abundance index relative to the SKT survey and provide some data to verify or refute some aspects of the volumetric expansion assumptions. Currently, abundance estimates from EDSM are very imprecise owing to low abundance and extensive variability in the catch densities among stations (USFWS 2017). Additional years of data collection will however provide insight on depth distributions and how they change with physical covariates (turbidity) or offshore-onshore position. In our model, such data would provide more reliable conversions of regional abundance to catch for fitting to the SKT data. Future investments in salvage efficiency estimates would be very useful for sorting among alternate PTMs, and would therefore lead to more reliable predictions of the effects of export regimes on proportional entrainment loss. Improving understanding of salvage efficiency through mark-recapture experiments will take a number of years to achieve in order to capture the range in abiotic and biotic conditions that influence variability in pre-screen losses. Furthermore, even if this aspect of the model is improved, there will likely be continued uncertainty about the reliability of the SKT data to estimate population abundance. Thus managers should be aware that developing a reliable model for estimating proportional entrainment is a distant goal, and one that may be difficult to achieve.

Acknowledgements

Funding for this study was provided by the United States Bureau of Reclamation, State and Federal Contractors Water Agency, and the California Department of Water Resources through the Collaborative Science Adaptive Management Program. This study was done under the direction of CSAMP's Collaborative Adaptive Management Team (CAMT) and the Delta Smelt Scoping Team (DSST). We would like to thank Ken Newman, Leo Polansky, and William Smith for providing much of the data used in our analysis and for many insightful conversations over the course of this project. Our analysis relied heavily on long-term trawl and salvage datasets. We thank the many biologists and technicians working for California Department of Fish and Wildlife, the US Fish and Wildlife Service, and Bureau of Reclamation for the collection and maintenance of these data. We thank the DSST for providing comments on an earlier draft of this manuscript.

References

Ahrestani, F.S., Hebblewhite, M., and Post, E. 2013. The importance of observation versus process error in analyses of global ungulate populations. Scientific Reports 3:3125. DOI: 10.1038/srep03125.

Bennett W.A. 2005. Critical assessment of the Delta Smelt population in the San Francisco Estuary, California. San Francisco Estuary and Watershed Science. 3(2).

Bennett W.A, and Burau J.R. 2015. Riders on the storm: Selective tidal movements facilitate the spawning migration of threatened Delta Smelt in the San Francisco Estuary. Estuaries and Coasts 38: 826–835.

Brown, L.R., Kimmerer, W., and R. Brown. 2009. Managing water to protect fish: A review of California's environmental water account, 2001-2005. Environmental Management 43:357-368.

Burnham, K. P., and Anderson, D. R. 2002. Model selection and multimodel inference, 2nd edition. Springer-Verlag, New York.

Castillo, G., Morinaka, J., Lindberg, J., Fujimura, R., Baskerville-Bridges, B., Hobbs, J., ... & Ellison, L.(2012 . Pre-screen loss and fish facility efficiency for Delta Smelt at the south Delta's State Water Project, California. *San Francisco Estuary and Watershed Science, 10*(4).

Culberson, S.D., Harrison, C.B., Enright, C. and Nobriga, M.L. 2004. Sensitivity of larval fish transport to location, timing, and behavior using a particle tracking model in Suisun March, California.

Feyrer F, Nobriga M, Sommer T. 2007. Multi-decadal trends for three declining fish species: habitat patterns and mechanisms in the San Francisco Estuary, California, U.S.A. Canadian Journal of Fisheries and Aquatic Sciences 64: 723–734.

Fournier, D.A., H.J. Skaug, Ancheta, J., Ianelli, J., Magnusson, A., Maunder, M.N., Nielsen, A., and Sibert, J. 2011. AD Model Builder: using automatic differentiation for statistical inference of highly parameterized complex nonlinear models. Optimization Methods & Software. Available from http://admb-project.org/ [accessed 17 February 2012].

Ginetz, R. M., and Larkin, P.A. 1976. Factors affecting rainbow trout (*Salmogairdneri*) predation outmigrant fry of sockeye salmon (*Oncorhynchus nerka*). Journal of the Fisheries Research Board of Canada 33:19–24.

Gradall, K. S., and Swenson, W.A. 1982. Response of brook trout and creek chubs to turbidity. Transactions of the American Fisheries Society111:392–395.

Gregory, R. S., and Levings, C.D. 1998. Turbidity reduces predation on migrating juvenile Pacific salmon. Transactions of the American Fisheries Society 127:275–285.

Grimaldo, L., T. Sommer, N. Van Ark, G. Jones, E. Holland, P. Moyle, P. Smith, and Herbold,B. 2009. Factors affecting fish entrainment into massive water diversions in a freshwater tidal estuary: can fish losses be managed? North American Journal of Fisheries Management 29:1253-1270.

Guthrie, D. M., and Muntz, W.R.A. 1993. Role of vision in fish behaviour. Pages 89–121 *in* T. J. Pitcher, editor. in. Chapman and Hall, New York.

Hilborn, R., and Walters, C.J. 1992. Quantitative fisheries stock assessment. Chapman and Hall, New York, NY. 570 pp.

International Commission on Large Dams (ICOLD). Register of Dams— general synthesis. (2015). http://www.icold-cigb.net/GB/World_register/ general_synthesis.asp. Accessed 24 Nov 2016.

Johnson, J. D., and Hines, R.T. 1999. Effect of suspended sediment on vulnerability of young razorback suckers to predation. Transactions of the American Fisheries Society 128:648–655.

Kimmerer, W. J. 2004. Open water processes of the San Francisco Estuary: from physical forcing to biological responses. San Francisco Estuary and Watershed Science 2(1):1.

Kimmerer, W.J. 2008. Losses of Sacramento River chinook salmon and Delta Smelt to entrainment in water diversions in the Sacramento-San Joaquin Delta. San Francisco Estuary and Watershed Science 6(2)

Kimmerer, W.J. 2011. Modeling Delta Smelt losses at the South Delta export facilities. San Francisco Estuary and Watershed Science 9(1).

Korman, J, Yard, M.D., and Yackulic, C.B. 2016. Factors controlling the abundance of rainbow trout in the Colorado River in Grand Canyon in a reach utilized by endangered humpback chub. Canadian Journal of Fisheries and Aquatic Sciences. Sci. 73:105-124.

Korman, J., and Yard, M.D. 2017. Effects of environmental covariates and density on the catchability of fish populations and the interpretation of catch per unit effort trends. Fish. Res. 189:18-34.

Latour, R.J. 2015. Explaining patterns of pelagic fish abundance in the Sacramento-San Joaquin Delta. Estuaries and Coasts 39:233-247.

Mac Nally, R., J.R. Thomson, W.J. Kimmerer, F. Feyrer, K.B. Newman, A. Sih, W. A. Bennett, L. Brown, E. Fleishman, S. D. Culberson, and G. Castillo. 2010. Analysis of pelagic species decline in the upper San Francisco Estuary using multivariate autoregressive modeling (MAR). Ecological Applications 20:1417-1430.

Maunder, M.N., and Deriso, R.B. 2011. A state-space multistage life cycle model to evaluate population impacts n the presence of density dependence: illustrated with application to Delta Smelt (*Hyposmesus transpacificus*). Canadian Journal of Fisheries and Aquatic Sciences 68:1285-1306.

Maunder, M.N. and Piner, K.R. 2014. Contemporary fisheries stock assessment: many issues still remain. ICES Journal of Marine Science 72:7-18.

Miner, J. G., and Stein, R.A. 1996. Detection of predators and habitat choice by small bluegills: effects of turbidity and alternative prey. Transactions of the American Fisheries Society 125:97–103.

Miller, W.J. 2011. Revisiting assumptions that underlie estimates of proportional entrainment of Delta Smelt by State and Federal water diversions from the Sacramento-San Joaquin Delta. San Francisco Estuary and Watershed Science 9(1).

Newman, K.B., Polansky, L., Mitchell, L., Kimmerer, W., Smith, P., Baxter, R., Bennet, W., Mander, M., Nobriga, M., Meiring, W., Laca, E., and Feyrer, F. 2014. A Delta Smelt life cycle model. Draft reported prepared by USFWS Dec 17, 2014.

Newman, K., Polansky, L., and L. Mitchell. 2015. Adult Delta Smelt entrainment estimation and monitoring plan (draft May 24, 2015).

Noble, H., Jennings, E., Cirss, A., Danner, E., Sridharan, V., Greene, C.M., Imaki, H., and Lindley, S.T. 2017. Model description for the Sacramento River winter-run chinook salmon life cycle model.

Resource Management Associates [RMA]. 2014. Estimates of Delta Smelt Hatching Distribution, Abundance and Entrainment using Three-Dimensional Hydrodynamic and Particle Tracking Model Results. Report submitted to IEP.

Resource Management Associates [RMA]. 2018. Estimation of adult Delta Smelt distribution for hypothesized swimming behaviors using hydrodynamic, suspended sediment, and particle-tracking models. Report prepared by Resource Management Associates. 52 pp.

Rose KA, Kimmerer WJ, Edwards KP, Bennett WA. 2013. Individual-based modeling of Delta Smelt population dynamics in the upper San Francisco Estuary: I. Model description and baseline results. Transactions of the American Fisheries Society 142: 1238–1259.

Rytwinski, T, Algera, D.A., Taylor, J.J., Smokorowski, K.E., Bennett, J.R., Harrison, P.M., and Cooke, S.J. 2017. Water are the consequences of fish entrainment and impingement associated with hydroelectric dams on fish productivity? A systematic review protocol. Environmental Evidence 6:8

Sommer T, Mejia F, Nobriga M, Feyrer F, Grimaldo L. 2011. The Spawning Migration of Delta Smelt in the Upper San Francisco Estuary. San Francisco Estuary and Watershed Science 9(2), 16 pages.

Thomson, J.R., Kimmerer, W.J., Brown, L.R., Newman, K.B., Mac Nally, R., Bennett,W.A., Feyrer, F., and E. Fleishman. 2010. Bayesian change point analysis of abundance trends for pelagic fishes in the upper San Francisco Estuary. Ecological Applications 20 (5),1431–1448.

Wanger, O. W. 2007. Findings of fact and conclusions of law re interim remedies re: Delta Smelt ESA remand and reconsultation. Case 1: 05-cv-01207-OWW-GSA. Document 561. United States District Court, Eastern District of California, Fresno, California, USA.

Wanger, O. W. 2010. Memorandum decision re. Cross motions for summary judgment. Case 1: 09-cv-00407-OWW-DLB. Document 561. United States District Court, Eastern District of California, Fresno, California, USA.

Yackulic, C.B., Korman, J., Yard, M.D., and Dzul, M. 2017. Inferring species interactions through joint mark-recapture analysis. Ecology (*in press)*.

Yard, M.D., Coggins, L.G. Jr., Baxter, C.V., G.E. Bennett, and Korman, J. 2011. Trout piscivory in the Colorado River, Grand Canyon: Effects of turbidity, temperature, and fish prey availability. Transactions of the American Fisheries Society 140:471-486.

US Fish and Wildlife Service (USFWS). 2008. 2008 Biological Opinion for Delta Smelt. https://www.fws.gov/sfbaydelta/documents/SWP-CVP_OPs_BO_12-15_final_OCR.pdf

US Fish and Wildlife Service (USFWS). 2017. Enhanced Delta Smelt monitoring. Preliminary abundance analysis (draft), March 31, 2017. 22 pp.

Table 1. Start and end dates of particle tracking model (PTM) simulations in relation to the last dates associated with Spring Kodiak Trawl (SKT) surveys and salvage observations.

Water	PTM Runs			SKT Data (last survey date)			Salvage (last observation)	
Year	Start	End	Days	March	April	May	in a Sequence	Last in Spring
2002	Dec-05-01	Apr-17-02	134	Mar-07			Mar-24	Apr-25
2004	Dec-12-03	Apr-17-04	128	Mar-12	Apr-08	May-07	Mar-17	May-16
2005	Dec-14-04	Apr-29-05	137	Mar-25	Apr-21		Feb-16	Feb-16
2011	Dec-17-10	Apr-17-11	122	Mar-10	Apr-07	May-05	Apr-01	Apr-01

Table 2. Summary of particle tracking model behaviors. See RMA 2018 for additional details.

PTM #	Model Name	Behavior Summary
1	passive	Passive particles move with water parcels.
2	turbidity_seeking	Seek higher turbidity by orienting swimming direction to be along the turbidity gradient towards higher turbidity.
3	tmd	Uses water column depth gradients to choose direction of swimming. Nearshore swimming toward shallow water could lead to repeated swimming into the shoreline so passive behavior is specified nearshore.
4	ptmd_sal_gt_1	Tidal migration in brackish water.This behavior triggers tidal migration in brackish water. Once tidal migration behavior is triggered it will continue for 24 hours. At that time it may be triggered again depending on the salinity at the particle location.
5	ptmd_si_pt_5	Persistent tidal migration when the salinity the particle experiences as it moves through the estuary increases.
6	ptmd_si_pt_5_shallow_ebb_t_gt_12	Persistent tidal migration when the salinity the particle experiences as it moves through the estuary increases. Otherwise move to shallow water on ebb when in turbid water.
7	ptmd_sal_gt_1_si_pt_5	Persistent tidal migration in brackish water or if perceived salinity is increasing.
8	ptmd_sal_gt_1_h8_ebb_shallow_t_gt_18_acclim	Persistent tidal migration in brackish water. Moving to shallow water and holding on ebb if acclimated turbidity is higher than 18 NTU.
9	tmd_sal_gt_1_ebb_shallow_t_gt_18	Tidal migration in brackish water. Movement to shallow water during ebb in turbid water.
10	tmd_sal_gt_1_ptmd_prtmd_sd_pt_1_switch	Tidal migration in brackish water. Persistent tidal migration as long as the salinity experienced by a particle is decreasing. Change direction of tidal migration if the salinity experienced by a particle increases substantially.

Table 3. Ratio of Spring Kodiak Trawl (SKT) tow volume (vtow) in 2002 to the regional volume over which Delta Smelt are distributed over (assumed depth of 4 m, Vreg). The inverse of this ratio can be used to expand the total catch on a trip across stations in a region to calculate abundance (see Eqn. 5b). Tow volumes values used in the ratios below represents the average tow volume for reach region.

Region Name	Region Abbreviation	Efficiency (vtow/Vreg)	Expansion (vtow/Vreg)^-1
Napa River	napa	2.20E-04	4,570
Carquinez Strait	carq	7.20E-05	13,986
West Suisun Bay	wsuisb	1.50E-04	6,591
Mid Suisun Bay	msuisb	1.20E-04	8,429
Suisun Marsh	smarsh	6.20E-04	1,617
Chipps Island	chipps	2.00E-04	5,078
Sacramento River near Sherman Lake	sac_sherm	2.20E-04	4,452
Sacramento River near Rio Vista	sac_rio	2.50E-04	3,965
Cache slough and SDWSC	cache_dwsc	2.40E-04	4,188
Sacramento River and Steamboat Slough	sac_steam	5.50E-04	1,822
San Joaquin River near Antioch	sjr_ant	2.60E-04	3,874
Central Delta and Franks Tract	cdelta	1.80E-04	5,526
North and South Forks Mokelumne River	mok	6.60E-04	1,518
San Joaquin near Stockton	sjr_stk	2.70E-04	3,697
South Delta	sdelta	1.90E-04	5,283
Average		2.80E-04	4,973

Table 4. Comparison of models based on 10 different particle-tracking model (PTM) behaviours (rows, see Table 2) and structures in the population dynamic models (columns) by water year and PTM type (2D or 3D), assuming poisson error in SKT catch data (variance-to-mean ratio of τ=1) or negative binomial error (τ=10). The ΔAIC tables show the difference between each models AIC relative to the model with the lowest AIC among all PTMs and population model structures (thus model with ΔAIC=0 has the lowest AIC and is considered the best model). Dark grey and grey shaded cells identify models within 2, or 2-7 units of the best model, respectively. The model rank table shows the rank of each PTM within each population model type (column, rank 1= best model). Dark grey, grey, and light grey shaded cells identify the 1st-, 2nd-, and 3rd-ranked PTMs, respectively. The proportional entrainment table shows the most likely estimate of the total proportional entrainment loss across facilities. The SWP salvage expansion table shows the average salvage expansion factor over the simulation at the state facility. Blank cells occur for models that do not meet non-linear convergence criteria.

Table 4. Con't.

a) 3D WY 2002 Poisson error in SKT data (τ=1)

Population model number	1	2	3	4	5	6	7	8	9	10
Salvage efficiency structure	**const**	**const**	**const**	**const**	**~turb**	**~turb**	**~turb**	**~turb**	**const**	**~turb**
Natural survival structure	S_c	S_{SKT}	S_d	S_W	S_c	S_{SKT}	S_d	S_W	S_d	S_d
SKT efficiency structure ($\theta_{c\text{-}SKT}$)	=1	=1	=1	=1	=1	=1	=1	=1	**~Secchi**	**~Secch**
ΔAIC										
1) passive	1,847	1,851	1,829	1,829	859	863	845	845	1,789	782
2) turbidity_seeking	6,430	6,370	6,367	6,416	4,752	4,738	4,739	4,749	6,106	4,497
3) tmd	4,787	4,778	4,778	4,778	2,339	2,334	2,339	2,339	4,778	2,030
4) ptmd_sal_gt_1	1,776	1,578	1,580	1,722	713	618	632	695	1,573	625
5) ptmd_si_pt_5	1,561	1,346	1,350	1,493	542	425	437	511	1,304	380
6) ptmd_si_pt_5_shallow_ebb_t_gt_12	1,089	975	971	1,046	83	24	28	63	943	0
7) ptmd_sal_gt_1_si_pt_5	1,314	1,108	1,110	1,249	290	180	189	260	1,101	176
8) ptmd_sal_gt_1_h8_ebb_shallow_t_gt_18_acclim	1,855	1,855	1,846	1,846	294	297	290	290	1,805	249
9) tmd_sal_gt_1_ebb_shallow_t_gt_18	1,531	1,512	1,534	1,534	147	142	145	149	1,525	134
10) tmd_sal_gt_1_ptmd_prtmd_sd_pt_1_switch	1,395	1,246	1,252	1,359	184	115	119	167	1,227	92
Model Rank										
1) passive	7	7	7	7	8	8	8	8	7	8
2) turbidity_seeking	10	10	10	10	10	10	10	10	10	10
3) tmd	9	9	9	9	9	9	9	9	9	9
4) ptmd_sal_gt_1	6	6	6	6	7	7	7	7	6	7
5) ptmd_si_pt_5	5	4	4	4	6	6	6	6	4	6
6) ptmd_si_pt_5_shallow_ebb_t_gt_12	1	1	1	1	1	1	1	1	1	1
7) ptmd_sal_gt_1_si_pt_5	2	2	2	2	4	4	4	4	2	4
8) ptmd_sal_gt_1_h8_ebb_shallow_t_gt_18_acclim	8	8	8	8	5	5	5	5	8	5
9) tmd_sal_gt_1_ebb_shallow_t_gt_18	4	5	5	5	2	3	3	2	5	3
10) tmd_sal_gt_1_ptmd_prtmd_sd_pt_1_switch	3	3	3	3	3	2	2	3	3	2
Proportional Entrainment Loss										
1) passive	0.02	0.02	0.02	0.02	0.02	0.02	0.03	0.03	0.02	0.03
2) turbidity_seeking	0.08	0.08	0.08	0.08	0.07	0.07	0.07	0.07	0.03	0.04
3) tmd	0.35	0.35	0.35	0.35	0.34	0.34	0.34	0.34	0.35	0.38
4) ptmd_sal_gt_1	0.06	0.06	0.06	0.06	0.08	0.08	0.08	0.08	0.06	0.08
5) ptmd_si_pt_5	0.20	0.20	0.20	0.20	0.22	0.22	0.22	0.22	0.20	0.22
6) ptmd_si_pt_5_shallow_ebb_t_gt_12	0.34	0.34	0.34	0.34	0.35	0.35	0.35	0.35	0.34	0.35
7) ptmd_sal_gt_1_si_pt_5	0.24	0.24	0.24	0.24	0.26	0.26	0.25	0.26	0.24	0.26
8) ptmd_sal_gt_1_h8_ebb_shallow_t_gt_18_acclim	0.60	0.60	0.60	0.60	0.60	0.60	0.60	0.60	0.61	0.61
9) tmd_sal_gt_1_ebb_shallow_t_gt_18	0.48	0.48	0.48	0.48	0.49	0.49	0.49	0.49	0.49	0.49
10) tmd_sal_gt_1_ptmd_prtmd_sd_pt_1_switch	0.46	0.46	0.46	0.46	0.47	0.47	0.46	0.47	0.46	0.47
SWP Salvage Expansion Factor										
1) passive	104	104	103	103	266	266	262	262	120	340
2) turbidity_seeking	26	24	24	25	69	66	65	67	51	140
3) tmd	63	68	61	61	226	240	219	219	61	419
4) ptmd_sal_gt_1	13	11	12	13	39	33	33	38	337	58
5) ptmd_si_pt_5	59	47	49	56	143	110	114	134	64	179
6) ptmd_si_pt_5_shallow_ebb_t_gt_12	55	44	45	52	130	100	103	122	48	114
7) ptmd_sal_gt_1_si_pt_5	103	92	91	100	222	190	194	215	101	219
8) ptmd_sal_gt_1_h8_ebb_shallow_t_gt_18_acclim	271	276	267	267	708	714	694	694	312	817
9) tmd_sal_gt_1_ebb_shallow_t_gt_18	140	148	137	137	351	364	359	351	144	380
10) tmd_sal_gt_1_ptmd_prtmd_sd_pt_1_switch	137	116	115	132	311	253	261	298	131	300

Table 4. Con't.

b) 3D WY 2002 negative binomial error in SKT data (τ=10)

Population model number	**1**	**2**	**3**	**4**	**5**	**6**	**7**	**8**	**9**	**10**
Salvage efficiency structure	**const**	**const**	**const**	**const**	**~turb**	**~turb**	**~turb**	**~turb**	**const**	**~turb**
Natural survival structure	S_c	S_{SKT}	S_d	S_W	S_c	S_{SKT}	S_d	S_W	S_d	S_d
SKT efficiency structure ($\theta_{c\text{-}SKT}$)	=1	=1	=1	=1	=1	=1	=1	=1	**~Secchi**	**~Secchi**
ΔAIC										
1) passive	1,336	1,339	1,328	1,328	297	301	292	292	1,332	288
2) turbidity_seeking	5,961	5,758	5,938	5,907	4,432	4,428	4,495	4,432	5,876	4,361
3) tmd	3,463	3,467	3,448	3,448	974	978	970	970	3,399	973
4) ptmd_sal_gt_1	1,324	1,107	1,121	1,279	290	214	224	281	1,125	228
5) ptmd_si_pt_5	1,242	961	1,008	1,188	277	155	175	262	1,011	179
6) ptmd_si_pt_5_shallow_ebb_t_gt_12	1,011	834	887	981	41	0	1	35	885	1
7) ptmd_sal_gt_1_si_pt_5	1,235	953	1,000	1,183	270	143	165	255	1,003	169
8) ptmd_sal_gt_1_h8_ebb_shallow_t_gt_18_acclin	1,790	1,791	1,783	1,783	210	214	209	209	1,785	211
9) tmd_sal_gt_1_ebb_shallow_t_gt_18	1,569	1,496	1,546	1,570	177	177	175	176	1,548	179
10) tmd_sal_gt_1_ptmd_prtmd_sd_pt_1_switch	1,348	1,084	1,154	1,321	182	95	111	178	1,158	115
Model Rank										
1) passive	5	6	6	6	8	8	8	8	6	8
2) turbidity_seeking	10	10	10	10	10	10	10	10	10	10
3) tmd	9	9	9	9	9	9	9	9	9	9
4) ptmd_sal_gt_1	4	5	4	4	7	6	7	7	4	7
5) ptmd_si_pt_5	3	3	3	3	6	4	4	6	3	4
6) ptmd_si_pt_5_shallow_ebb_t_gt_12	1	1	1	1	1	1	1	1	1	1
7) ptmd_sal_gt_1_si_pt_5	2	2	2	2	5	3	3	5	2	3
8) ptmd_sal_gt_1_h8_ebb_shallow_t_gt_18_acclin	8	8	8	8	4	7	6	4	8	6
9) tmd_sal_gt_1_ebb_shallow_t_gt_18	7	7	7	7	2	5	5	2	7	5
10) tmd_sal_gt_1_ptmd_prtmd_sd_pt_1_switch	6	4	5	5	3	2	2	3	5	2
Proportional Entrainment Loss										
1) passive	0.02	0.02	0.02	0.02	0.03	0.03	0.03	0.03	0.02	0.03
2) turbidity_seeking	0.02	0.02	0.02	0.02	0.04	0.04	0.06	0.04	0.02	0.03
3) tmd	0.39	0.39	0.39	0.39	0.38	0.38	0.38	0.38	0.40	0.38
4) ptmd_sal_gt_1	0.06	0.06	0.06	0.06	0.08	0.07	0.07	0.08	0.06	0.07
5) ptmd_si_pt_5	0.19	0.19	0.18	0.19	0.21	0.21	0.21	0.21	0.18	0.21
6) ptmd_si_pt_5_shallow_ebb_t_gt_12	0.35	0.35	0.34	0.35	0.36	0.36	0.36	0.36	0.34	0.36
7) ptmd_sal_gt_1_si_pt_5	0.24	0.24	0.23	0.24	0.26	0.26	0.25	0.26	0.23	0.25
8) ptmd_sal_gt_1_h8_ebb_shallow_t_gt_18_acclin	0.60	0.59	0.60	0.60	0.59	0.59	0.59	0.59	0.60	0.59
9) tmd_sal_gt_1_ebb_shallow_t_gt_18	0.48	0.46	0.47	0.48	0.49	0.48	0.49	0.49	0.47	0.49
10) tmd sal gt 1 ptmd prtmd sd pt 1 switch	0.49	0.48	0.47	0.48	0.49	0.49	0.48	0.49	0.47	0.48
SWP Salvage Expansion Factor										
1) passive	57	57	57	57	137	137	135	135	57	186
2) turbidity seeking	8	5	7	7	53	45	61	51	49	135
3) tmd	50	50	48	48	188	188	184	184	97	185
4) ptmd sal gt 1	10	9	9	10	27	23	24	26	316	24
5) ptmd si pt 5	39	31	32	38	93	67	72	87	808	72
6) ptmd si pt 5 shallow ebb t gt 12	46	36	37	44	106	74	80	98	959	81
7) ptmd sal gt 1 si pt 5	91	87	82	88	195	162	166	186	94	177
8) ptmd sal gt 1 h8 ebb shallow t gt 18 acclin	219	231	215	215	570	570	556	556	241	561
9) tmd sal gt 1 ebb shallow t gt 18	118	141	131	120	297	306	296	310	156	324
10) tmd sal gt 1 ptmd prtmd sd pt 1 switch	135	115	113	130	302	217	238	284	>1000	247

Table 4. Con't.

c) 2D WY 2002 Poisson error in SKT data (τ=1)

Population model number	**1**	**2**	**3**	**4**	**5**	**6**	**7**	**8**	**9**	**10**
Salvage efficiency structure	**const**	**const**	**const**	**const**	**~turb**	**~turb**	**~turb**	**~turb**	**const**	**~turb**
Natural survival structure	S_c	S_{SKT}	S_d	S_W	S_c	S_{SKT}	S_d	S_W	S_d	S_d
SKT efficiency structure ($\theta_{c\text{-}SKT}$)	=1	=1	=1	=1	=1	=1	=1	=1	~Secchi	~Secchi
ΔAIC										
1) passive	1,509	1,513	1,498	1,498	652	656	642	642	1,471	609
2) turbidity seeking	49,649	49,653	49,635	49,635	49,642	49,646	49,629	49,629	49,392	49,387
3) tmd	2,426	2,381	2,389	2,425	1,082	1,069	1,092	1,082	2,267	945
4) ptmd sal gt 1	2,383	2,109	2,107	2,296	1,364	1,217	1,230	1,325	1,863	989
5) ptmd si pt 5	2,643	2,341	2,374	2,590	1,000	843	877	976	2,199	711
6) ptmd si pt 5 shallow ebb t gt 12	1,694	1,557	1,564	1,644	507	453	446	482	1,510	386
7) ptmd sal gt 1 si pt 5	2,544	2,249	2,282	2,493	997	841	874	973	2,124	721
8) ptmd sal gt 1 h8 ebb shallow t gt 18 acclim	958	922	933	934	45	27	38	37	895	0
9) tmd sal gt 1 ebb shallow t gt 18	1,556	1,479	1,553	1,549	370	351	372	360	1,535	334
10) tmd sal gt 1 ptmd prtmd sd pt 1 switch	1,387	1,346	1,381	1,386	508	495	509	507	1,197	321
Model Rank										
1) passive	3	4	3	3	5	5	5	5	3	5
2) turbidity seeking	10	10	10	10	10	10	10	10	10	10
3) tmd	7	9	9	7	8	8	8	8	9	8
4) ptmd_sal_gt_1	6	6	6	6	9	9	9	9	6	9
5) ptmd si pt 5	9	8	8	9	7	7	7	7	8	6
6) ptmd si pt 5 shallow ebb t gt 12	5	5	5	5	3	3	3	3	4	4
7) ptmd sal gt 1 si pt 5	8	7	7	8	6	6	6	6	7	7
8) ptmd sal gt 1 h8 ebb shallow t gt 18 acclim	1	1	1	1	1	1	1	1	1	1
9) tmd sal gt 1 ebb shallow t gt 18	4	3	4	4	2	2	2	2	5	3
10) tmd sal gt 1 ptmd prtmd sd pt 1 switch	2	2	2	2	4	4	4	4	2	2
Proportional Entrainment Loss										
1) passive	0 02	0 02	0 02	0 02	0 03	0 03	0 03	0 03	0 03	0 03
2) turbidity_seeking	0 00	0 00	0 00	0 00	0 00	0 00	0 00	0 00	0 00	0 00
3) tmd	0 37	0 36	0 36	0 37	0 36	0 36	0 36	0 36	0 38	0 38
4) ptmd sal gt 1	0 06	0 05	0 05	0 05	0 06	0 06	0 06	0 06	0 05	0 06
5) ptmd si pt 5	0 22	0 22	0 21	0 22	0 25	0 24	0 24	0 25	0 21	0 24
6) ptmd si pt 5 shallow ebb t gt 12	0 35	0 35	0 35	0 35	0 36	0 36	0 35	0 35	0 35	0 36
7) ptmd_sal_gt_1_si_pt_5	0 23	0 22	0 22	0 22	0 25	0 24	0 24	0 24	0 22	0 24
8) ptmd sal gt 1 h8 ebb shallow t gt 18 acclim	0 36	0 36	0 36	0 35	0 37	0 36	0 37	0 37	0 36	0 37
9) tmd sal gt 1 ebb shallow t gt 18	0 35	0 35	0 35	0 35	0 37	0 36	0 36	0 36	0 35	0 36
10) tmd sal gt 1 ptmd prtmd sd pt 1 switch	0 47	0 47	0 47	0 47	0 47	0 47	0 48	0 47	0 49	0 49
SWP Salvage Expansion Factor										
1) passive	101	102	100	100	218	218	214	214	114	254
2) turbidity seeking	5	5	5	5	6	6	6	6	36	42
3) tmd	60	65	63	61	149	149	137	151	85	198
4) ptmd sal gt 1	24	19	19	22	59	45	45	54	291	756
5) ptmd_si_pt_5	70	64	66	71	215	183	189	212	>1000	>1000
6) ptmd si pt 5 shallow ebb t gt 12	107	96	92	103	250	211	210	238	112	266
7) ptmd sal gt 1 si pt 5	68	63	65	69	194	166	172	192	>1000	>1000
8) ptmd sal gt 1 h8 ebb shallow t gt 18 acclim	87	86	81	85	178	207	167	175	89	185
9) tmd sal gt 1 ebb shallow t gt 18	106	100	105	105	255	320	256	249	110	297
10) tmd_sal_gt_1_ptmd_prtmd_sd_pt_1_switch	130	129	128	129	243	288	234	242	171	396

Table 4. Con't.

d) 2D WY 2002 negative binomial error in SKT data (τ=10)

Population model number	**1**	**2**	**3**	**4**	**5**	**6**	**7**	**8**	**9**	**10**
Salvage efficiency structure	**const**	**const**	**const**	**const**	**~turb**	**~turb**	**~turb**	**~turb**	**const**	**~turb**
Natural survival structure	S_c	S_{SKT}	S_d	S_W	S_c	S_{SKT}	S_d	S_W	S_d	S_d
SKT efficiency structure ($\theta_{c\text{-}SKT}$)	**=1**	**=1**	**=1**	**=1**	**=1**	**=1**	**=1**	**=1**	**~Secchi**	**~Secchi**
ΔAIC										
1) passive	1,102	1,106	1,095	1,095	232	236	226	226	1,094	224
2) turbidity seeking	47,530	47,534	47,531	47,531	47,514	47,511	47,516	47,515	47,533	47,520
3) tmd	1,795	1,727	1,786	1,794	384	386	384	382	1,767	365
4) ptmd sal gt 1	1,315	1,075	1,075	1,251	294	215	216	279	1,073	220
5) ptmd si pt 5	2,062	1,788	1,819	2,026	430	322	340	393	1,819	344
6) ptmd si pt 5 shallow ebb t gt 12	1,298	1,040	1,156	1,267	125	89	87	119	1,144	79
7) ptmd sal gt 1 si pt 5	1,993	1,725	1,754	1,958	452	345	362	443	1,755	366
8) ptmd sal gt 1 h8 ebb shallow t gt 18 acclim	882	681	864	869	16	0	15	17	867	14
9) tmd sal gt 1 ebb shallow t gt 18	1,164	797	1,152	1,130	73	32	69	71	1,150	70
10) tmd sal gt 1 ptmd prtmd sd pt 1 switch	893	712	880	831	70	57	70	61	869	57
Model Rank										
1) passive	3	6	4	3	5	6	6	5	4	6
2) turbidity seeking	10	10	10	10	10	10	10	10	10	10
3) tmd	7	8	8	7	7	9	9	7	8	8
4) ptmd_sal_gt_1	6	5	3	5	6	5	5	6	3	5
5) ptmd_si_pt_5	9	9	9	9	8	7	7	8	9	7
6) ptmd_si_pt_5_shallow_ebb_t_gt_12	5	4	6	6	4	4	4	4	5	4
7) ptmd_sal_gt_1_si_pt_5	8	7	7	8	9	8	8	9	7	9
8) ptmd sal gt 1 h8 ebb shallow t gt 18 acclim	1	1	1	2	1	1	1	1	1	1
9) tmd sal gt 1 ebb shallow t gt 18	4	3	5	4	3	2	2	3	6	3
10) tmd sal gt 1 ptmd prtmd sd pt 1 switch	2	2	2	1	2	3	3	2	2	2
Proportional Entrainment Loss										
1) passive	0 03	0 03	0 03	0 03	0 03	0 03	0 03	0 03	0 03	0 03
2) turbidity seeking	0 00	0 00	0 00	0 00	0 00	0 00	0 00	0 00	0 00	0 00
3) tmd	0 41	0 40	0 41	0 41	0 40	0 40	0 40	0 40	0 41	0 40
4) ptmd sal gt 1	0 06	0 05	0 05	0 05	0 07	0 07	0 06	0 07	0 05	0 06
5) ptmd si pt 5	0 23	0 21	0 21	0 22	0 25	0 24	0 24	0 24	0 21	0 24
6) ptmd si pt 5 shallow ebb t gt 12	0 39	0 38	0 38	0 38	0 39	0 39	0 39	0 39	0 37	0 39
7) ptmd sal gt 1 si pt 5	0 23	0 22	0 21	0 22	0 25	0 24	0 24	0 24	0 21	0 24
8) ptmd sal gt 1 h8 ebb shallow t gt 18 acclim	0 34	0 34	0 34	0 34	0 37	0 37	0 36	0 37	0 34	0 36
9) tmd sal gt 1 ebb shallow t gt 18	0 33	0 33	0 33	0 34	0 36	0 36	0 36	0 36	0 33	0 36
10) tmd sal gt 1 ptmd prtmd sd pt 1 switch	0 50	0 50	0 51	0 50	0 51	0 51	0 51	0 51	0 51	0 51
SWP Salvage Expansion Factor										
1) passive	78	78	76	76	163	163	160	160	96	206
2) turbidity seeking	2	2	2	2	4	4	4	4	38	4
3) tmd	48	66	55	47	109	116	105	117	84	183
4) ptmd_sal_gt_1	12	10	10	11	26	23	23	25	270	23
5) ptmd_si_pt_5	40	41	42	42	111	105	107	131	>1000	107
6) ptmd_si_pt_5_shallow_ebb_t_gt_12	82	76	71	79	186	155	154	175	96	193
7) ptmd_sal_gt_1_si_pt_5	40	40	41	41	104	98	101	104	>1000	101
8) ptmd_sal_gt_1_h8_ebb_shallow_t_gt_18_acclim	75	71	74	74	154	139	162	151	76	181
9) tmd sal gt 1 ebb shallow t gt 18	82	63	82	82	199	151	211	203	105	214
10) tmd sal gt 1 ptmd prtmd sd pt 1 switch	118	122	117	124	214	197	222	219	151	301

Table 4. Con't.

e) 2D WY 2004 Poisson error in SKT data (τ=1)

Population model number	**1**	**2**	**3**	**4**	**5**	**6**	**7**	**8**	**9**	**10**
Salvage efficiency structure	**const**	**const**	**const**	**const**	**~turb**	**~turb**	**~turb**	**~turb**	**const**	**~turb**
Natural survival structure	S_c	S_{SKT}	S_d	S_W	S_c	S_{SKT}	S_d	S_W	S_d	S_d
SKT efficiency structure ($\theta_{c\text{-}SKT}$)	**=1**	**=1**	**=1**	**=1**	**=1**	**=1**	**=1**	**=1**	**~Secchi**	**~Secchi**
ΔAIC										
1) passive	4,390	4,382	4,325	4,325	3,025	3,008	2,974	2,974	4,127	2,770
2) turbidity seeking	53,542	53,548	53,517	53,517	52,894	52,900	52,881	52,881	53,341	52,684
3) tmd	1,812	1,698	1,811	1,806	1,088	997	1,013	1,043	1,528	830
4) ptmd sal gt 1	4,909	4,913	4,846	4,846	3,451	3,455	3,397	3,397	4,736	3,290
5) ptmd si pt 5	4,346	4,331	4,290	4,290	3,037	3,023	2,996	2,996	4,126	2,842
6) ptmd si pt 5 shallow ebb t gt 12	1,392	1,301	1,384	1,384	722	649	717	717	1,205	539
7) ptmd sal gt 1 si pt 5	4,430	4,418	4,373	4,373	3,146	3,135	3,104	3,104	4,214	2,955
8) ptmd sal gt 1 h8 ebb shallow t gt 18 acclim	1,103	934	1,073	1,095	594	439	586	598	745	220
9) tmd sal gt 1 ebb shallow t gt 18	1,414	1,351	1,411	1,411	538	485	533	533	1,086	211
10) tmd sal gt 1 ptmd prtmd sd pt 1 switch	771	689	770	770	222	154	227	211	542	0
Model Rank										
1) passive	7	7	7	7	6	6	6	6	7	6
2) turbidity seeking	10	10	10	10	10	10	10	10	10	10
3) tmd	5	5	5	5	5	5	5	5	5	5
4) ptmd sal gt 1	9	9	9	9	9	9	9	9	9	9
5) ptmd si pt 5	6	6	6	6	7	7	7	7	6	7
6) ptmd si pt 5 shallow ebb t gt 12	3	3	3	3	4	4	4	4	4	4
7) ptmd sal gt 1 si pt 5	8	8	8	8	8	8	8	8	8	8
8) ptmd sal gt 1 h8 ebb shallow t gt 18 acclim	2	2	2	2	3	2	3	3	2	3
9) tmd sal gt 1 ebb shallow t gt 18	4	4	4	4	2	3	2	2	3	2
10) tmd sal gt 1 ptmd prtmd sd pt 1 switch	1	1	1	1	1	1	1	1	1	1
Proportional Entrainment Loss										
1) passive	0 03	0 03	0 03	0 03	0 06	0 06	0 06	0 06	0 03	0 06
2) turbidity seeking	0 02	0 02	0 02	0 02	0 04	0 04	0 04	0 04	0 04	0 04
3) tmd	0 43	0 42	0 43	0 42	0 41	0 41	0 40	0 40	0 41	0 40
4) ptmd_sal_gt_1	0 05	0 05	0 05	0 05	0 10	0 10	0 10	0 10	0 05	0 10
5) ptmd si pt 5	0 18	0 18	0 18	0 18	0 30	0 30	0 30	0 30	0 18	0 30
6) ptmd si pt 5 shallow ebb t gt 12	0 20	0 19	0 20	0 20	0 20	0 19	0 20	0 20	0 19	0 19
7) ptmd sal gt 1 si pt 5	0 22	0 22	0 22	0 22	0 35	0 36	0 35	0 35	0 22	0 35
8) ptmd sal gt 1 h8 ebb shallow t gt 18 acclim	0 29	0 28	0 27	0 30	0 27	0 26	0 28	0 25	0 26	0 24
9) tmd_sal_gt_1_ebb_shallow_t_gt_18	0 37	0 36	0 37	0 37	0 36	0 36	0 37	0 37	0 36	0 35
10) tmd sal gt 1 ptmd prtmd sd pt 1 switch	0 50	0 49	0 51	0 51	0 50	0 49	0 50	0 49	0 49	0 49
SWP Salvage Expansion Factor										
1) passive	96	96	96	96	462	473	447	447	89	426
2) turbidity_seeking	2	2	2	2	>1000	>1000	>1000	>1000	6	>1000
3) tmd	52	57	51	55	87	89	94	93	57	90
4) ptmd sal gt 1	9	9	9	9	96	97	92	92	9	95
5) ptmd si pt 5	25	27	25	25	180	191	170	170	28	184
6) ptmd si pt 5 shallow ebb t gt 12	33	35	33	32	50	54	50	50	34	52
7) ptmd_sal_gt_1_si_pt_5	30	32	29	29	201	213	190	190	33	204
8) ptmd sal gt 1 h8 ebb shallow t gt 18 acclim	33	36	35	32	42	47	42	43	37	49
9) tmd sal gt 1 ebb shallow t gt 18	54	59	54	54	88	94	87	87	68	109
10) tmd sal gt 1 ptmd prtmd sd pt 1 switch	71	74	71	71	100	105	100	102	77	109

Table 4. Con't.

f) 2D WY 2004 negative binomial error in SKT data (τ=10)

Population model number	1	2	3	4	5	6	7	8	9	10
Salvage efficiency structure	const	const	const	const	~turb	~turb	~turb	~turb	const	~turb
Natural survival structure	S_c	S_{SKT}	S_d	S_W	S_c	S_{SKT}	S_d	S_W	S_d	S_d
SKT efficiency structure ($\theta_{c\text{-}SKT}$)	=1	=1	=1	=1	=1	=1	=1	=1	~Secchi	~Secchi
ΔAIC										
1) passive	3,544	3,550	3,479	3,479	1,922	1,928	1,867	1,867	3,447	1,871
2) turbidity seeking	48,211	48,217	48,197	48,197	47,538	47,535	47,538	47,538	48,196	47,538
3) tmd	1,320	1,273	1,302	1,302	319	320	312	312	1,271	316
4) ptmd sal gt 1	3,338	3,344	3,275	3,275	1,758	1,764	1,705	1,705	3,267	1,706
5) ptmd si pt 5	3,394	3,400	3,328	3,328	1,933	1,939	1,881	1,881	3,314	1,885
6) ptmd si pt 5 shallow ebb t gt 12	1,290	1,275	1,271	1,271	389	394	368	368	1,250	370
7) ptmd sal gt 1 si pt 5	3,559	3,565	3,493	3,493	2,124	2,130	2,071	2,071	3,479	2,074
8) ptmd sal gt 1 h8 ebb shallow t gt 18 acclim	1,194	1,174	1,173	1,173	402	406	385	385	1,136	580
9) tmd sal gt 1 ebb shallow t gt 18	1,065	1,069	1,053	1,053	19	25	1	1	1,010	0
10) tmd sal gt 1 ptmd prtmd sd pt 1 switch	672	668	663	663	111	115	106	106	652	98
Model Rank										
1) passive	8	8	8	8	7	7	7	7	8	7
2) turbidity seeking	10	10	10	10	10	10	10	10	10	10
3) tmd	5	4	5	5	3	3	3	3	5	3
4) ptmd_sal_gt_1	6	6	6	6	6	6	6	6	6	6
5) ptmd_si_pt_5	7	7	7	7	8	8	8	8	7	8
6) ptmd_si_pt_5_shallow_ebb_t_gt_12	4	5	4	4	4	4	4	4	4	4
7) ptmd_sal_gt_1_si_pt_5	9	9	9	9	9	9	9	9	9	9
8) ptmd sal gt 1 h8 ebb shallow t gt 18 acclim	3	3	3	3	5	5	5	5	3	5
9) tmd sal gt 1 ebb shallow t gt 18	2	2	2	2	1	1	1	1	2	1
10) tmd sal gt 1 ptmd prtmd sd pt 1 switch	1	1	1	1	2	2	2	2	1	2
Proportional Entrainment Loss										
1) passive	0 03	0 03	0 03	0 03	0 10	0 10	0 10	0 10	0 03	0 10
2) turbidity seeking	0 02	0 02	0 02	0 02	0 06	0 07	0 06	0 06	0 02	0 06
3) tmd	0 30	0 21	0 31	0 31	0 33	0 32	0 33	0 33	0 29	0 33
4) ptmd sal gt 1	0 04	0 04	0 04	0 04	0 10	0 10	0 10	0 10	0 04	0 10
5) ptmd si pt 5	0 18	0 18	0 18	0 18	0 31	0 31	0 31	0 31	0 18	0 31
6) ptmd si pt 5 shallow ebb t gt 12	0 18	0 17	0 18	0 18	0 14	0 14	0 14	0 14	0 18	0 14
7) ptmd sal gt 1 si pt 5	0 22	0 22	0 22	0 22	0 37	0 37	0 37	0 37	0 22	0 36
8) ptmd sal gt 1 h8 ebb shallow t gt 18 acclim	0 22	0 22	0 23	0 23	0 14	0 14	0 14	0 14	0 22	0 20
9) tmd sal gt 1 ebb shallow t gt 18	0 25	0 25	0 26	0 26	0 18	0 18	0 18	0 18	0 25	0 18
10) tmd sal gt 1 ptmd prtmd sd pt 1 switch	0 52	0 52	0 52	0 52	0 52	0 52	0 52	0 52	0 52	0 52
SWP Salvage Expansion Factor										
1) passive	19	19	18	18	169	169	167	167	40	167
2) turbidity seeking	1	1	1	1	>1000	>1000	>1000	>1000	19	>1000
3) tmd	12	8	12	12	>1000	>1000	>1000	>1000	22	>1000
4) ptmd_sal_gt_1	4	4	4	4	115	115	113	113	241	112
5) ptmd_si_pt_5	15	15	14	14	100	100	98	98	18	98
6) ptmd_si_pt_5_shallow_ebb_t_gt_12	12	13	12	12	146	147	152	152	31	151
7) ptmd_sal_gt_1_si_pt_5	17	17	16	16	100	100	97	97	20	97
8) ptmd_sal_gt_1_h8_ebb_shallow_t_gt_18_acclim	14	16	13	13	53	54	51	51	23	24
9) tmd sal gt 1 ebb shallow t gt 18	17	18	17	17	22	22	23	23	31	23
10) tmd sal gt 1 ptmd prtmd sd pt 1 switch	43	46	43	43	57	59	56	56	54	72

Table 4. Con't.

g) 2D WY 2005 Poisson error in SKT data (τ=1)

Population model number	**1**	**2**	**3**	**4**	**5**	**6**	**7**	**8**	**9**	**10**
Salvage efficiency structure	**const**	**const**	**const**	**const**	**~turb**	**~turb**	**~turb**	**~turb**	**const**	**~turb**
Natural survival structure	S_c	S_{SKT}	S_d	S_W	S_c	S_{SKT}	S_d	S_W	S_d	S_d
SKT efficiency structure ($\theta_{c\text{-}SKT}$)	**=1**	**=1**	**=1**	**=1**	**=1**	**=1**	**=1**	**=1**	**~Secchi**	**~Secchi**
ΔAIC										
1) passive	1,164	947	1,192	1,056	1,131	920	1,164	1,023	1,134	932
2) turbidity seeking	14,979	14,982	14,978	14,978	14,983	14,986	14,982	14,982	14,682	14,686
3) tmd	804	731	784	780	650	546	602	578	722	557
4) ptmd sal gt 1	1,071	886	938	968	1,047	867	918	945	898	877
5) ptmd si pt 5	919	714	792	810	899	699	776	791	793	777
6) ptmd si pt 5 shallow ebb t gt 12	468	293	360	351	461	281	350	343	205	196
7) ptmd sal gt 1 si pt 5	875	670	749	766	859	657	735	750	751	738
8) ptmd sal gt 1 h8 ebb shallow t gt 18 acclim	153	11	71	51	153	14	73	53	0	2
9) tmd sal gt 1 ebb shallow t gt 18	261	198	227	215	190	95	134	121	119	34
10) tmd sal gt 1 ptmd prtmd sd pt 1 switch	318	220	271	252	271	146	205	183	175	122
Model Rank										
1) passive	9	9	9	9	9	9	9	9	9	9
2) turbidity seeking	10	10	10	10	10	10	10	10	10	10
3) tmd	5	7	6	6	5	5	5	5	5	5
4) ptmd_sal_gt_1	8	8	8	8	8	8	8	8	8	8
5) ptmd si pt 5	7	6	7	7	7	7	7	7	7	7
6) ptmd si pt 5 shallow ebb t gt 12	4	4	4	4	4	4	4	4	4	4
7) ptmd sal gt 1 si pt 5	6	5	5	5	6	6	6	6	6	6
8) ptmd sal gt 1 h8 ebb shallow t gt 18 acclim	1	1	1	1	1	1	1	1	1	1
9) tmd sal gt 1 ebb shallow t gt 18	2	2	2	2	2	2	2	2	2	2
10) tmd sal gt 1 ptmd prtmd sd pt 1 switch	3	3	3	3	3	3	3	3	3	3
Proportional Entrainment Loss										
1) passive	0 06	0 06	0 06	0 06	0 06	0 06	0 06	0 06	0 10	0 10
2) turbidity_seeking	0 00	0 00	0 00	0 00	0 00	0 00	0 00	0 00	0 01	0 01
3) tmd	0 16	0 15	0 16	0 16	0 17	0 16	0 16	0 16	0 19	0 18
4) ptmd sal gt 1	0 09	0 09	0 09	0 09	0 09	0 09	0 09	0 09	0 10	0 11
5) ptmd si pt 5	0 15	0 15	0 15	0 15	0 15	0 15	0 15	0 15	0 15	0 16
6) ptmd si pt 5 shallow ebb t gt 12	0 09	0 10	0 10	0 10	0 10	0 10	0 10	0 10	0 12	0 12
7) ptmd_sal_gt_1_si_pt_5	0 16	0 16	0 16	0 16	0 16	0 16	0 16	0 16	0 16	0 16
8) ptmd sal gt 1 h8 ebb shallow t gt 18 acclim	0 14	0 16	0 15	0 15	0 15	0 16	0 15	0 15	0 17	0 17
9) tmd sal gt 1 ebb shallow t gt 18	0 15	0 15	0 15	0 15	0 15	0 15	0 15	0 15	0 15	0 16
10) tmd sal gt 1 ptmd prtmd sd pt 1 switch	0 30	0 30	0 30	0 30	0 29	0 30	0 29	0 29	0 31	0 31
SWP Salvage Expansion Factor										
1) passive	116	133	81	145	134	144	89	162	>1000	>1000
2) turbidity seeking	>1000	>1000	>1000	>1000	>1000	>1000	>1000	>1000	>1000	>1000
3) tmd	45	38	42	41	64	62	62	64	764	>1000
4) ptmd sal gt 1	41	47	46	52	50	53	52	61	>1000	>1000
5) ptmd_si_pt_5	57	65	62	72	62	67	64	76	>1000	>1000
6) ptmd si pt 5 shallow ebb t gt 12	59	55	54	60	61	57	56	62	>1000	>1000
7) ptmd sal gt 1 si pt 5	58	65	62	73	63	68	65	76	>1000	>1000
8) ptmd sal gt 1 h8 ebb shallow t gt 18 acclim	83	75	76	80	87	75	77	81	>1000	>1000
9) tmd sal gt 1 ebb shallow t gt 18	72	68	69	69	81	86	82	84	>1000	>1000
10) tmd_sal_gt_1_ptmd_prtmd_sd_pt_1_switch	116	105	108	107	125	123	121	123	>1000	>1000

Table 4. Con't.

h) 2D WY 2005 negative binomial error in SKT data (τ=10)

Population model number	1	2	3	4	5	6	7	8	9	10
Salvage efficiency structure	const	const	const	const	~turb	~turb	~turb	~turb	const	~turb
Natural survival structure	S_c	S_{SKT}	S_d	S_W	S_c	S_{SKT}	S_d	S_W	S_d	S_d
SKT efficiency structure ($\theta_{c\text{-}SKT}$)	=1	=1	=1	=1	=1	=1	=1	=1	~Secchi	~Secchi
ΔAIC										
1) passive	764	765	758	758	734	736	729	729	755	726
2) turbidity seeking	14,285	14,291	14,286	14,286	14,289	14,295	14,290	14,290	14,285	14,293
3) tmd	606	409	604	607	445	355	431	427	607	435
4) ptmd sal gt 1	747	744	742	742	727	724	722	722	746	726
5) ptmd si pt 5	727	717	723	723	711	701	707	707	720	704
6) ptmd si pt 5 shallow ebb t gt 12	294	258	274	280	274	248	261	268	276	262
7) ptmd sal gt 1 si pt 5	686	675	682	682	672	662	668	668	677	664
8) ptmd sal gt 1 h8 ebb shallow t gt 18 acclim	64	37	47	48	66	39	75	50	51	49
9) tmd sal gt 1 ebb shallow t gt 18	123	39	121	123	34	0	27	26	124	28
10) tmd sal gt 1 ptmd prtmd sd pt 1 switch	195	112	183	182	143	91	126	122	183	126
Model Rank										
1) passive	9	9	9	9	9	9	9	9	9	8
2) turbidity seeking	10	10	10	10	10	10	10	10	10	10
3) tmd	5	5	5	5	5	5	5	5	5	5
4) ptmd_sal_gt_1	8	8	8	8	8	8	8	8	8	9
5) ptmd_si_pt_5	7	7	7	7	7	7	7	7	7	7
6) ptmd_si_pt_5_shallow_ebb_t_gt_12	4	4	4	4	4	4	4	4	4	4
7) ptmd_sal_gt_1_si_pt_5	6	6	6	6	6	6	6	6	6	6
8) ptmd_sal_gt_1_h8_ebb_shallow_t_gt_18_acclim	1	1	1	1	2	2	2	2	1	2
9) tmd sal gt 1 ebb shallow t gt 18	2	2	2	2	1	1	1	1	2	1
10) tmd sal gt 1 ptmd prtmd sd pt 1 switch	3	3	3	3	3	3	3	3	3	3
Proportional Entrainment Loss										
1) passive	0 10	0 09	0 10	0 10	0 10	0 10	0 10	0 10	0 10	0 11
2) turbidity seeking	0 01	0 01	0 01	0 01	0 01	0 01	0 01	0 01	0 01	0 01
3) tmd	0 12	0 12	0 12	0 12	0 11	0 12	0 11	0 10	0 12	0 11
4) ptmd sal gt 1	0 09	0 09	0 09	0 09	0 10	0 10	0 10	0 10	0 09	0 10
5) ptmd si pt 5	0 15	0 15	0 15	0 15	0 15	0 15	0 15	0 15	0 15	0 15
6) ptmd si pt 5 shallow ebb t gt 12	0 14	0 14	0 14	0 14	0 14	0 14	0 14	0 14	0 14	0 14
7) ptmd sal gt 1 si pt 5	0 16	0 16	0 16	0 16	0 16	0 16	0 16	0 16	0 16	0 16
8) ptmd sal gt 1 h8 ebb shallow t gt 18 acclim	0 17	0 18	0 18	0 17	0 17	0 18	0 18	0 17	0 18	0 18
9) tmd sal gt 1 ebb shallow t gt 18	0 16	0 16	0 16	0 16	0 16	0 16	0 16	0 16	0 16	0 16
10) tmd sal gt 1 ptmd prtmd sd pt 1 switch	0 33	0 33	0 33	0 33	0 33	0 33	0 33	0 33	0 33	0 33
SWP Salvage Expansion Factor										
1) passive	105	133	100	100	116	145	110	110	111	122
2) turbidity seeking	>1000	>1000	>1000	>1000	>1000	>1000	>1000	>1000	>1000	>1000
3) tmd	30	20	29	29	35	26	33	33	332	33
4) ptmd sal gt 1	25	35	24	24	29	41	28	28	24	56
5) ptmd_si_pt_5	32	50	30	30	33	52	31	31	687	431
6) ptmd_si_pt_5_shallow_ebb_t_gt_12	34	58	48	50	33	55	48	48	48	>1000
7) ptmd_sal_gt_1_si_pt_5	32	51	30	30	33	52	32	32	853	583
8) ptmd_sal_gt_1_h8_ebb_shallow_t_gt_18_acclim	48	69	59	65	49	71	34	66	59	61
9) tmd sal gt 1 ebb shallow t gt 18	66	61	68	67	62	66	69	71	>1000	71
10) tmd sal gt 1 ptmd prtmd sd pt 1 switch	126	126	127	127	124	130	131	134	>1000	134

Table 4. Con't.

i) 2D WY 2011 Poisson error in SKT data (τ=1)

Population model number	**1**	**2**	**3**	**4**	**5**	**6**	**7**	**8**	**9**	**10**
Salvage efficiency structure	**const**	**const**	**const**	**const**	**~turb**	**~turb**	**~turb**	**~turb**	**const**	**~turb**
Natural survival structure	S_c	S_{SKT}	S_d	S_W	S_c	S_{SKT}	S_d	S_W	S_d	S_d
SKT efficiency structure ($\theta_{c\text{-}SKT}$)	=1	=1	=1	=1	=1	=1	=1	=1	**~Secchi**	**~Secchi**
ΔAIC										
1) passive	38	33	40	40	41	36	43	43	28	31
2) turbidity seeking	2,104	2,110	2,103	2,103	2,108	2,114	2,107	2,107	2,073	2,076
3) tmd	91	84	92	91	94	88	96	95	80	84
4) ptmd sal gt 1	517	454	488	483	519	457	553	486	464	467
5) ptmd_si_pt_5	445	426	436	435	448	429	440	439	398	401
6) ptmd si pt 5 shallow ebb t gt 12	13	0	14	12	17	4	17	16	1	4
7) ptmd sal gt 1 si pt 5	504	485	494	494	507	488	497	497	456	459
8) ptmd sal gt 1 h8 ebb shallow t gt 18 acclim	121	98	123	122	124	101	126	125	100	102
9) tmd sal gt 1 ebb shallow t gt 18	552	513	554	553	555	517	557	556	555	559
10) tmd sal gt 1 ptmd prtmd sd pt 1 switch	293	274	281	281	296	278	285	285	250	253
Model Rank										
1) passive	2	2	2	2	2	2	2	2	2	2
2) turbidity seeking	10	10	10	10	10	10	10	10	10	10
3) tmd	3	3	3	3	3	3	3	3	3	3
4) ptmd_sal_gt_1	8	7	7	7	8	7	8	7	8	8
5) ptmd_si_pt_5	6	6	6	6	6	6	6	6	6	6
6) ptmd si pt 5 shallow ebb t gt 12	1	1	1	1	1	1	1	1	1	1
7) ptmd sal gt 1 si pt 5	7	8	8	8	7	8	7	8	7	7
8) ptmd sal gt 1 h8 ebb shallow t gt 18 acclim	4	4	4	4	4	4	4	4	4	4
9) tmd sal gt 1 ebb shallow t gt 18	9	9	9	9	9	9	9	9	9	9
10) tmd_sal_gt_1_ptmd_prtmd_sd_pt_1_switch	5	5	5	5	5	5	5	5	5	5
Proportional Entrainment Loss										
1) passive	0 01	0 01	0 01	0 01	0 01	0 01	0 01	0 01	0 01	0 01
2) turbidity seeking	0 01	0 01	0 01	0 01	0 01	0 01	0 01	0 01	0 02	0 02
3) tmd	0 10	0 09	0 10	0 09	0 09	0 09	0 09	0 09	0 12	0 12
4) ptmd_sal_gt_1	0 02	0 02	0 02	0 02	0 02	0 02	0 00	0 02	0 02	0 02
5) ptmd si pt 5	0 03	0 03	0 03	0 03	0 03	0 03	0 03	0 03	0 02	0 02
6) ptmd si pt 5 shallow ebb t gt 12	0 03	0 03	0 03	0 03	0 03	0 03	0 03	0 03	0 03	0 03
7) ptmd sal gt 1 si pt 5	0 03	0 03	0 03	0 03	0 03	0 03	0 03	0 03	0 02	0 02
8) ptmd sal gt 1 h8 ebb shallow t gt 18 acclim	0 03	0 03	0 03	0 03	0 03	0 03	0 03	0 03	0 04	0 04
9) tmd_sal_gt_1_ebb_shallow_t_gt_18	0 03	0 03	0 03	0 03	0 03	0 03	0 03	0 03	0 03	0 03
10) tmd sal gt 1 ptmd prtmd sd pt 1 switch	0 12	0 12	0 12	0 12	0 12	0 12	0 12	0 12	0 12	0 12
SWP Salvage Expansion Factor										
1) passive	>1000	>1000	>1000	>1000	>1000	>1000	>1000	>1000	>1000	>1000
2) turbidity seeking	>1000	>1000	>1000	>1000	>1000	>1000	>1000	>1000	>1000	>1000
3) tmd	>1000	>1000	>1000	>1000	>1000	>1000	>1000	>1000	>1000	>1000
4) ptmd sal gt 1	>1000	>1000	>1000	>1000	>1000	>1000	>1000	>1000	>1000	>1000
5) ptmd si pt 5	>1000	>1000	>1000	>1000	>1000	>1000	>1000	>1000	>1000	>1000
6) ptmd si pt 5 shallow ebb t gt 12	>1000	>1000	>1000	>1000	>1000	>1000	>1000	>1000	>1000	>1000
7) ptmd sal gt 1 si pt 5	>1000	>1000	>1000	>1000	>1000	>1000	>1000	>1000	>1000	>1000
8) ptmd_sal_gt_1_h8_ebb_shallow_t_gt_18_acclim	>1000	>1000	>1000	>1000	>1000	>1000	>1000	>1000	>1000	>1000
9) tmd_sal_gt_1_ebb_shallow_t_gt_18	>1000	>1000	>1000	>1000	>1000	>1000	>1000	>1000	>1000	>1000
10) tmd sal gt 1 ptmd prtmd sd pt 1 switch	>1000	>1000	>1000	>1000	>1000	>1000	>1000	>1000	>1000	>1000

Table 4. Con't.

j) 2D WY 2011 negative binomial error in SKT data (τ=10)

Population model number	**1**	**2**	**3**	**4**	**5**	**6**	**7**	**8**	**9**	**10**
Salvage efficiency structure	**const**	**const**	**const**	**const**	**~turb**	**~turb**	**~turb**	**~turb**	**const**	**~turb**
Natural survival structure	S_c	S_{SKT}	S_d	S_W	S_c	S_{SKT}	S_d	S_W	S_d	S_d
SKT efficiency structure ($\theta_{c\text{-}SKT}$)	**=1**	**=1**	**=1**	**=1**	**=1**	**=1**	**=1**	**=1**	**~Secch**	**~Secch**
ΔAIC										
1) passive	88	94	90	90	92	98	93	93	91	92
2) turbidity seeking	319	325	320	320	323	329	324	324	319	321
3) tmd	7	13	2,017	9	11	17	14	13	11	15
4) ptmd sal gt 1	144	145	143	142	146	147	146	144	145	150
5) ptmd_si_pt_5	77	83	79	79	81	86	83	83	78	81
6) ptmd si pt 5 shallow ebb t gt 12	14	19	15	15	17	23	1,332	19	20	24
7) ptmd_sal_gt_1_si_pt_5	130	135	132	132	133	138	135	135	139	136
8) ptmd sal gt 1 h8 ebb shallow t gt 18 acclim	61	66	63	63	63	69	65	65	64	67
9) tmd sal gt 1 ebb shallow t gt 18	127	133	129	129	131	136	133	133	132	158
10) tmd_sal_gt_1_ptmd_prtmd_sd_pt_1_switch	0	5	348	3	3	9	5	5	0	4
Model Rank										
1) passive	6	6	4	6	6	6	5	6	6	6
2) turbidity_seeking	10	10	8	10	10	10	9	10	10	10
3) tmd	2	2	10	2	2	2	2	2	2	2
4) ptmd_sal_gt_1	9	9	7	9	9	9	8	9	9	8
5) ptmd si pt 5	5	5	3	5	5	5	4	5	5	5
6) ptmd si pt 5 shallow ebb t gt 12	3	3	1	3	3	3	10	3	3	3
7) ptmd_sal_gt_1_si_pt_5	8	8	6	8	8	8	7	8	8	7
8) ptmd sal gt 1 h8 ebb shallow t gt 18 acclim	4	4	2	4	4	4	3	4	4	4
9) tmd_sal_gt_1_ebb_shallow_t_gt_18	7	7	5	7	7	7	6	7	7	9
10) tmd sal gt 1 ptmd prtmd sd pt 1 switch	1	1	9	1	1	1	1	1	1	1
Proportional Entrainment Loss										
1) passive	0.03	0.03	0.03	0.03	0.03	0.03	0.03	0.03	0.03	0.04
2) turbidity seeking	0.03	0.03	0.03	0.03	0.03	0.03	0.03	0.03	0.03	0.04
3) tmd	0.14	0 14	0.00	0.14	0.14	0.14	0.14	0.14	0.14	0.14
4) ptmd sal gt 1	0.06	0.06	0.06	0.06	0.06	0.06	0.06	0.06	0.06	0.06
5) ptmd si pt 5	0.07	0.07	0.07	0.07	0.07	0.07	0.07	0.07	0.06	0.06
6) ptmd_si_pt_5_shallow_ebb_t_gt_12	0.07	0.07	0.07	0.07	0.07	0.07	0.03	0.07	0.06	0.07
7) ptmd sal gt 1 si pt 5	0.08	0.08	0.08	0.07	0.08	0.08	0.08	0.08	0.08	0.07
8) ptmd_sal_gt_1_h8_ebb_shallow_t_gt_18_acclim	0.06	0.07	0.07	0.07	0.07	0.07	0.07	0.07	0.06	0.06
9) tmd sal gt 1 ebb shallow t gt 18	0.08	0.08	0.08	0.08	0.08	0.08	0.08	0.08	0.08	0.01
10) tmd_sal_gt_1_ptmd_prtmd_sd_pt_1_switch	0.14	0.14	0.11	0.14	0.14	0.14	0.14	0.14	0.14	0.14
SWP Salvage Expansion Factor										
1) passive	>1000	>1000	>1000	>1000	>1000	>1000	>1000	>1000	>1000	>1000
2) turbidity seeking	>1000	>1000	>1000	>1000	>1000	>1000	>1000	>1000	>1000	>1000
3) tmd	>1000	>1000	1	>1000	>1000	>1000	>1000	>1000	>1000	>1000
4) ptmd sal gt 1	>1000	>1000	>1000	>1000	>1000	>1000	>1000	>1000	>1000	>1000
5) ptmd_si_pt_5	>1000	>1000	>1000	>1000	>1000	>1000	>1000	>1000	>1000	>1000
6) ptmd si pt 5 shallow ebb t gt 12	>1000	>1000	>1000	>1000	>1000	>1000	>1000	>1000	>1000	>1000
7) ptmd_sal_gt_1_si_pt_5	>1000	>1000	>1000	>1000	>1000	>1000	>1000	>1000	>1000	>1000
8) ptmd sal gt 1 h8 ebb shallow t gt 18 acclim	>1000	>1000	>1000	>1000	>1000	>1000	>1000	>1000	>1000	>1000
9) tmd_sal_gt_1_ebb_shallow_t_gt_18	>1000	>1000	>1000	>1000	>1000	>1000	>1000	>1000	>1000	>1000
10) tmd_sal_gt_1_ptmd_prtmd_sd_pt_1_switch	>1000	>1000	1	>1000	>1000	>1000	>1000	>1000	>1000	>1000

Table 5. Comparison of salvage expansion factors (θ_S^{-1}) from previous studies. Expansion factors from Castillo et al. (2012) were determined from mark-recapture based estimates of louver efficiency and pre-screen losses, while those from Kimmerer and Smith et al. were based on the ratio of estimated entrainment to observed salvage, where entrainment was calculated as the product of population size and a hydrodynamic-based entrainment rate. Rows a)-e) demonstrate how efficiency and pre-screen losses are combined to estimate the total efficiency (θ_S) and expansion factor (θ_S^{-1}). Rows f)-i) demonstrate how the Castillo et al. total efficiency estimates can be separated from the salvage efficiencies estimated from the population dynamics model in this study to determine the additional loss between the entrainment point and the Clifton Court Forebay (CCF) gates, which was the boundary of the Castillo et al. study.

		Castillo et al. (2009) - SWP		**Kimmerer (CVP=SWP)**		**Smith et al. (2017)**	
		February	**March**	**2008**	**2011**	**CVP**	**SWP**
a) Lourver efficiency		0.53	0.44				
b) Pre-screen loss		0.942	0.991				
c) Pre-screen efficiency (1 -b)		0.058	0.009				
d) Total efficiency (a*b)		0.03074	0.00396				
e) Salvage expansion factor (1/d)		32.5	252.5	29 (9-49)	22 (13-33)	35	50
f) Example salvage efficiency (θ_S) from population model for SWP	0.0025						
g) Example salvage expansion (1/f)	400						
h) Proporiton lost from entrainment point to CCF (1-f/d)		0.92	0.37				
i) Expansion factor upstream of CCF (1/h)		12.3	1.6				

Table 6. Comparison of 10 particle-tracking models (PTMs) for each water year and PTM type (2D or 3D) scenario based on differences in AIC (ΔAIC) within scenarios (columns). Results are based on the population model with survival varying with model day (S_d) and salvage efficiency varying with turbidity (θ_{turb}, model 7 in Table 4), assuming a) negative binomial and b) poisson error in SKT catch data. Also shown are the total proportional entrainment losses. Dark-, medium-, and light-grey shaded cells identify the 1st-, 2nd-, and 3rd-ranked models, respectively.

a) Poisson error in SKT data (variance to mean ratio, τ=1)

PTM Type	3D	2D			
Water Year	**2002**	**2002**	**2004**	**2005**	**2011**
ΔAIC					
1) passive	817	604	2,747	1,091	25
2) turbidity_seeking	4,711	49,591	52,654	14,909	2,090
3) tmd	2,311	1,054	786	528	78
4) ptmd_sal_gt_1	604	1,192	3,170	845	536
5) ptmd_si_pt_5	409	839	2,769	703	423
6) ptmd_si_pt_5_shallow_ebb_t_gt_12	0	408	490	277	0
7) ptmd_sal_gt_1_si_pt_5	161	836	2,877	662	480
8) ptmd_sal_gt_1_h8_ebb_shallow_t_gt_18_acclim	263	0	359	0	108
9) tmd_sal_gt_1_ebb_shallow_t_gt_18	117	334	306	60	540
10) tmd_sal_gt_1_ptmd_prtmd_sd_pt_1_switch	91	471	0	132	268
Proportional Entrainment Loss					
1) passive	0.03	0.03	0.06	0.06	0.01
2) turbidity_seeking	0.07	0.00	0.04	0.00	0.01
3) tmd	0.34	0.36	0.40	0.16	0.09
4) ptmd_sal_gt_1	0.08	0.06	0.10	0.09	0.00
5) ptmd_si_pt_5	0.22	0.24	0.30	0.15	0.03
6) ptmd_si_pt_5_shallow_ebb_t_gt_12	0.35	0.35	0.20	0.10	0.03
7) ptmd_sal_gt_1_si_pt_5	0.25	0.24	0.35	0.16	0.03
8) ptmd_sal_gt_1_h8_ebb_shallow_t_gt_18_acclim	0.60	0.37	0.28	0.15	0.03
9) tmd_sal_gt_1_ebb_shallow_t_gt_18	0.49	0.36	0.37	0.15	0.03
10) tmd_sal_gt_1_ptmd_prtmd_sd_pt_1_switch	0.46	0.48	0.50	0.29	0.12

Table 6. Con't.

b) Negative binomial error in SKT data (variance to mean ratio, τ=10)

PTM Type	3D	2D			
Water Year	**2002**	**2002**	**2004**	**2005**	**2011**
ΔAIC					
1) passive	291	211	1,866	701	88
2) turbidity_seeking	4,495	47,501	47,537	14,262	319
3) tmd	970	370	311	403	9
4) ptmd_sal_gt_1	223	201	1,704	694	140
5) ptmd_si_pt_5	174	325	1,880	679	78
6) ptmd_si_pt_5_shallow_ebb_t_gt_12	0	72	367	233	1,326
7) ptmd_sal_gt_1_si_pt_5	164	348	2,070	641	130
8) ptmd_sal_gt_1_h8_ebb_shallow_t_gt_18_acclim	208	0	384	48	60
9) tmd_sal_gt_1_ebb_shallow_t_gt_18	175	54	0	0	128
10) tmd_sal_gt_1_ptmd_prtmd_sd_pt_1_switch	111	56	105	99	0
Proportional Entrainment Loss					
1) passive	0.03	0.03	0.10	0.10	0.03
2) turbidity_seeking	0.06	0.00	0.06	0.01	0.03
3) tmd	0.38	0.40	0.33	0.11	0.14
4) ptmd_sal_gt_1	0.07	0.06	0.10	0.10	0.06
5) ptmd_si_pt_5	0.21	0.24	0.31	0.15	0.07
6) ptmd_si_pt_5_shallow_ebb_t_gt_12	0.36	0.39	0.14	0.14	0.03
7) ptmd_sal_gt_1_si_pt_5	0.25	0.24	0.37	0.16	0.08
8) ptmd_sal_gt_1_h8_ebb_shallow_t_gt_18_acclim	0.59	0.36	0.14	0.18	0.07
9) tmd_sal_gt_1_ebb_shallow_t_gt_18	0.49	0.36	0.18	0.16	0.08
10) tmd_sal_gt_1_ptmd_prtmd_sd_pt_1_switch	0.48	0.51	0.52	0.33	0.14

Table 7. Comparison of fit statistics (log likelihood) by data source for 1st- and 2nd -ranked PTMs in water year 2002 (3D PTM) and 2004 assuming poisson error (τ=1) in SKT catch data. Results are based on population model 7 (Table 4) where daily survival rate is a smooth function of model day and salvage expansion factors depend on turbidity. A higher log likelihood (closer to 0) indicates better fit. As the number of estimated parameters are the same for both PTMs, twice the difference in the total log likelihood between models is equivalent to the difference in AIC (Table 6).

Likelihood Source	**3D WY 2002**		**2D 2004**	
	PTM 6	**PTM 10**	**PTM 10**	**PTM 9**
FMWT	-50	-40	-49	-78
SKT	-800	-786	-1,385	-1,504
Salvage	-450	-520	-949	-955
Total	-1,300	-1,346	-2,383	-2,537
ΔAIC		91		306

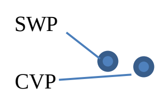

Figure 1. Boundaries of CAMT regions and the location of the State Water Project (SWP) and federal Central Valley Project (CVP) pumping plants.

Figure 2. Overview of modelling approaches used to evaluate alternate Particle Tracking Models (PTMs) and predict proportional entrainment loss for adult Delta Smelt.

a)

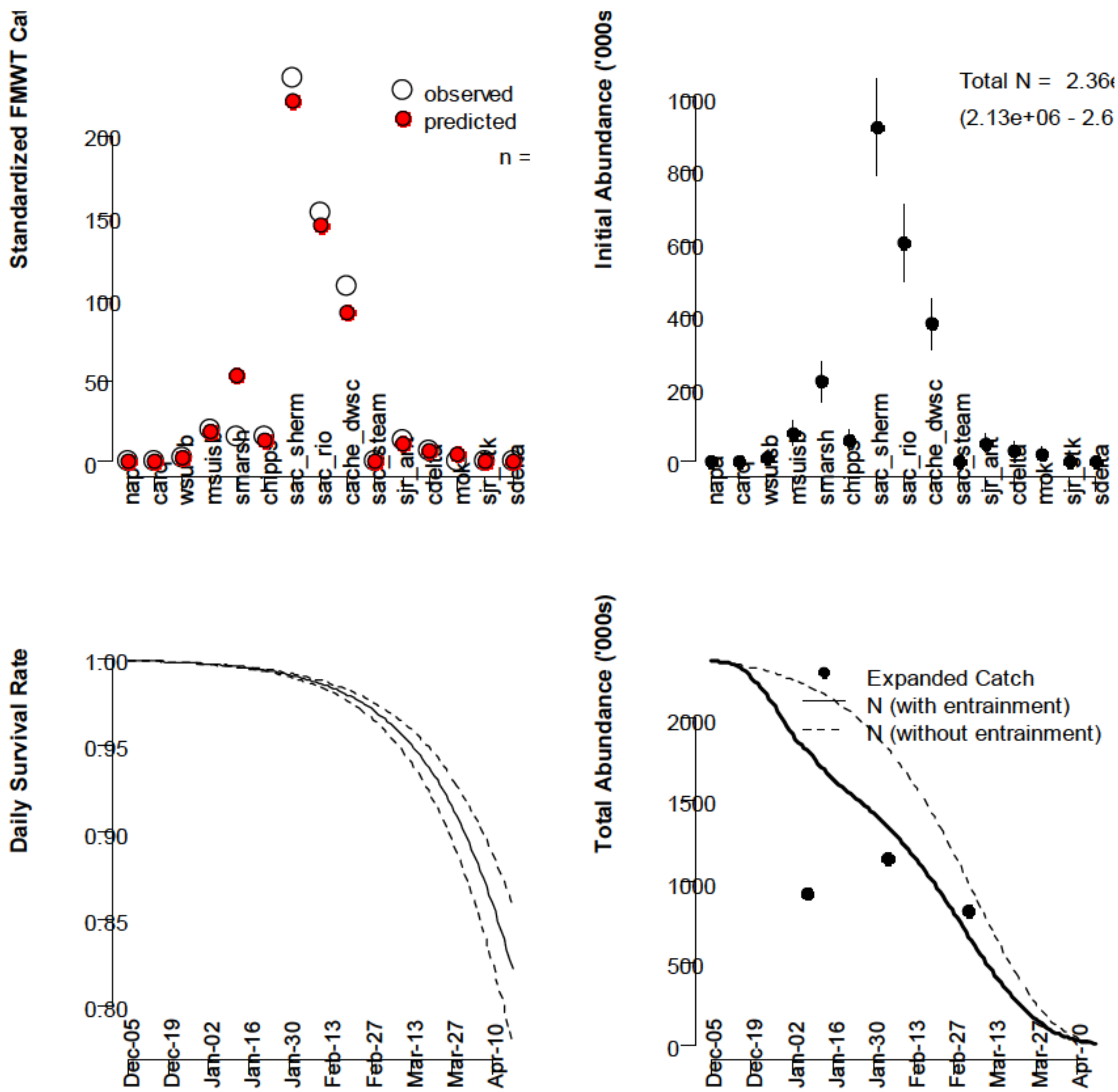

Figure 3. Model fit and predictions for the 3D-based PTM model 6 and population model 10 with poisson error in SKT catch data applied in water year 2002 (Table 4a). a) shows predicted and observed FMWT volume-corrected FMWT catch (top-left plot, observed catch summed across Sep, Oct, Nov, and Dec. surveys), regional population estimates with 95% credible intervals (top –right plot), predictions of the daily survival rate (solid line, bottom-left plot) with 95% credible intervals (dashed lines), and predicted total abundance across regions (bottom-right plot, solid and dashed lines) compared to estimates based on expanding the catch by the ratio of 4 m volume to the volume of tows and accounting for the estimated Secchi depth effect on SKT sampling efficiency.

b)

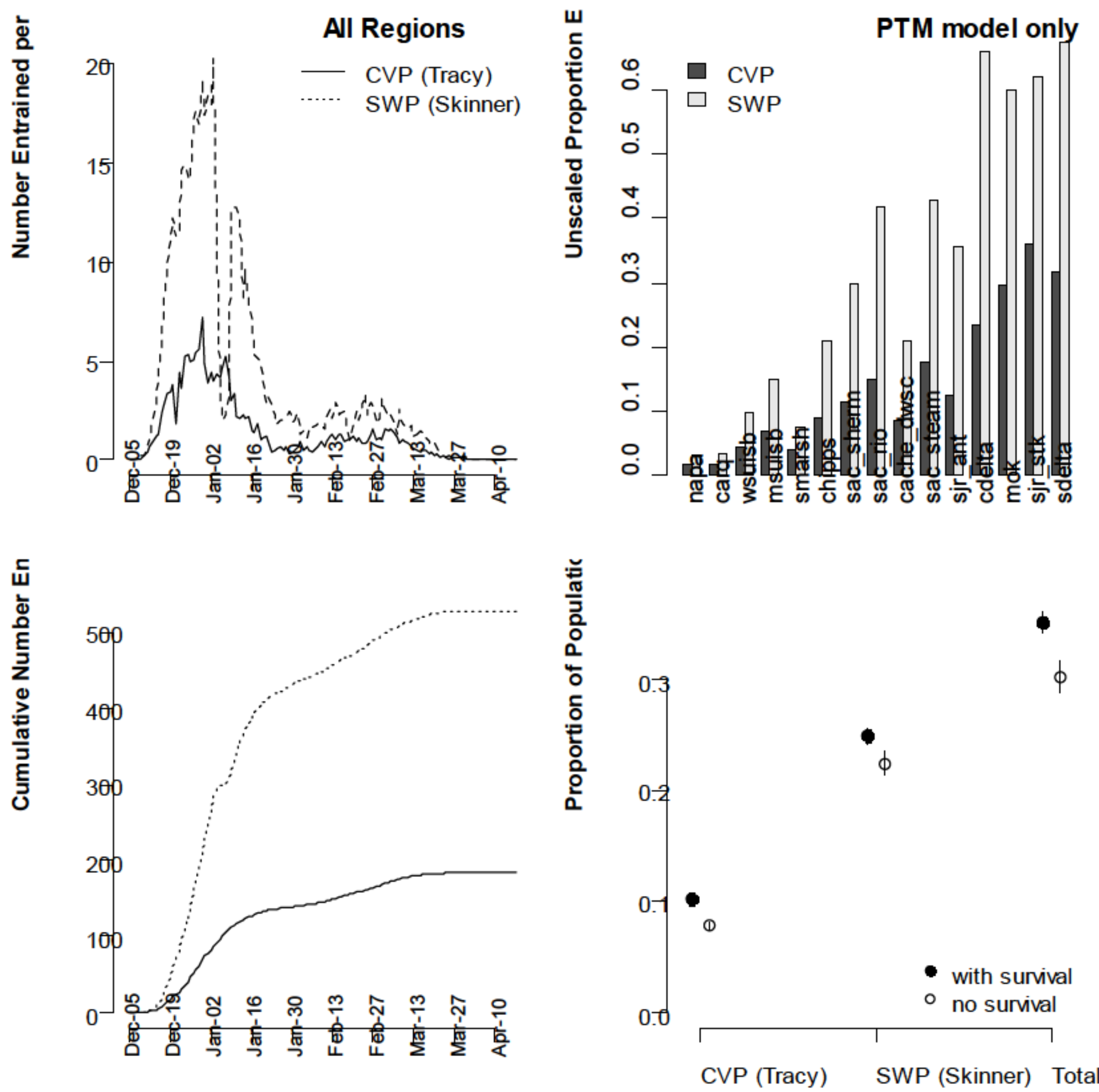

Figure 3. Con't. Predictions of daily salvage (left plots), the cumulative unscaled proportional entrainment for each region predicted by the PTM (top-right), and estimates of proportional entrainment (which include survival effects) and discrete proportional entrainment (which do not include survival effects as they are based on ratio of entrainment to initial abundance).

c)

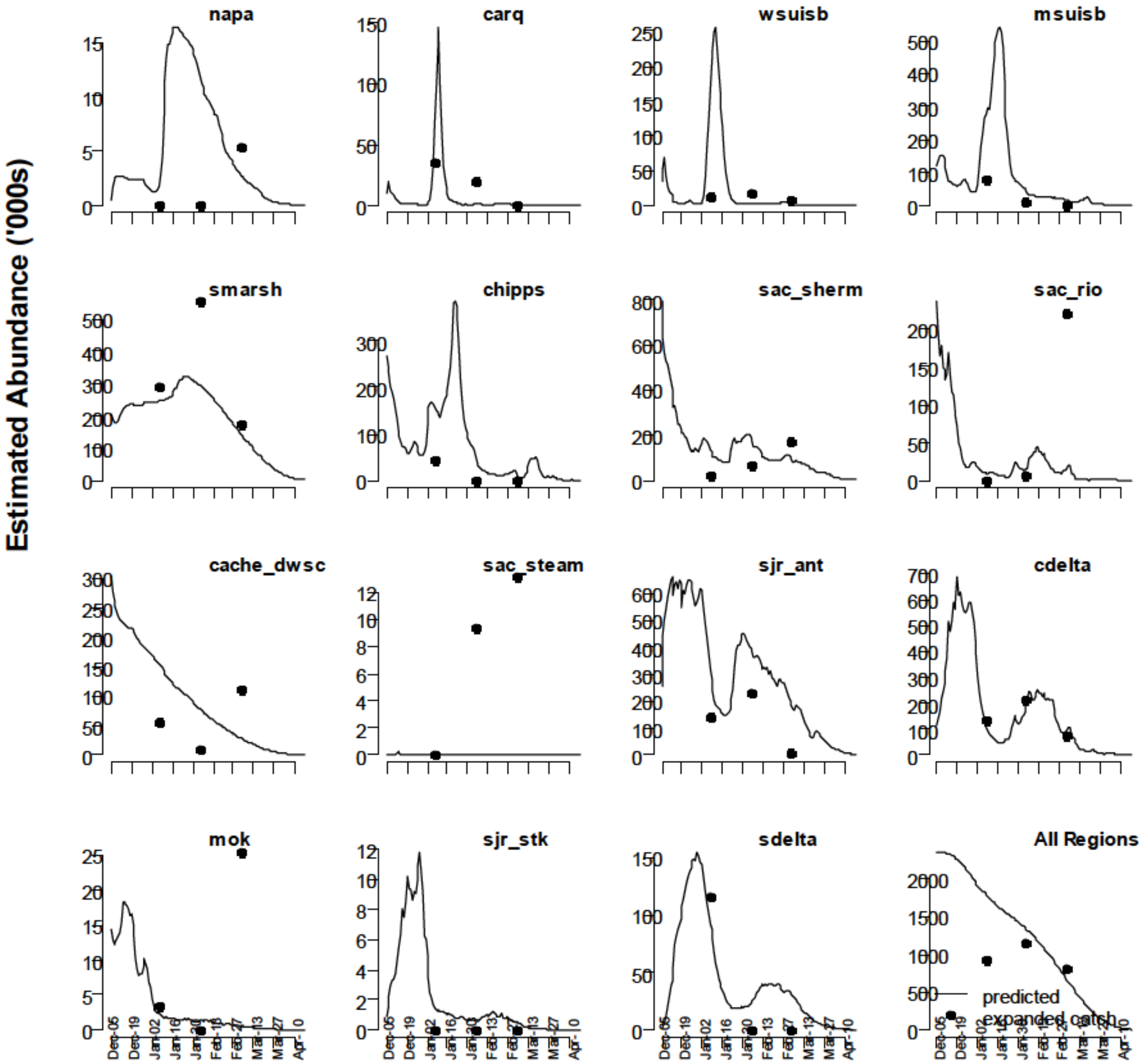

Figure 3. Con't. Abundance estimates by region and model day (lines) compared to estimates based on expanded catch (points). Note different y-axis scales among panels.

d)

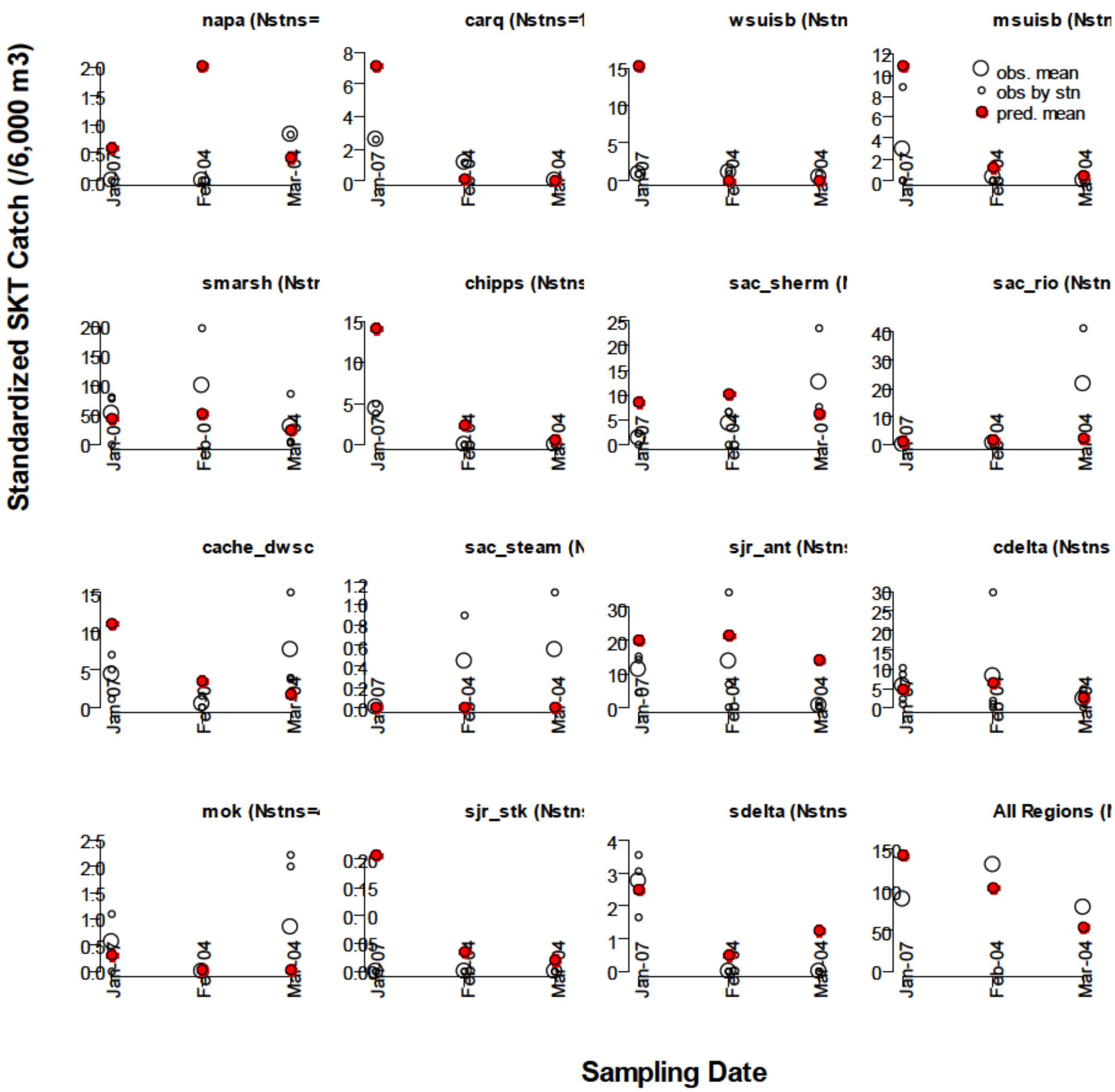

Figure 3. Con't. Comparison of predicted (red points) and mean observed (large open points) SKT catch by trip and region where catches are standardized by the approximate average tow volume. Also shown are the standardized station-specific standardized catches (small open points).

e)

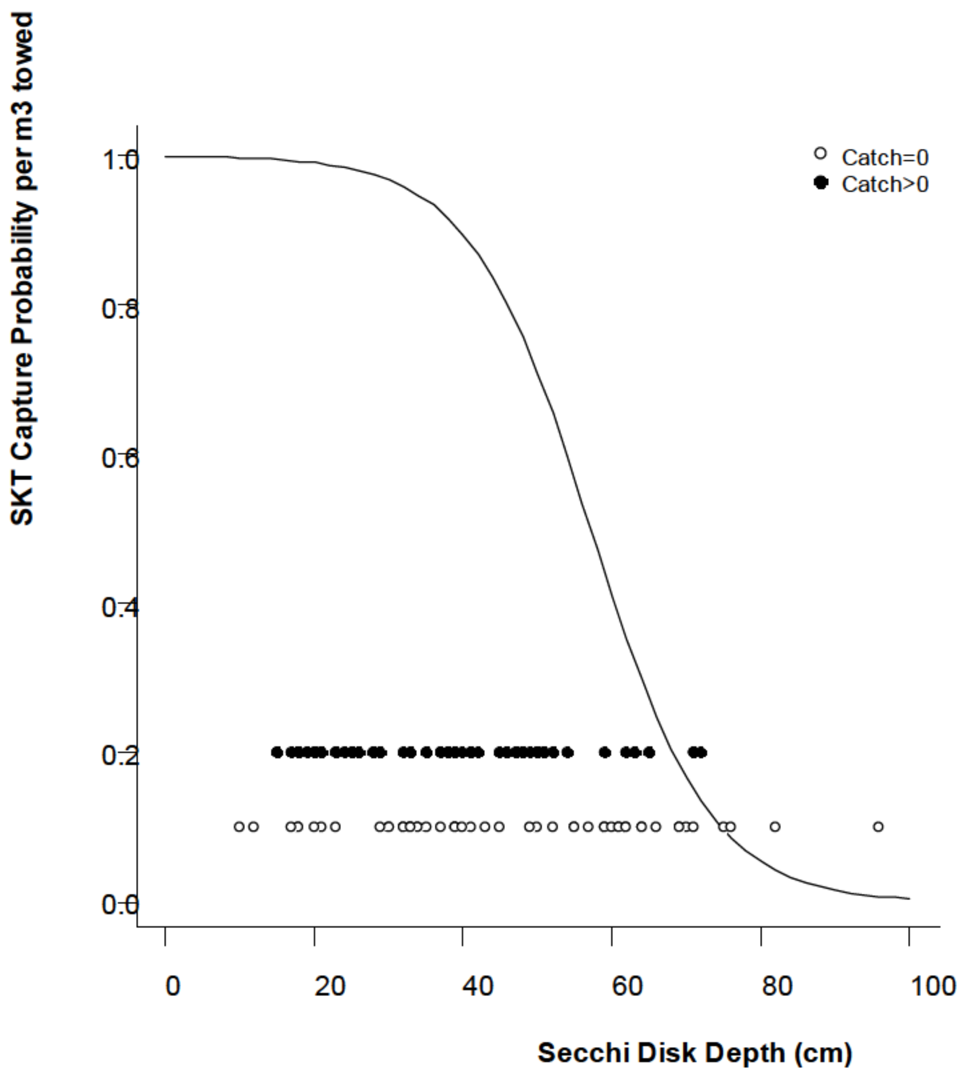

Figure 3. Con't. Estimated relationship between SKT efficiency and Secchi depth (eqn. 5c). Points show the measured Secchi depths across all surveys and stations where Delta Smelt were (closed) and were not (open) captured.

f)

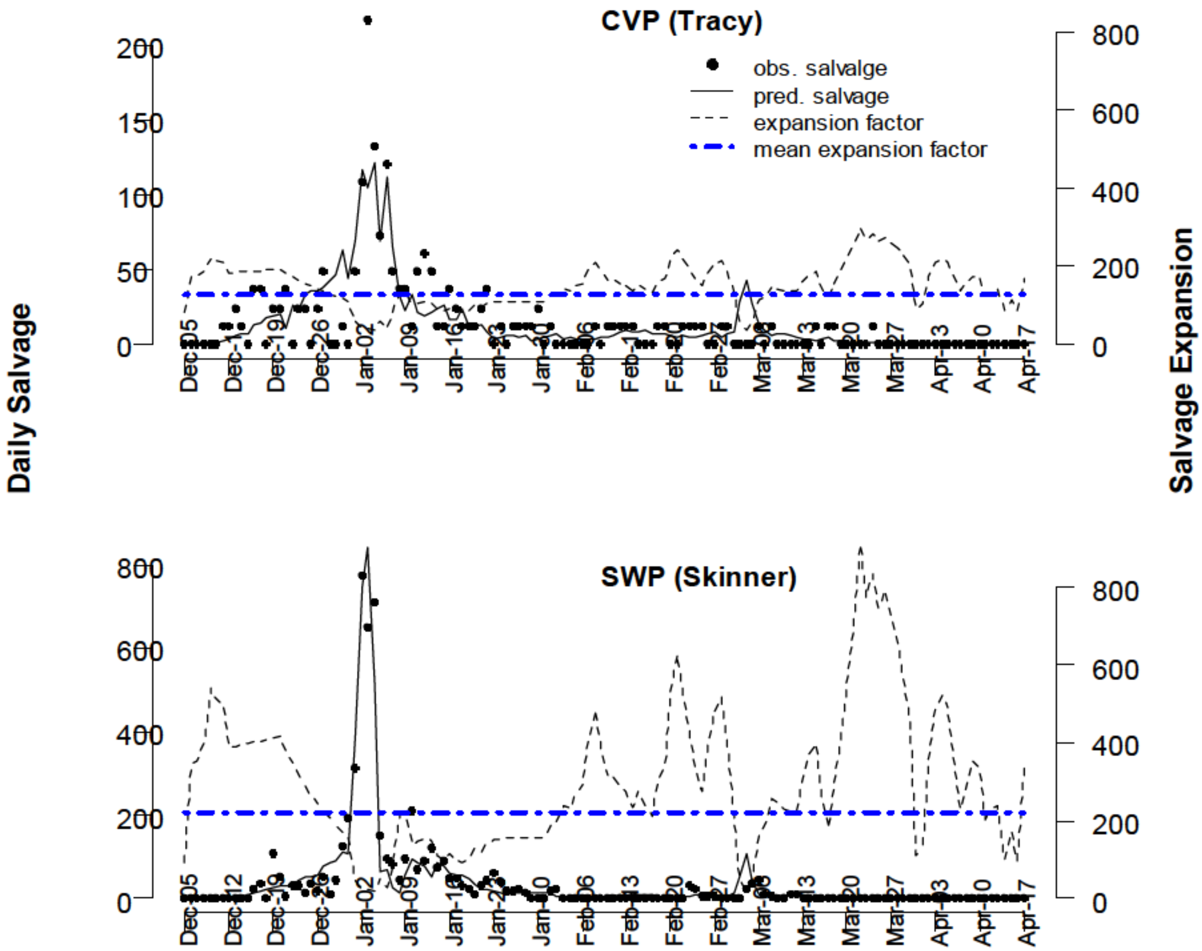

Figure 3. Con't. Predicted (solid line) and observed (points) daily salvage (left axis). Also shown are the daily salvage expansion factors ($1/\theta_S$, black dashed line right-hand axis) and the salvage-weighted average value across days (blue dashed line).

g)

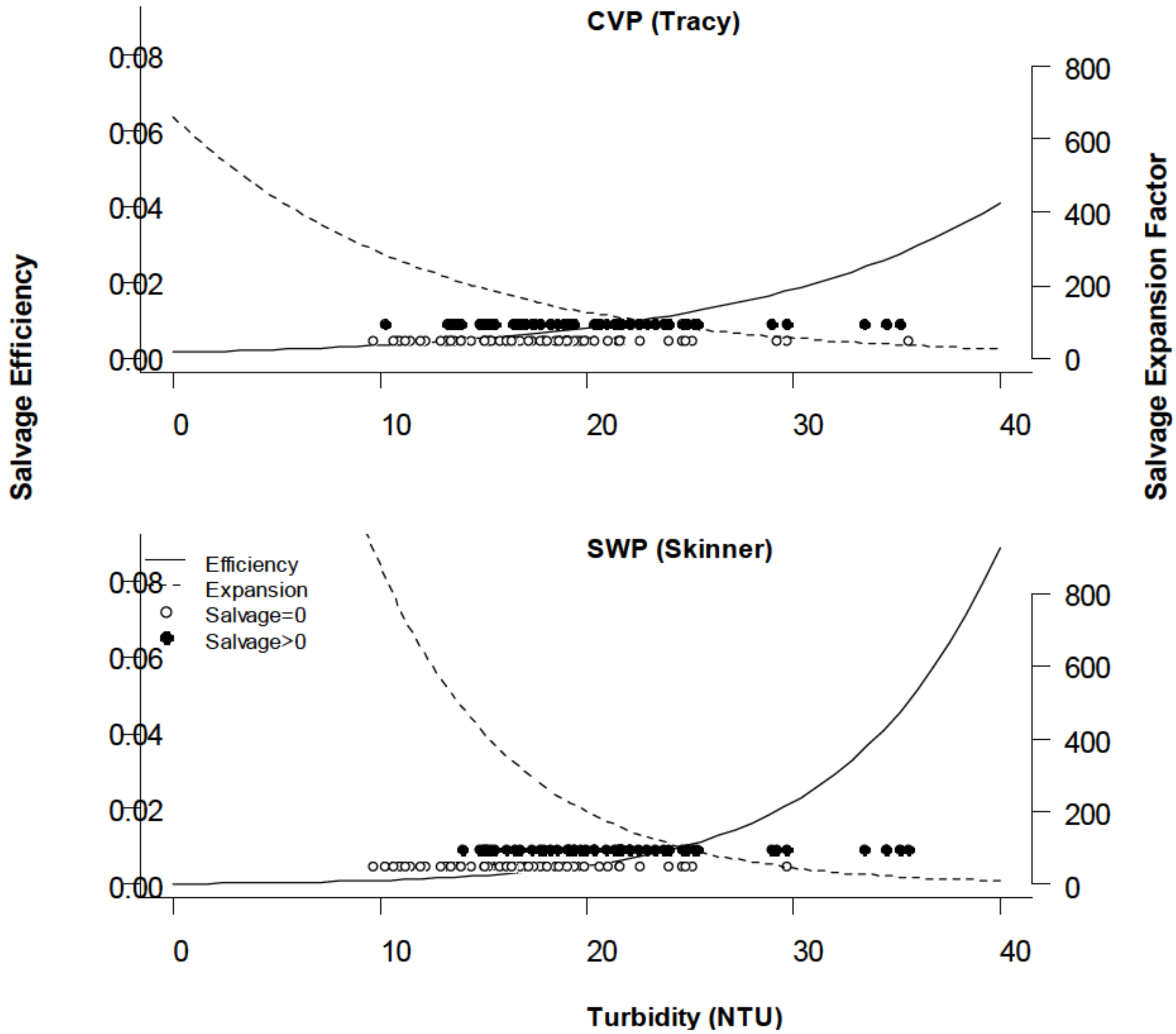

Figure 3. Con't. Estimated salvage efficiency-turbidity relationship (sold line, left-hand axis) and the inverse (expansion factor relationship, dashed line, right-hand axis). The solid and open points show the turbidity levels when salvage was and was not observed.

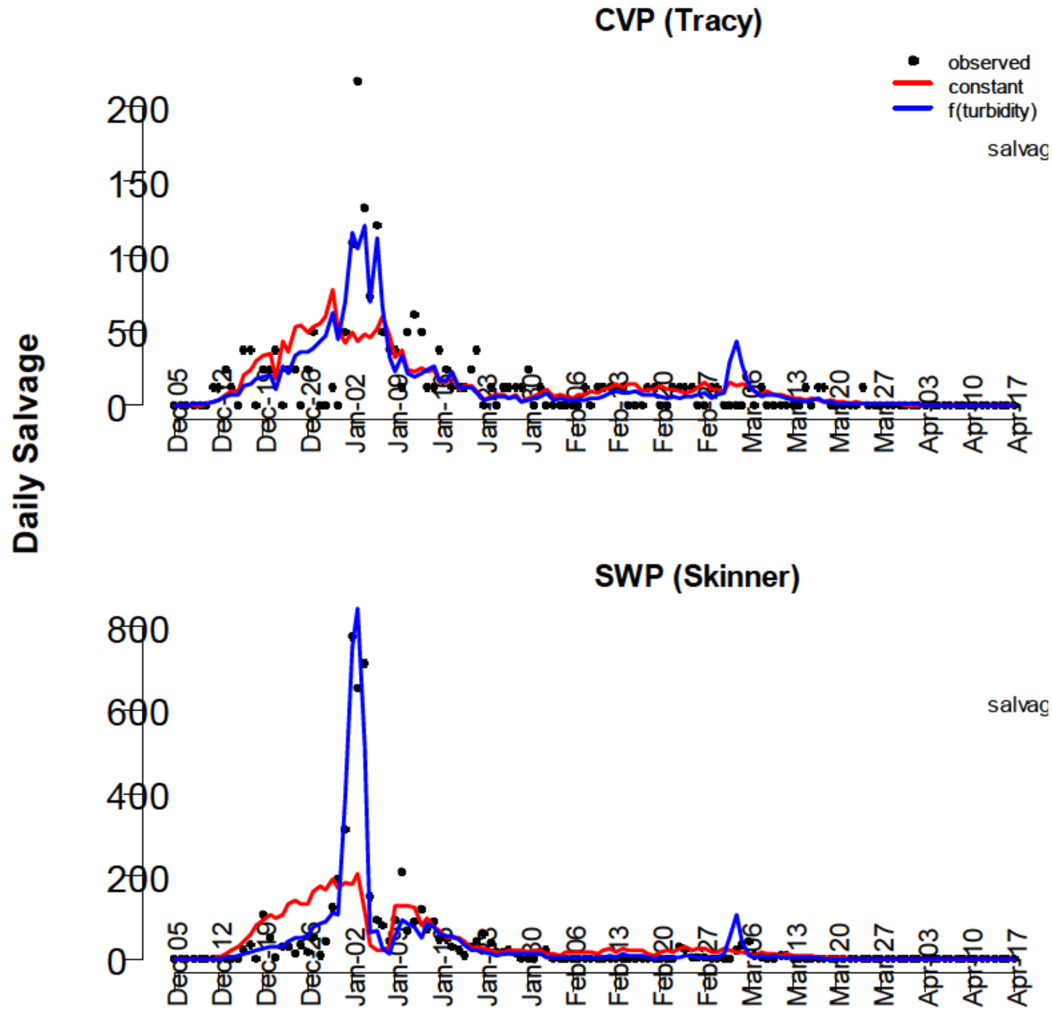

Figure 4. Comparison of fits to salvage in water year 2002 based on constant and turbidity-varying salvage efficiency models for 3D PTM 6 (population dynamic models 3 and 7, Table 4a).

a)

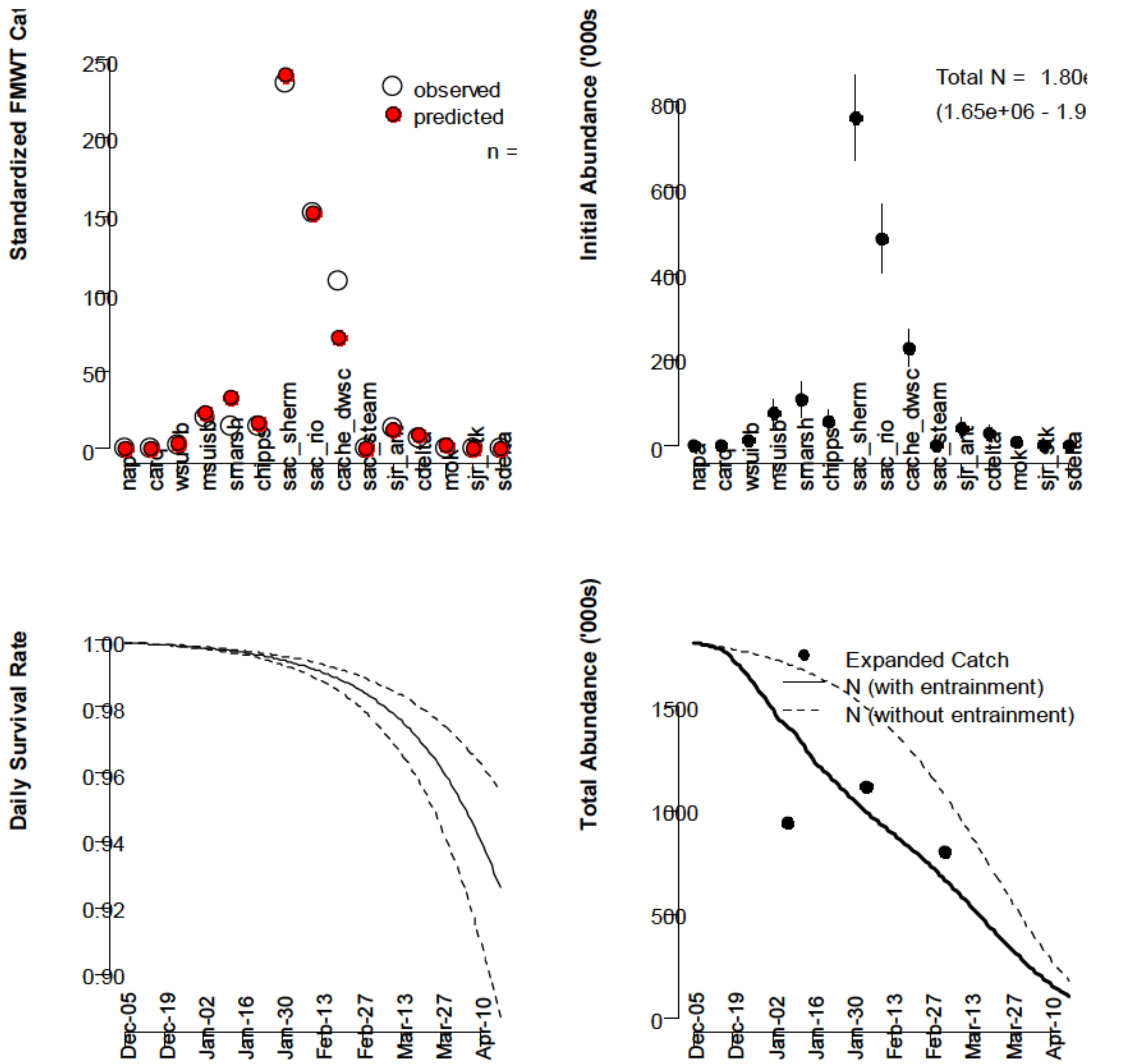

Figure 5. Model fit and predictions for the 2D-based PTM model 8 and population model 10 with poisson error in SKT catch data applied in water year 2002 (Table 4c). a) shows predicted and observed FMWT volume-corrected FMWT catch (top-left plot, observed catch summed across Sep, Oct, Nov, and Dec. surveys), regional population estimates with 95% credible intervals (top –right plot), predictions of the daily survival rate (solid line, bottom-left plot) with 95% credible intervals (dashed lines), and predicted total abundance across regions (bottom-right plot, solid and dashed lines) compared to estimates based on expanding the catch by the ratio of 4 m volume to the volume of tows and accounting for the estimated Secchi depth effect on SKT sampling efficiency.

b)

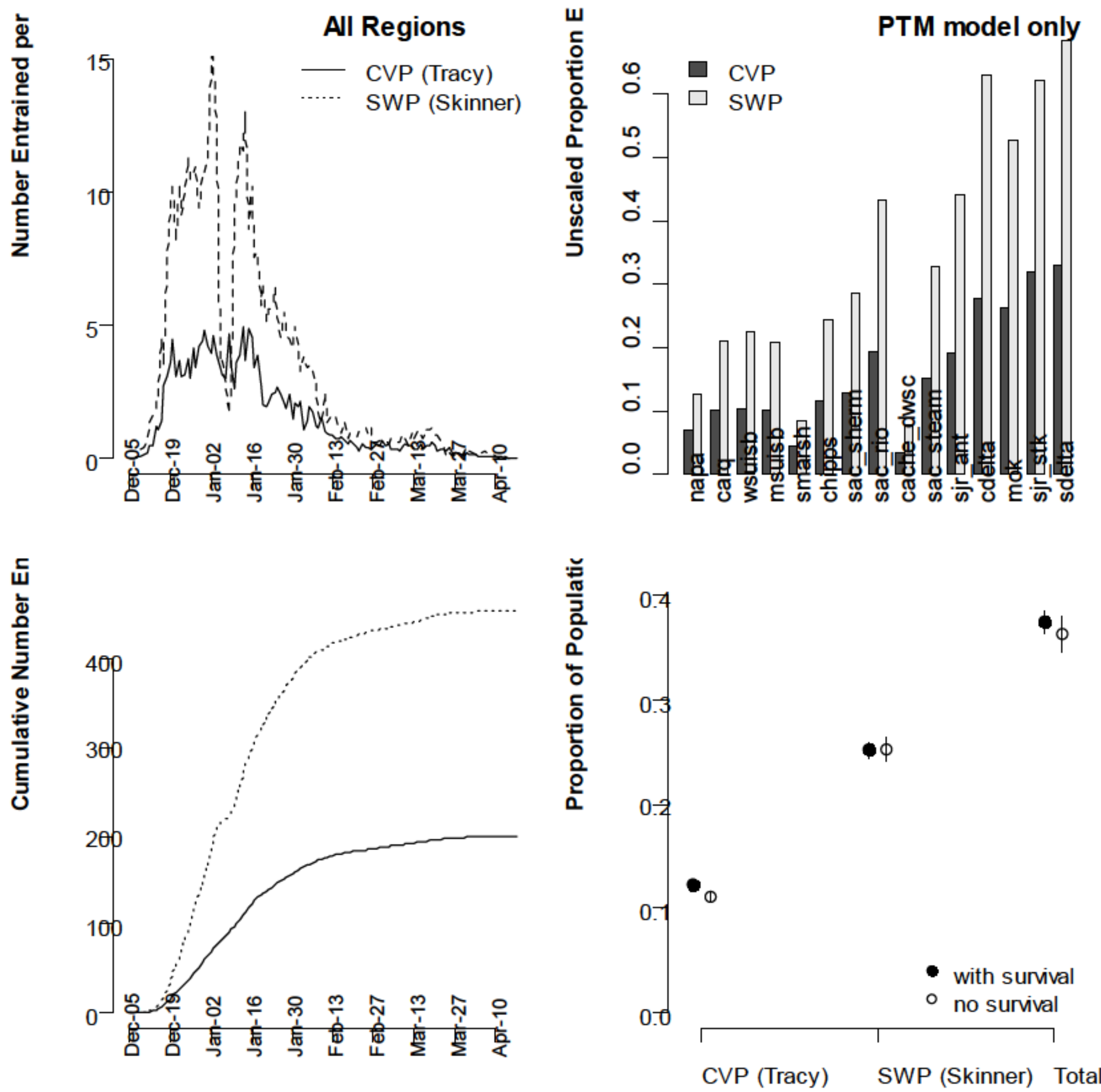

Figure 5. Con't. Predictions of daily salvage (left plots), the cumulative unscaled proportional entrainment for each region predicted by the PTM (top-right), and estimates of proportional entrainment (which include survival effects) and discrete proportional entrainment (which do not include survival effects as they are based on ratio of entrainment to initial abundance).

c)

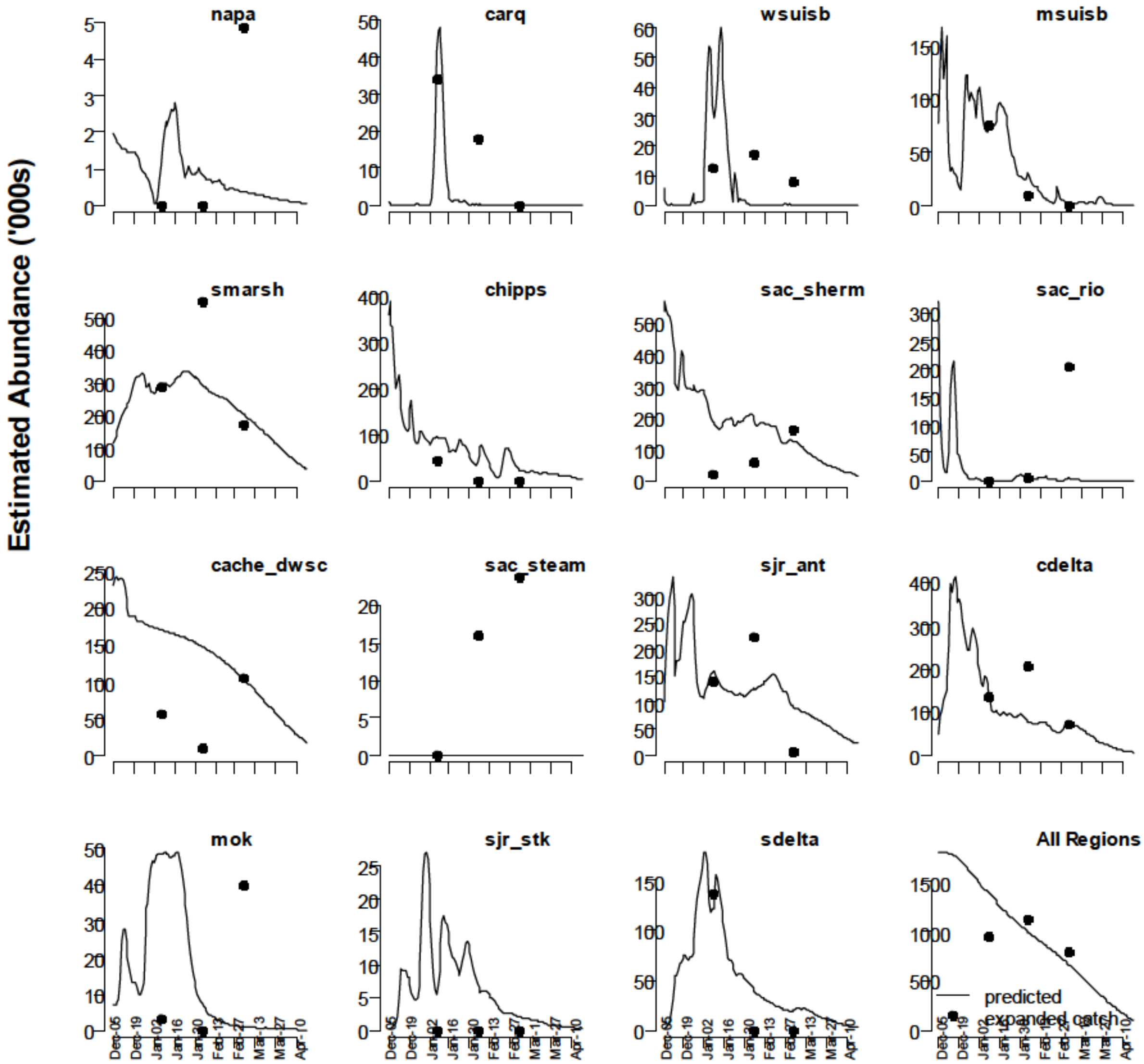

Figure 5. Con't. Abundance estimates by region and model day (lines) compared to estimates based on expanded catch (points).

d)

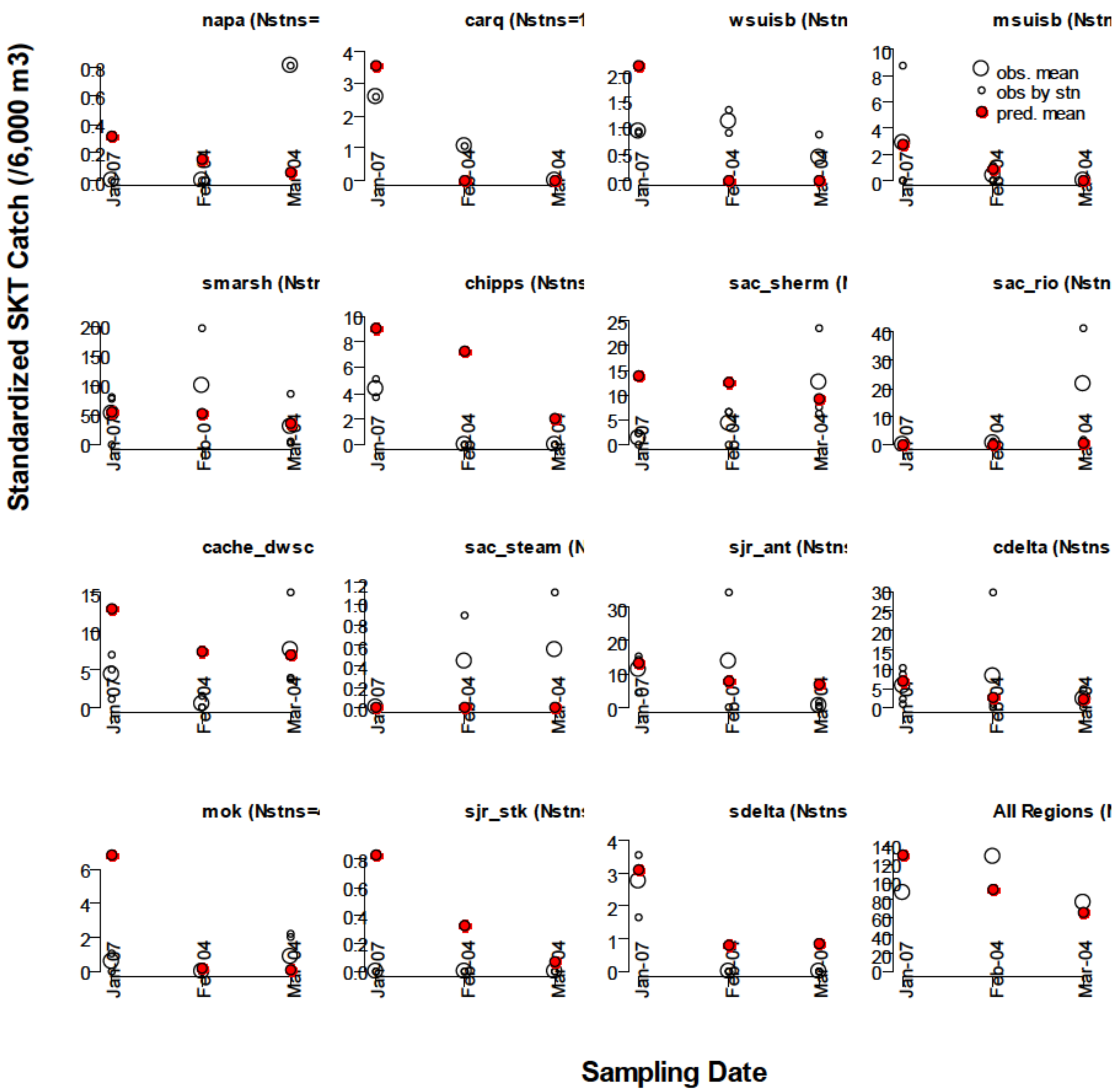

Figure 5. Con't. Comparison of predicted (red points) and mean observed (large open points) SKT catch by trip and region where catches are standardized by the approximate average tow volume. Also shown are the standardized station-specific standardized catches (small open points).

e)

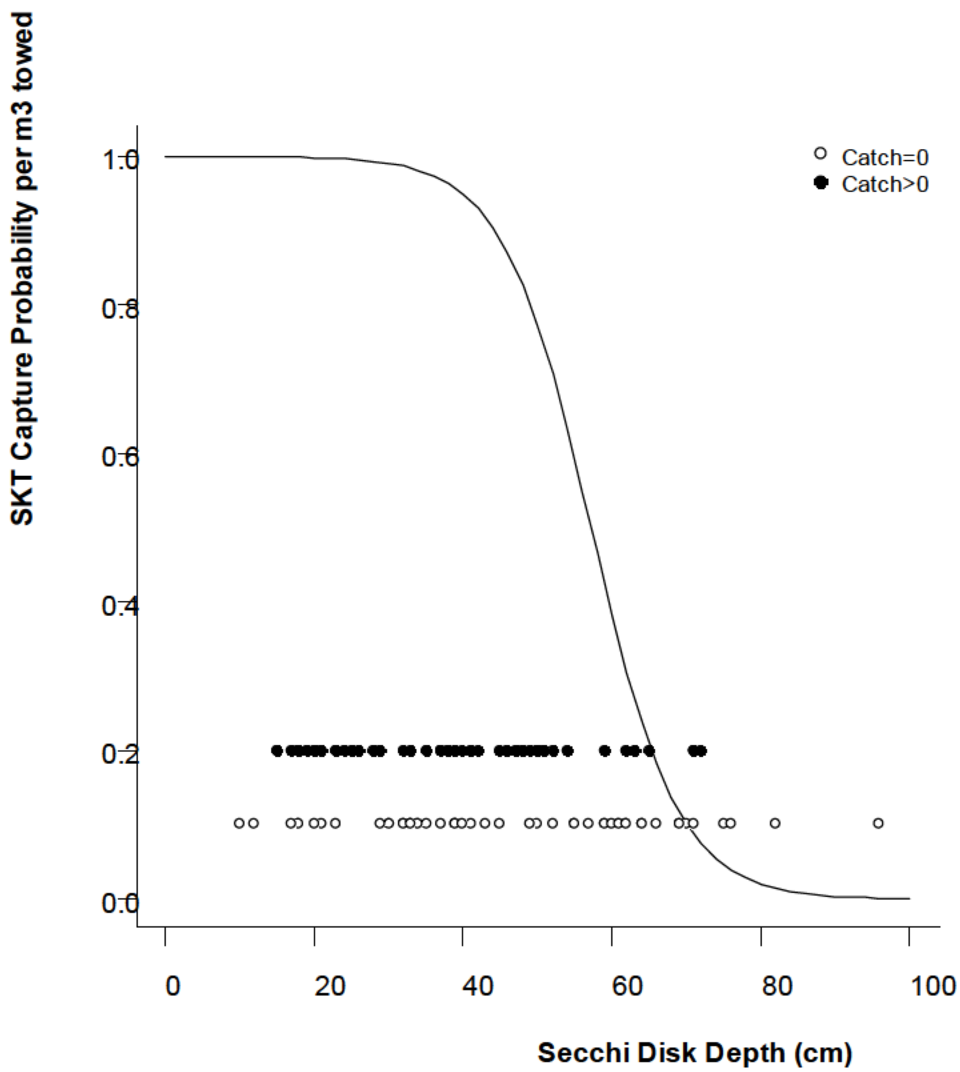

Figure 5. Con't. Estimated relationship between SKT efficiency and Secchi depth (eqn. 5c). Points show the measured Secchi depths across all surveys and stations where Delta Smelt were (closed) and were not (open) captured.

f)

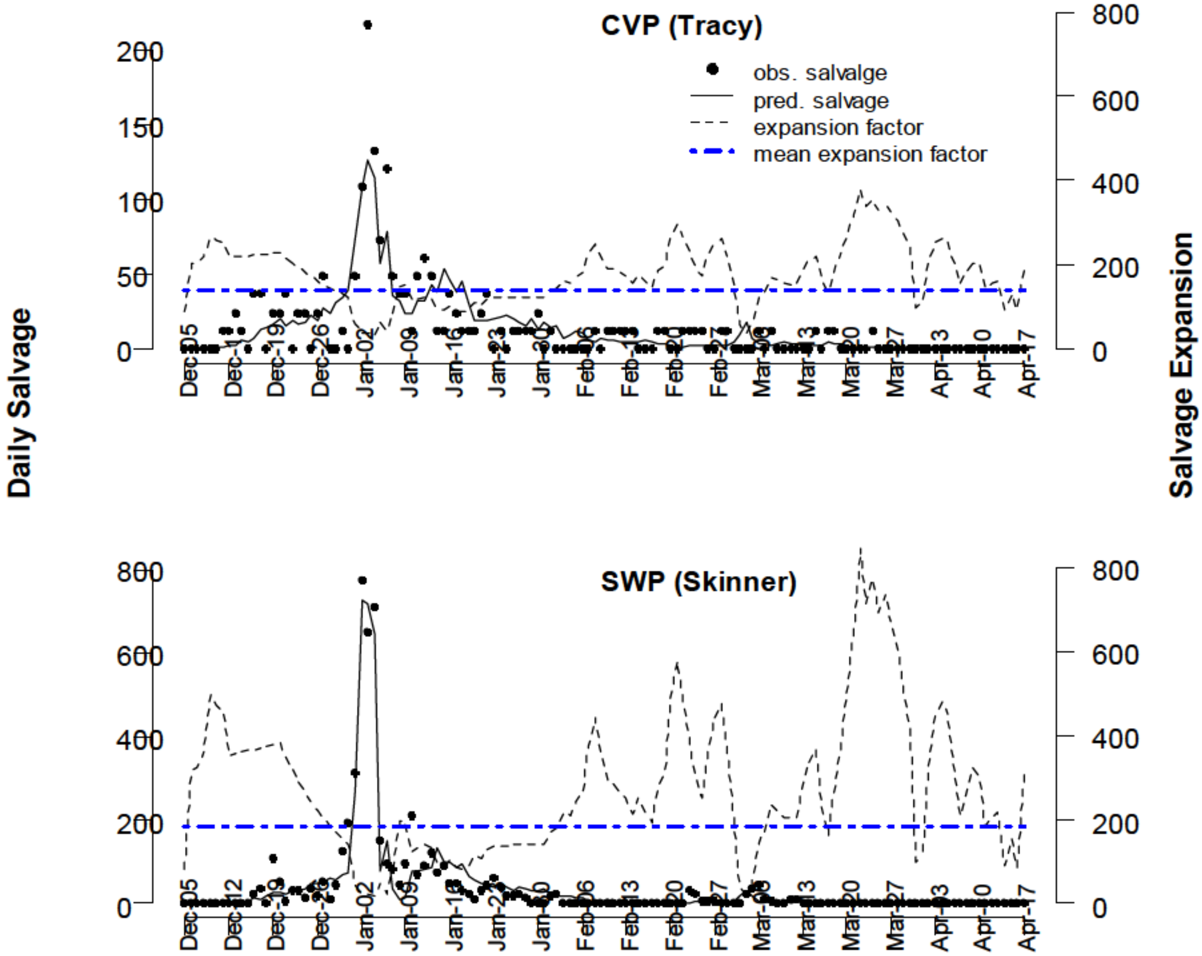

Figure 5. Con't. Predicted (solid line) and observed (points) daily salvage (left axis). Also shown are the daily salvage expansion factors ($1/\theta_S$, black dashed line right-hand axis) and the salvage-weighted average value across days (blue dashed line).

g)

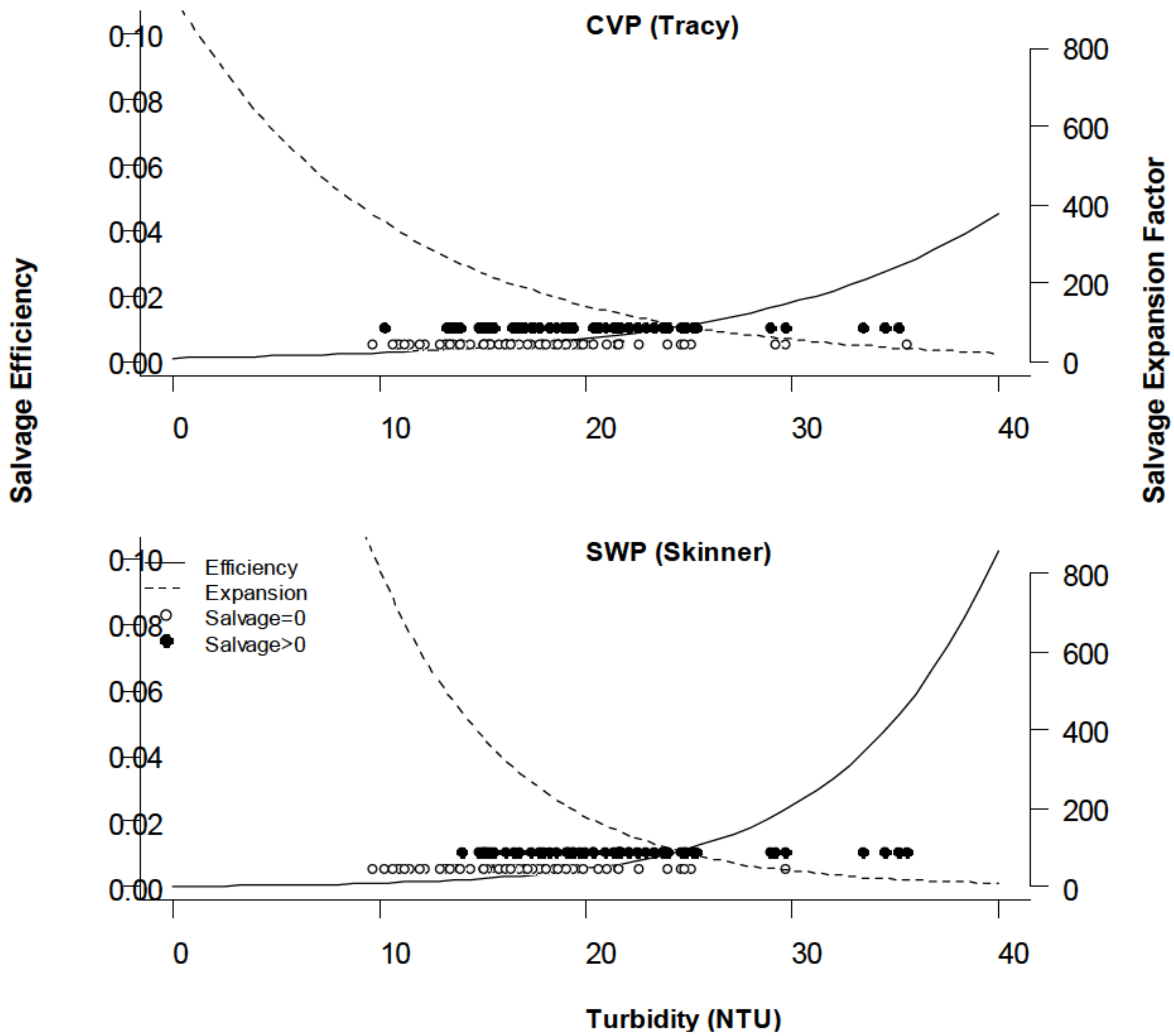

Figure 5. Con't. Estimated salvage efficiency-turbidity relationship (sold line, left-hand axis) and the inverse (expansion factor relationship, dashed line, right-hand axis). The solid and open points show the turbidity levels when salvage was and was not observed.

a)

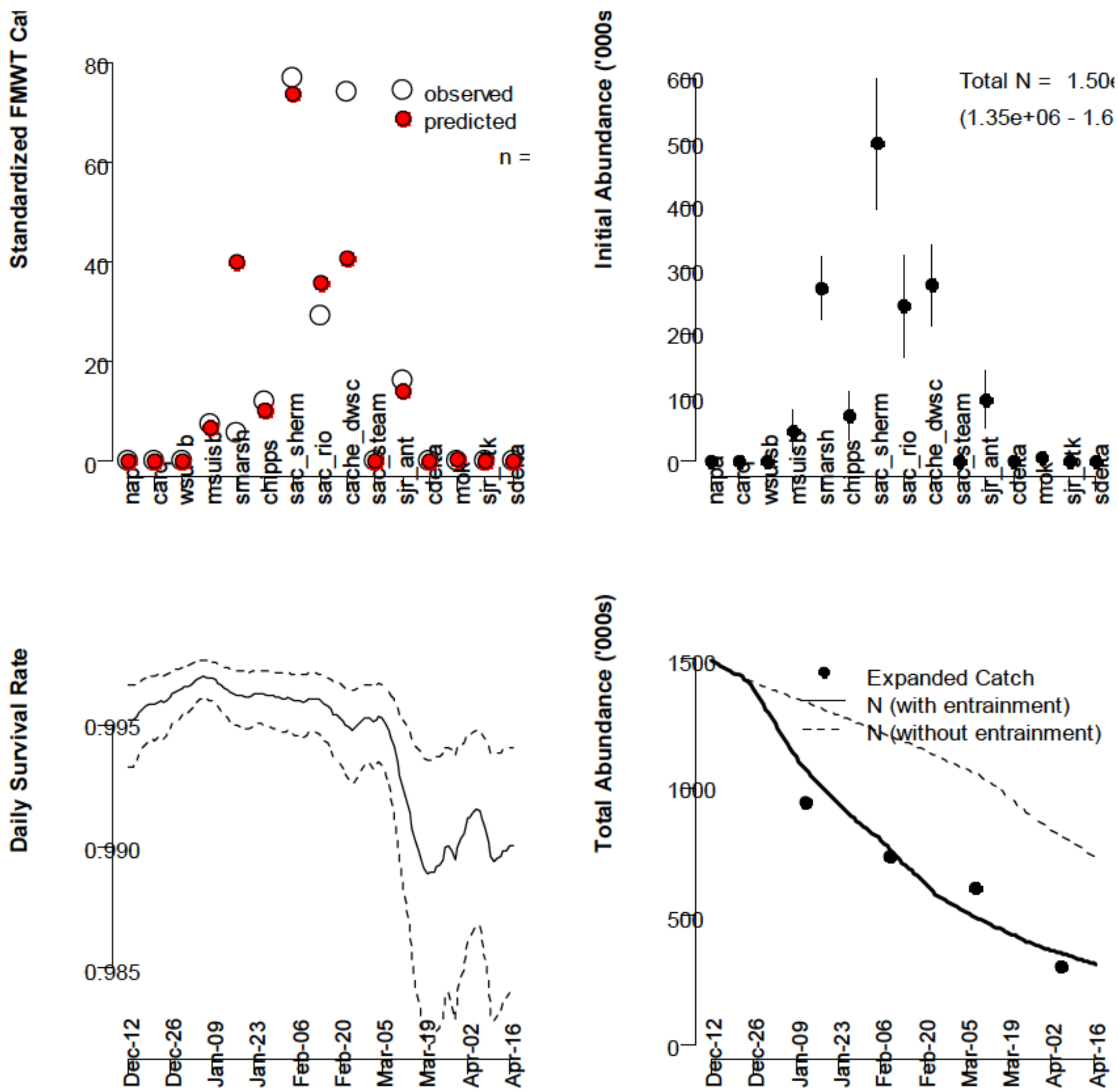

Figure 6. Model fit and predictions for the 2D-based PTM model 10 and population model 8 with poisson error in SKT catch data applied in water year 2004 (Table 4e). a) shows predicted and observed FMWT volume-corrected FMWT catch (top-left plot, observed catch summed across Sep, Oct, Nov, and Dec. surveys), regional population estimates with 95% credible intervals (top –right plot), predictions of the daily survival rate (solid line, bottom-left plot) with 95% credible intervals (dashed lines), and predicted total abundance across regions (bottom-right plot, solid and dashed lines) compared to estimates based on expanding the catch by the ratio of 4 m volume to the volume of tows.

b)

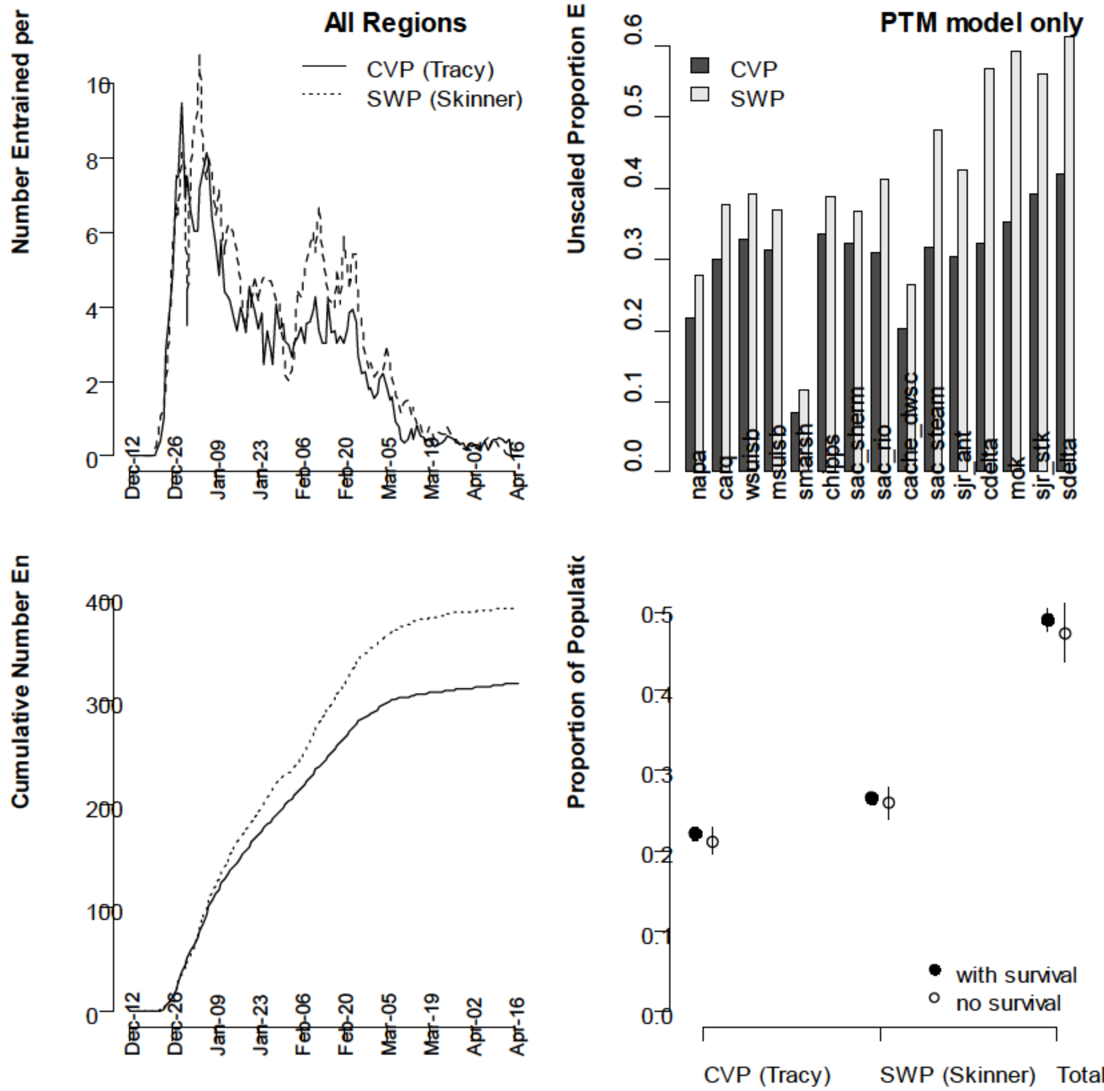

Figure 6. Con't. Predictions of daily salvage (left plots), the cumulative unscaled proportional entrainment for each region predicted by the PTM (top-right), and estimates of proportional entrainment (which include survival effects) and discrete proportional entrainment (which do not include survival effects as they are based on ratio of entrainment to initial abundance).

c)

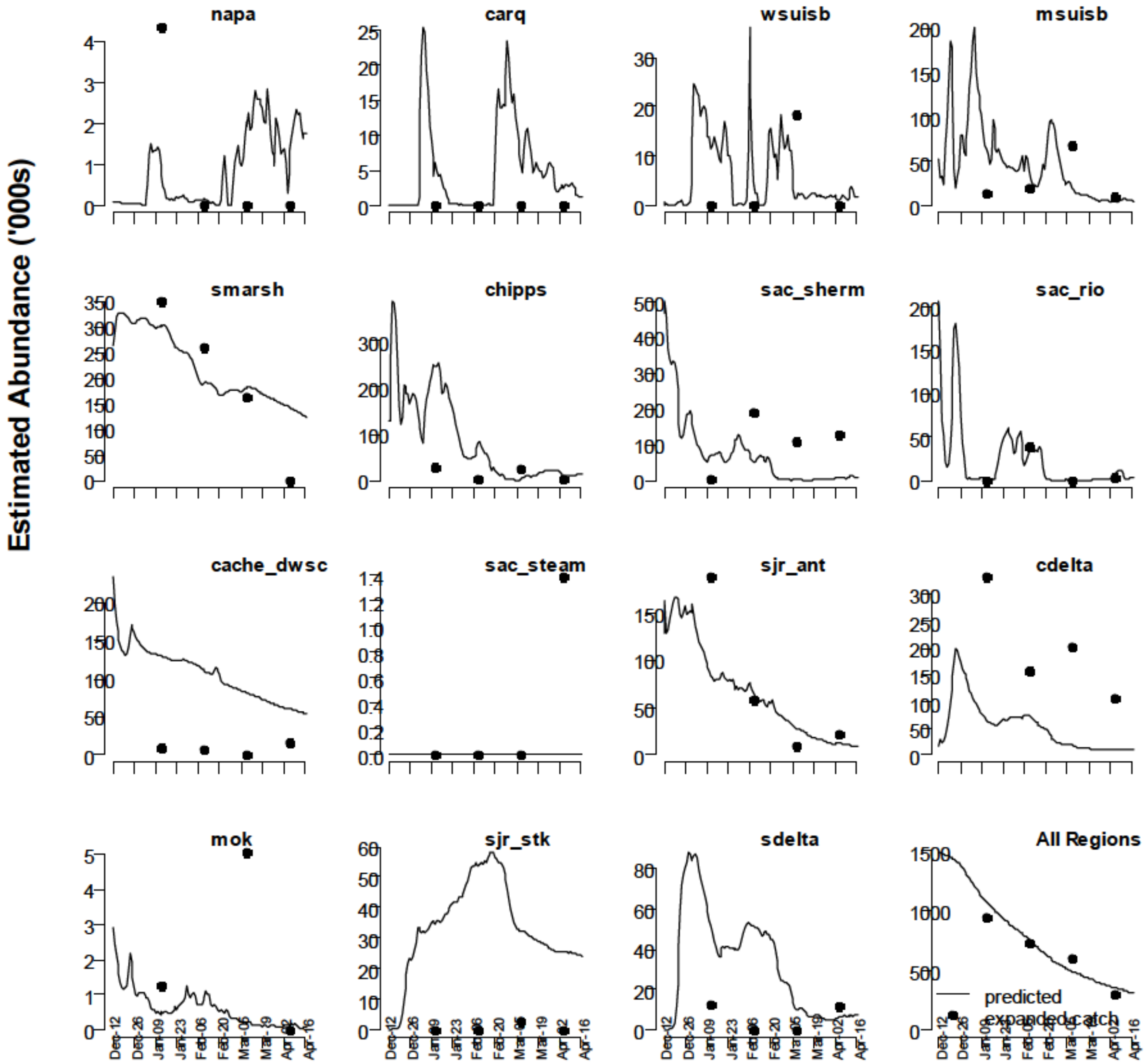

Figure 6. Con't. Abundance estimates by region and model day (lines) compared to estimates based on expanded catch (points).

d)

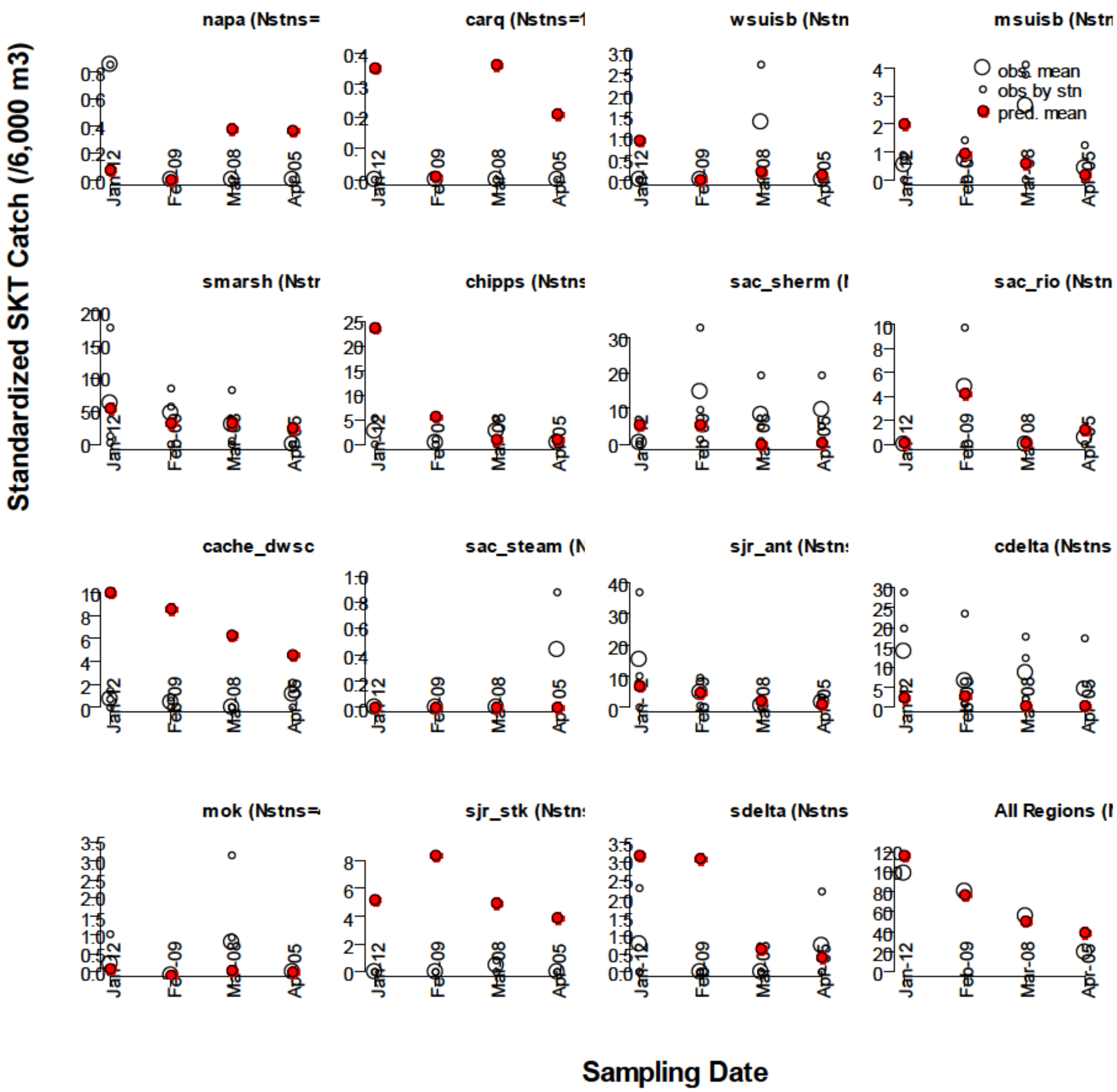

Figure 6. Con't. Comparison of predicted (red points) and mean observed (large open points) SKT catch by trip and region where catches are standardized by the approximate average tow volume. Also shown are the standardized station-specific standardized catches (small open points).

e)

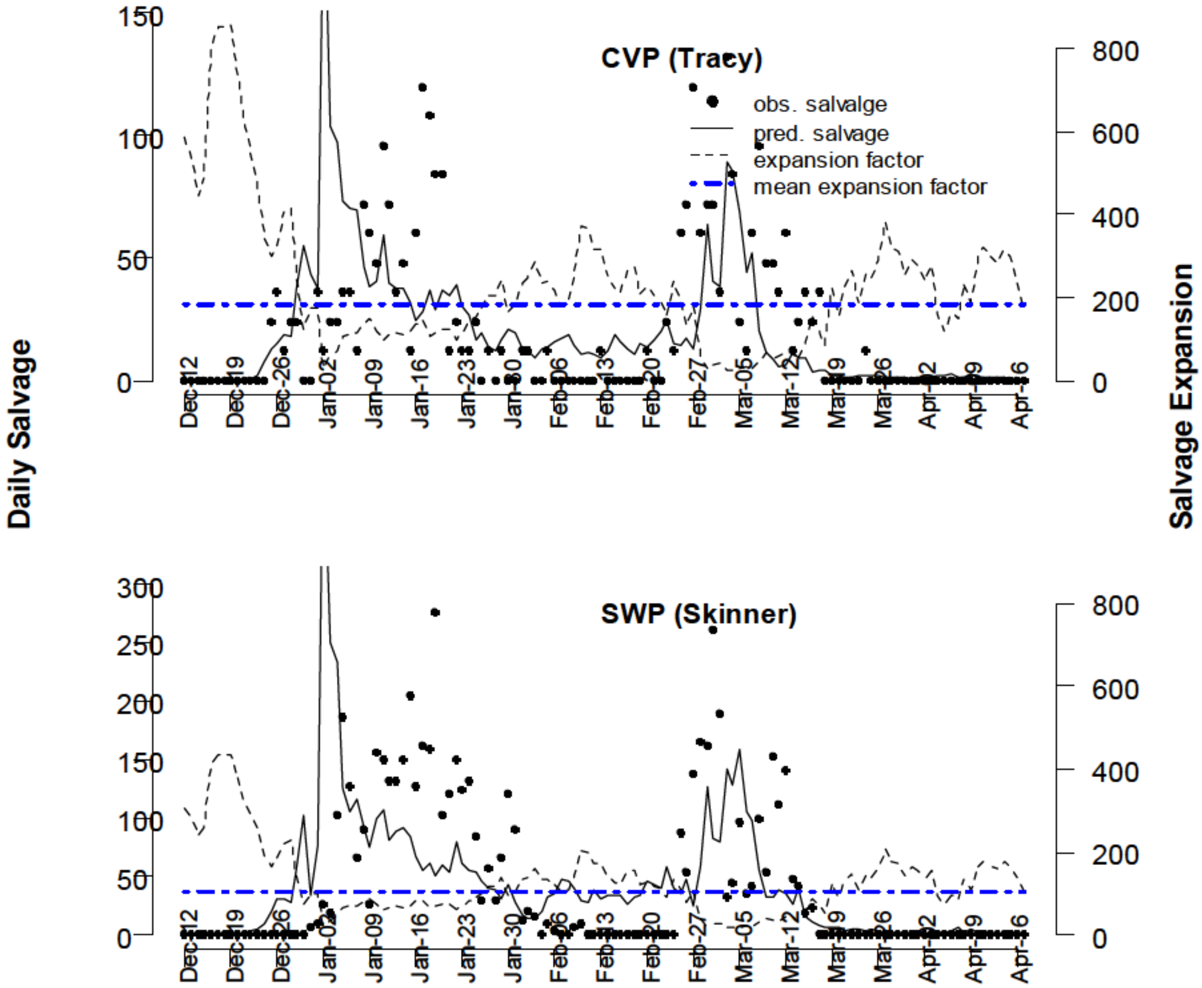

Figure 6. Con't. Predicted (solid line) and observed (points) daily salvage (left axis). Also shown are the daily salvage expansion factors ($1/\theta_S$, black dashed line right-hand axis) and the salvage-weighted average value across days (blue dashed line).

f)

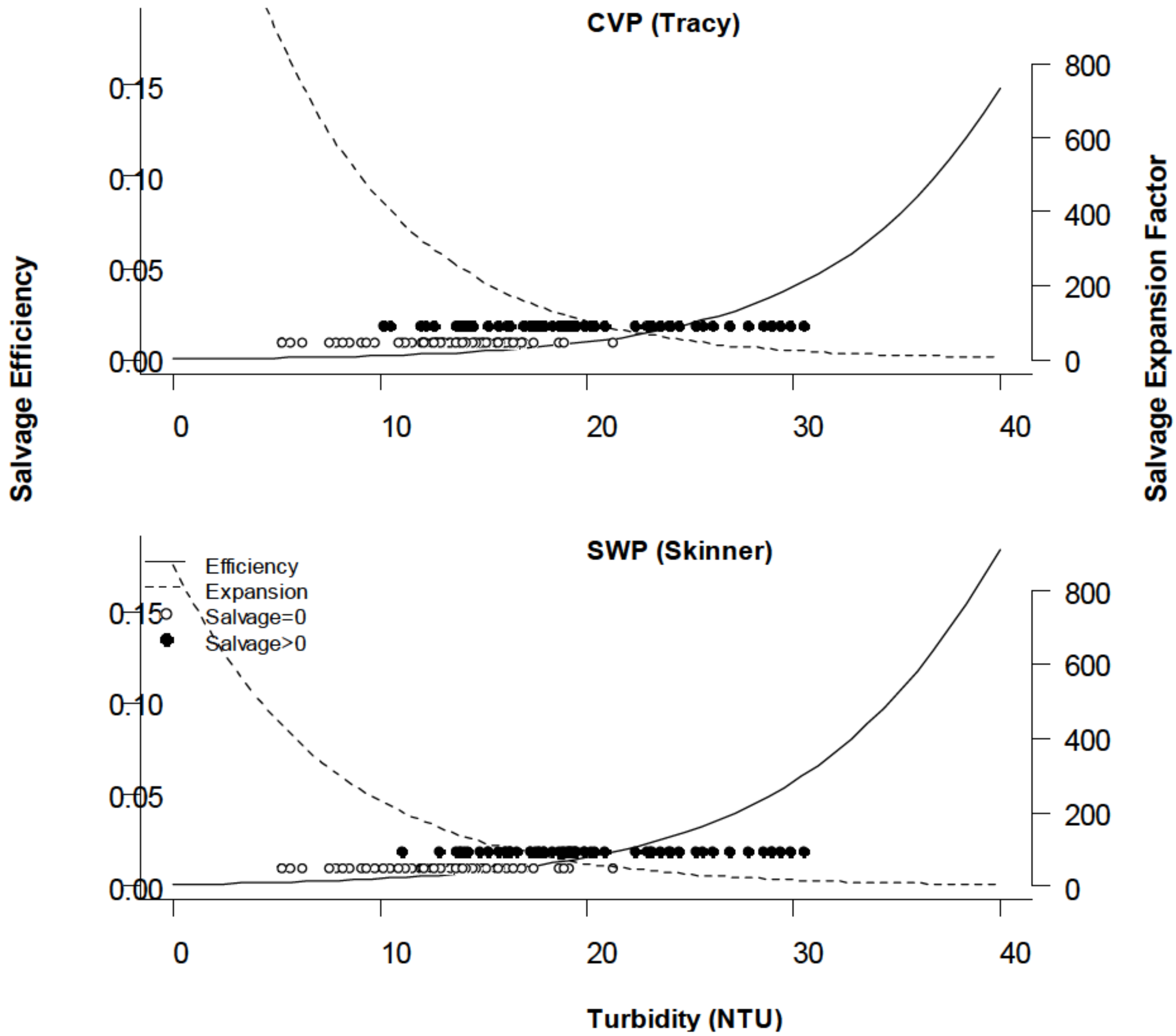

Figure 6. Con't. Estimated salvage efficiency-turbidity relationship (sold line, left-hand axis) and the inverse (expansion factor relationship, dashed line, right-hand axis). The solid and open points show the turbidity levels when salvage was and was not observed.

a)

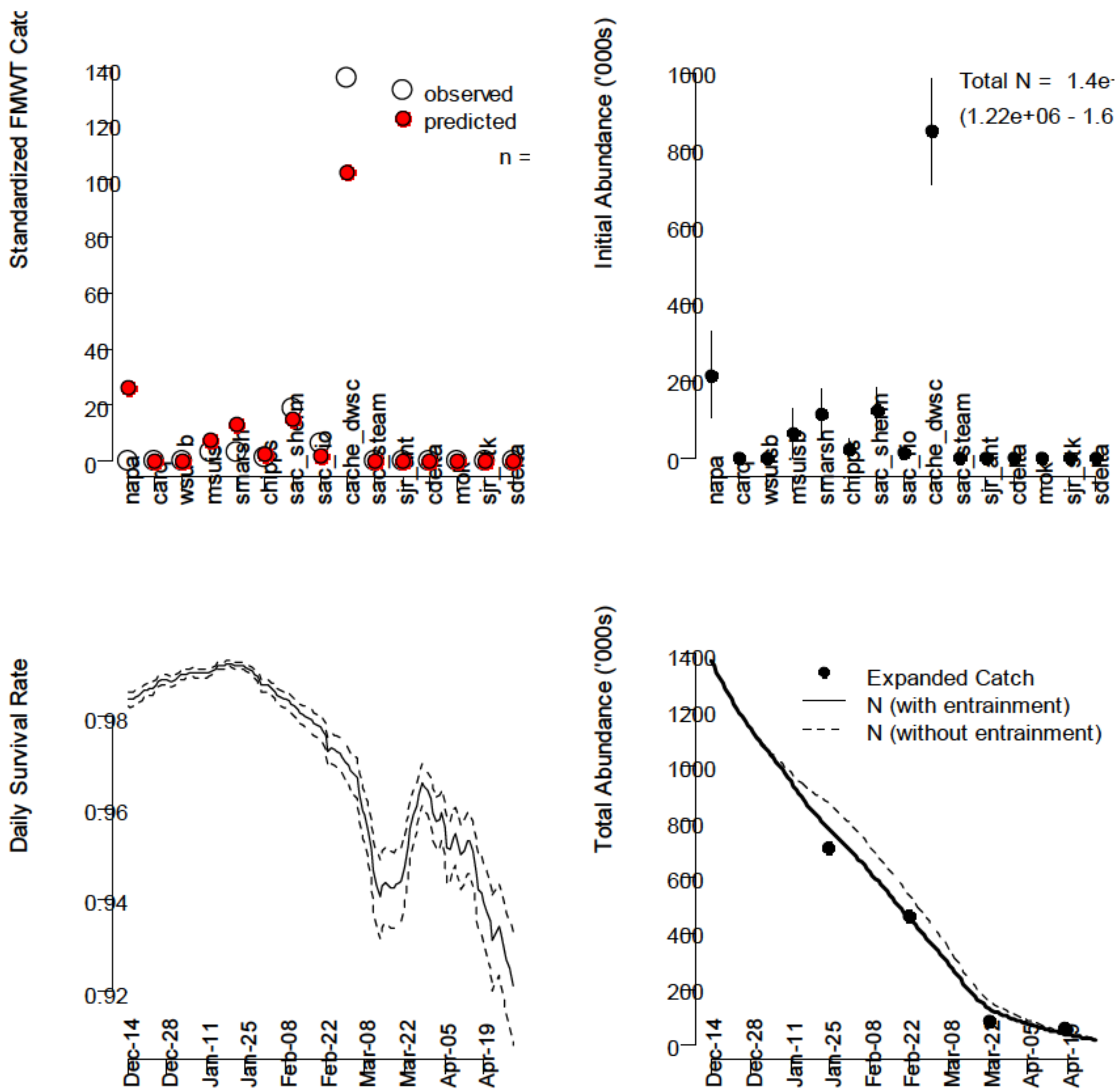

Figure 7. Model fit and predictions for the 2D-based PTM model 8 and population model 4 with poisson error in SKT catch data applied in water year 2005 (Table 4g). a) shows predicted and observed FMWT volume-corrected FMWT catch (top-left plot, observed catch summed across Sep, Oct, Nov, and Dec. surveys), regional population estimates with 95% credible intervals (top –right plot), predictions of the daily survival rate (solid line, bottom-left plot) with 95% credible intervals (dashed lines), and predicted total abundance across regions (bottom-right plot, solid and dashed lines) compared to estimates based on expanding the catch by the ratio of 4 m volume to the volume of tows.

b)

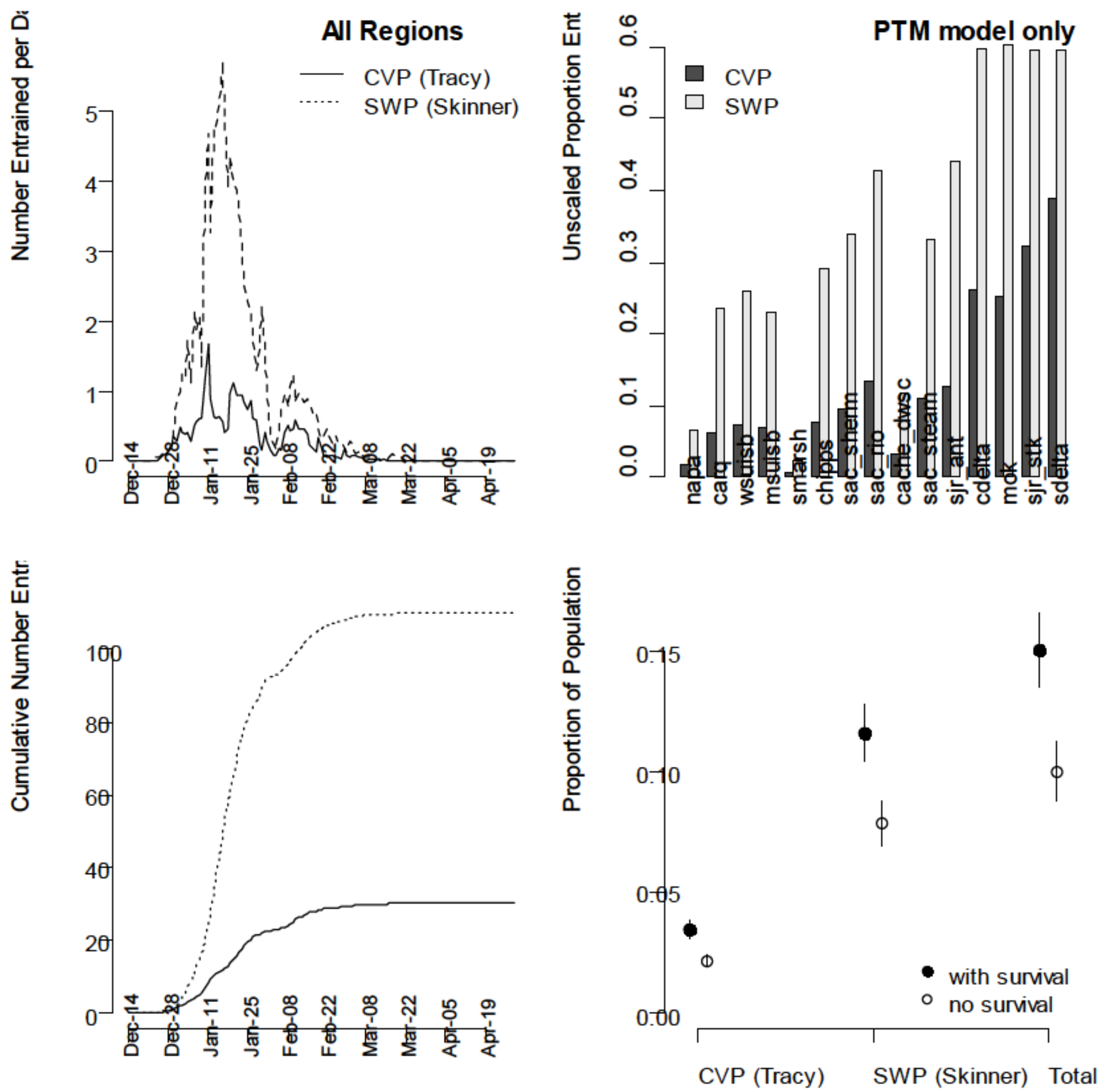

Figure 7. Con't. Predictions of daily salvage (left plots), the cumulative unscaled proportional entrainment for each region predicted by the PTM (top-right), and estimates of proportional entrainment (which include survival effects) and discrete proportional entrainment (which do not include survival effects as they are based on ratio of entrainment to initial abundance).

c)

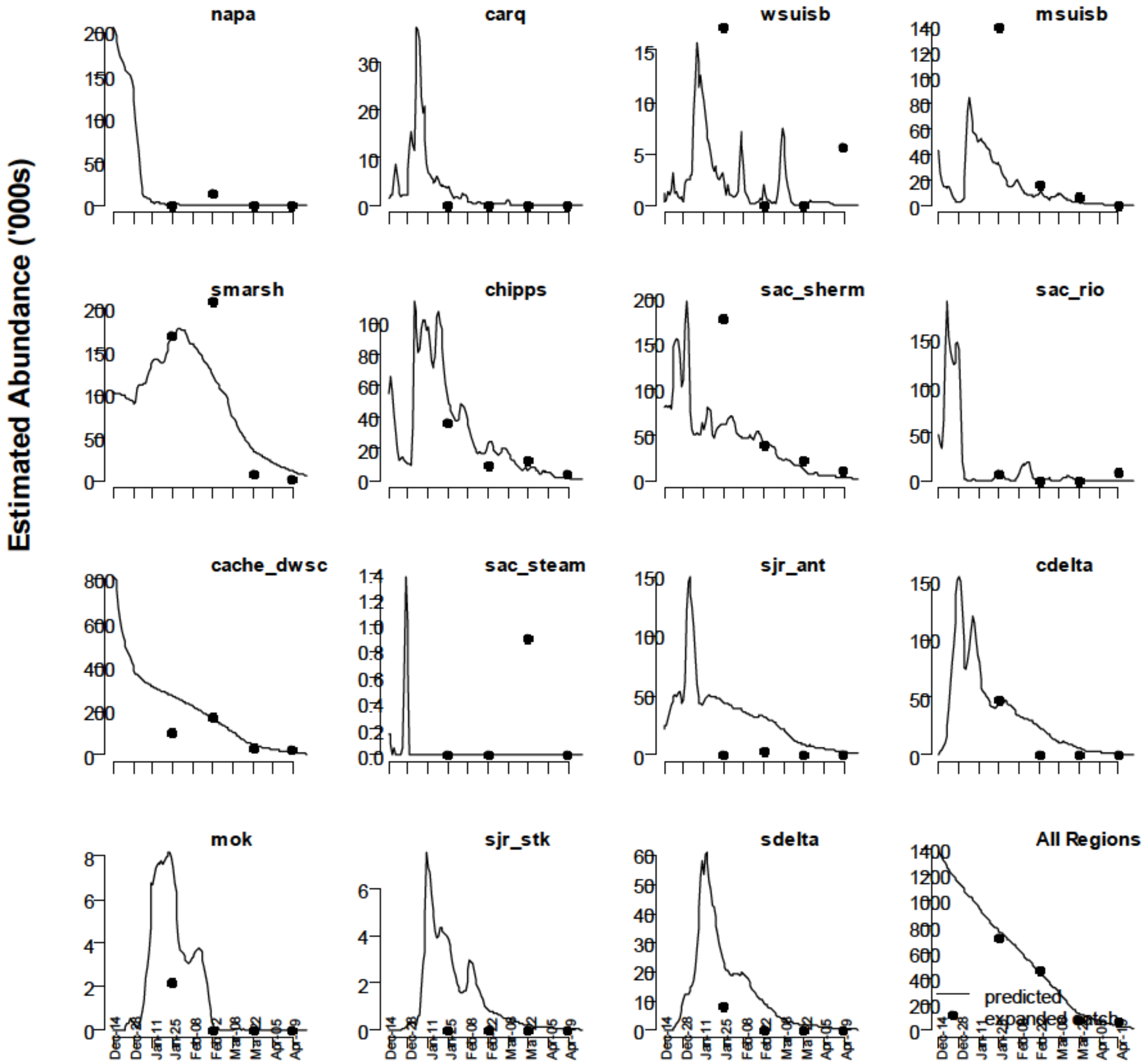

Figure 7. Con't. Abundance estimates by region and model day (lines) compared to estimates based on expanded catch (points).

d)

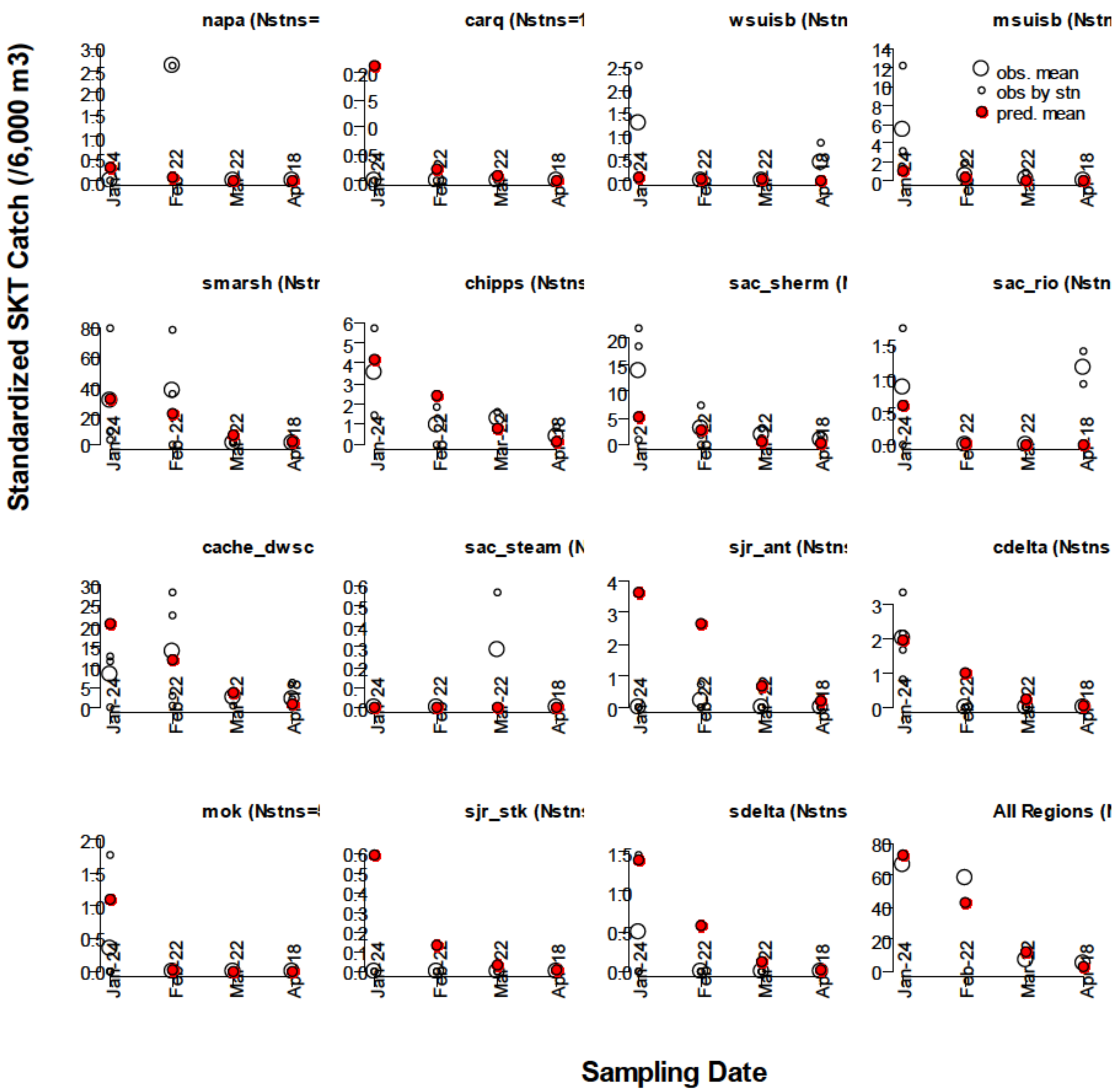

Figure 7. Con't. Comparison of predicted (red points) and mean observed (large open points) SKT catch by trip and region where catches are standardized by the approximate average tow volume. Also shown are the standardized station-specific standardized catches (small open points).

e)

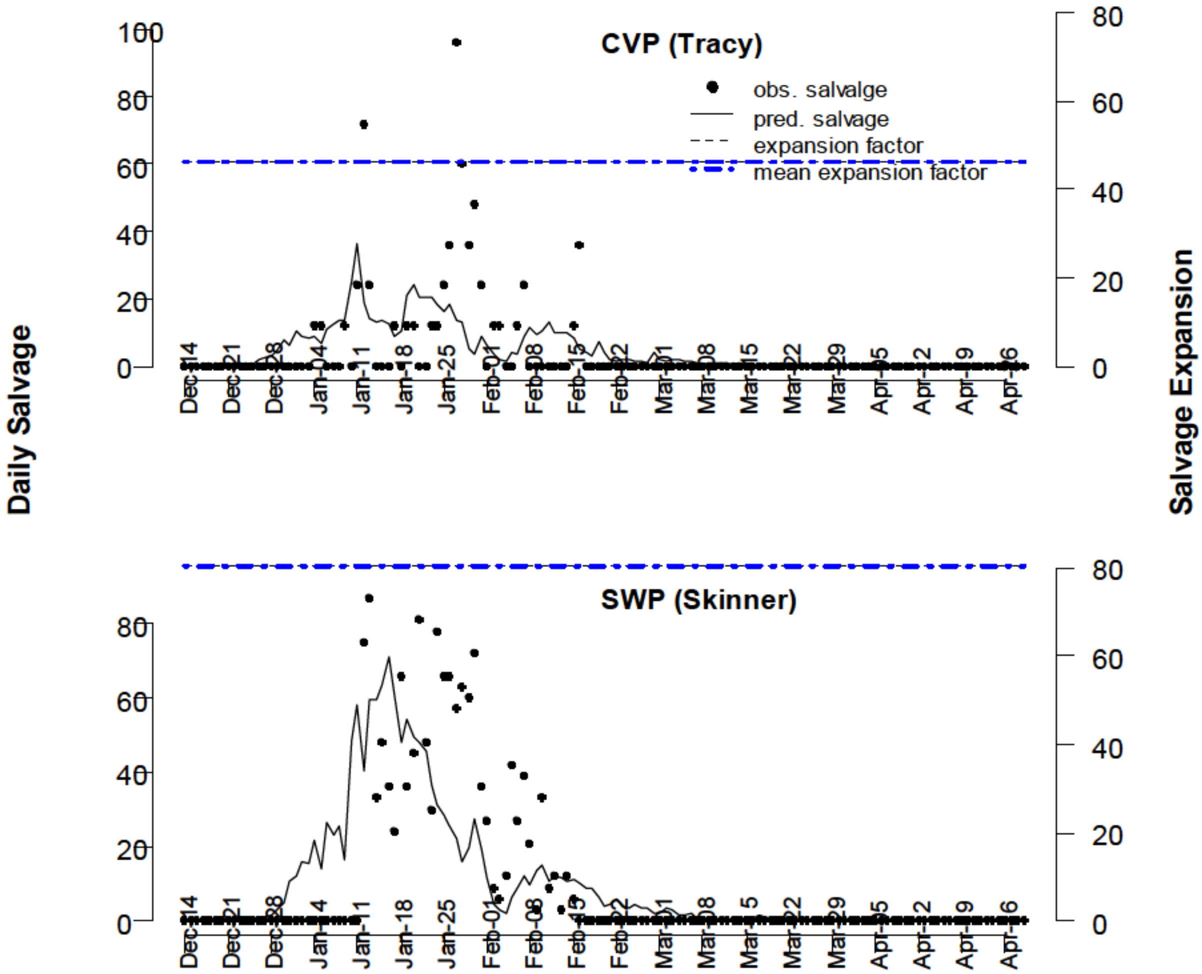

Figure 7. Con't. Predicted (solid line) and observed (points) daily salvage (left axis). Also shown are the daily salvage expansion factors ($1/\theta_S$, black dashed line right-hand axis) and the salvage-weighted average value across days (blue dashed line).

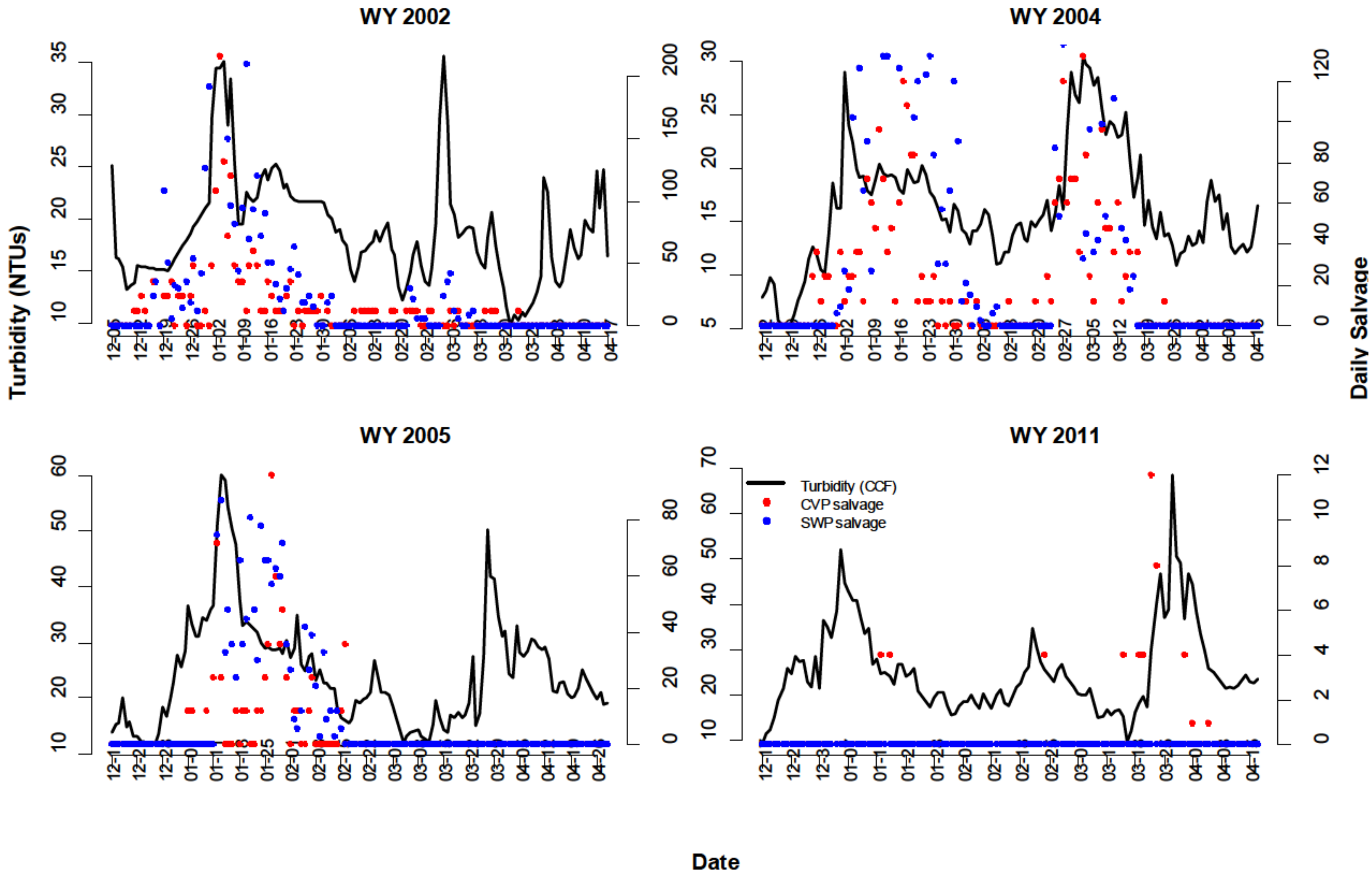

Figure 8. Relationship between turbidity measured at Clifton Court Forebay (CCF) and observed daily salvage at federal (CVP) and state (SWP) fish collection facilities.

a)

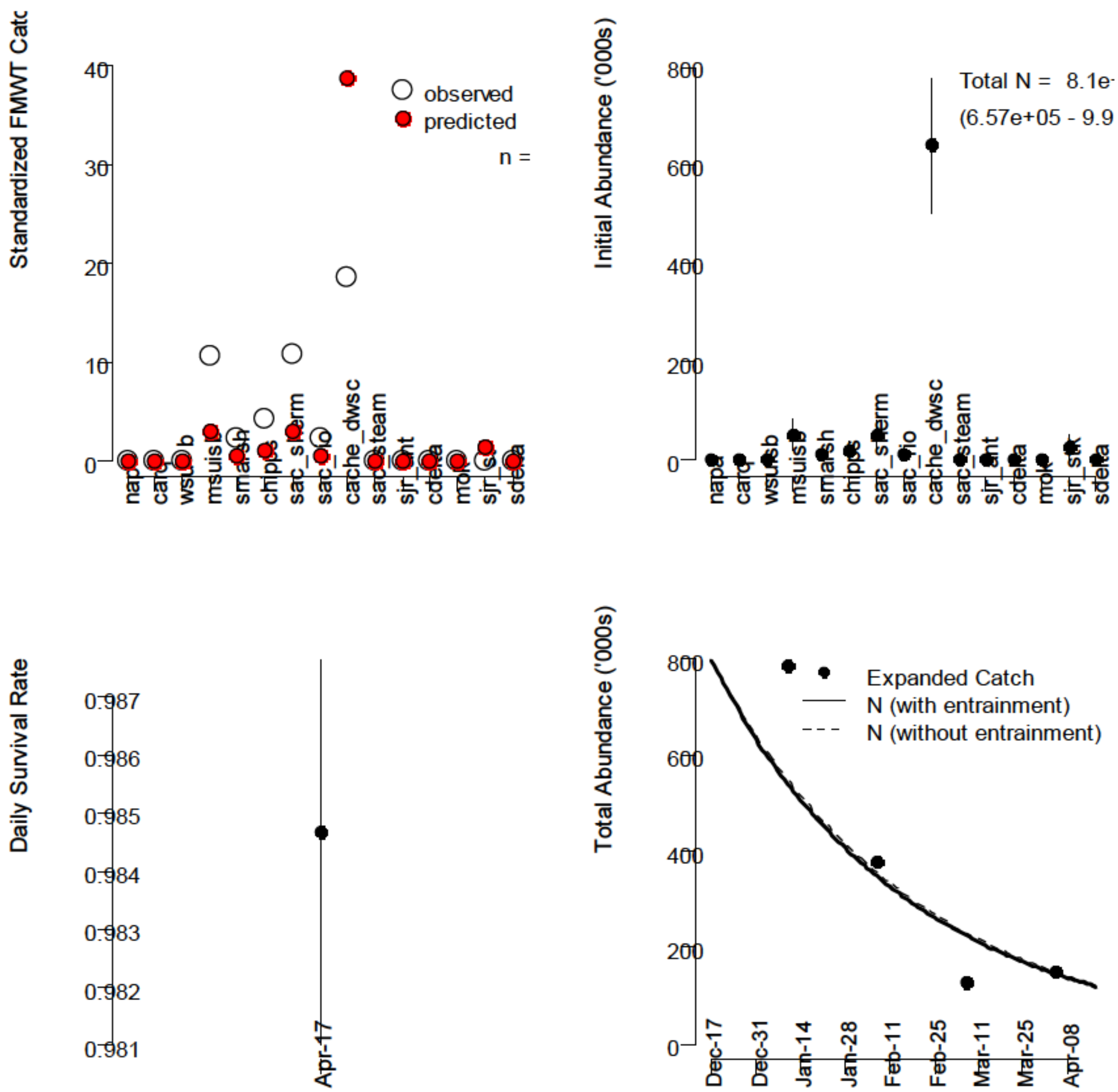

Figure 9. Model fit and predictions for the 2D-based PTM model 6 and population model 1 with poisson error in SKT catch data applied in water year 2011 (Table 4i). a) shows predicted and observed FMWT volume-corrected FMWT catch (top-left plot, observed catch summed across Sep, Oct, Nov, and Dec. surveys), regional population estimates with 95% credible intervals (top –right plot), predictions of the daily survival rate (solid line, bottom-left plot) with 95% credible intervals (dashed lines), and predicted total abundance across regions (bottom-right plot, solid and dashed lines) compared to estimates based on expanding the catch by the ratio of 4 m volume to the volume of tows.

b)

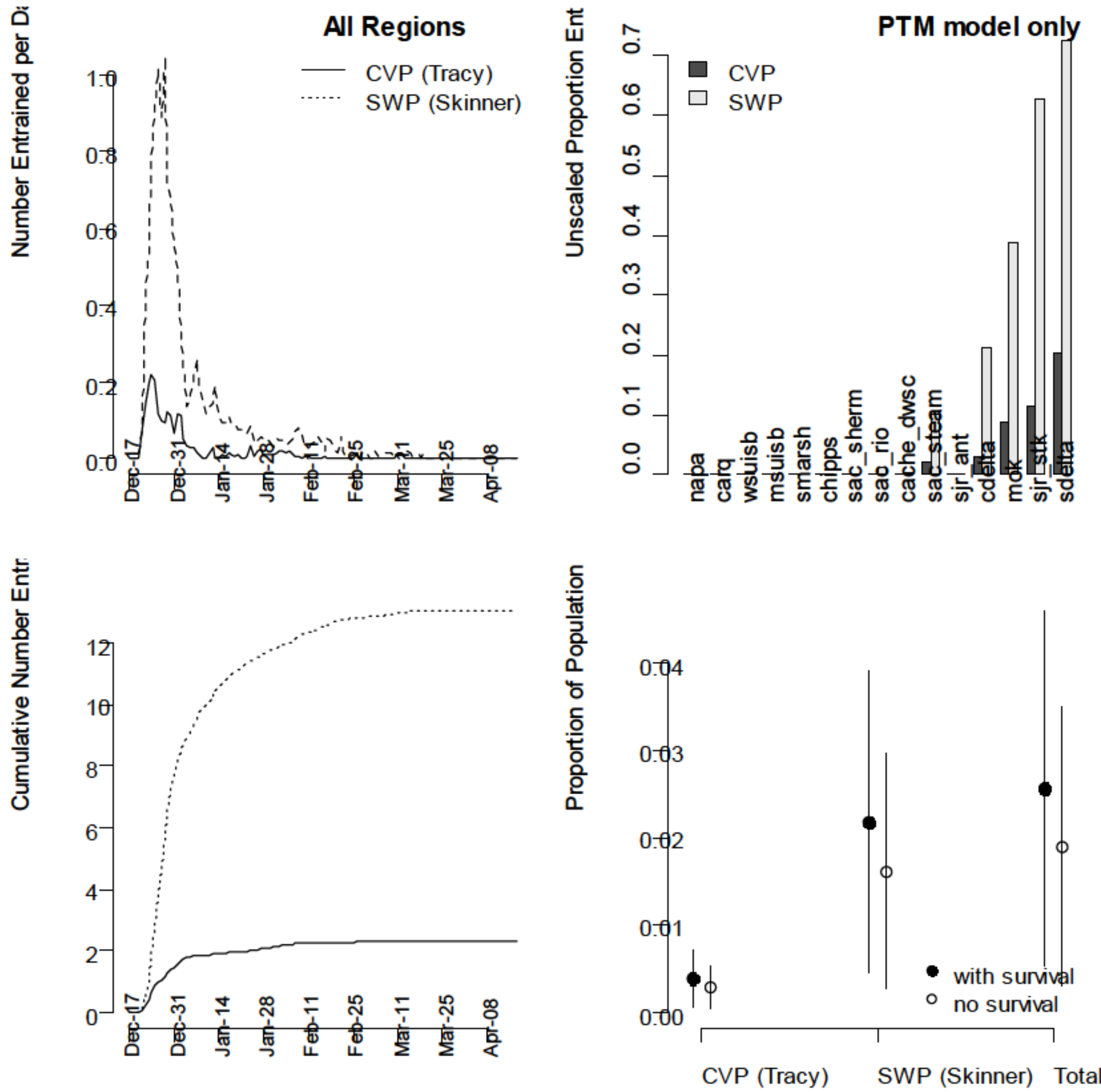

Figure 9. Con't. Predictions of daily salvage (left plots), the cumulative unscaled proportional entrainment for each region predicted by the PTM (top-right), and estimates of proportional entrainment (which include survival effects) and discrete proportional entrainment (which do not include survival effects as they are based on ratio of entrainment to initial abundance).

c)

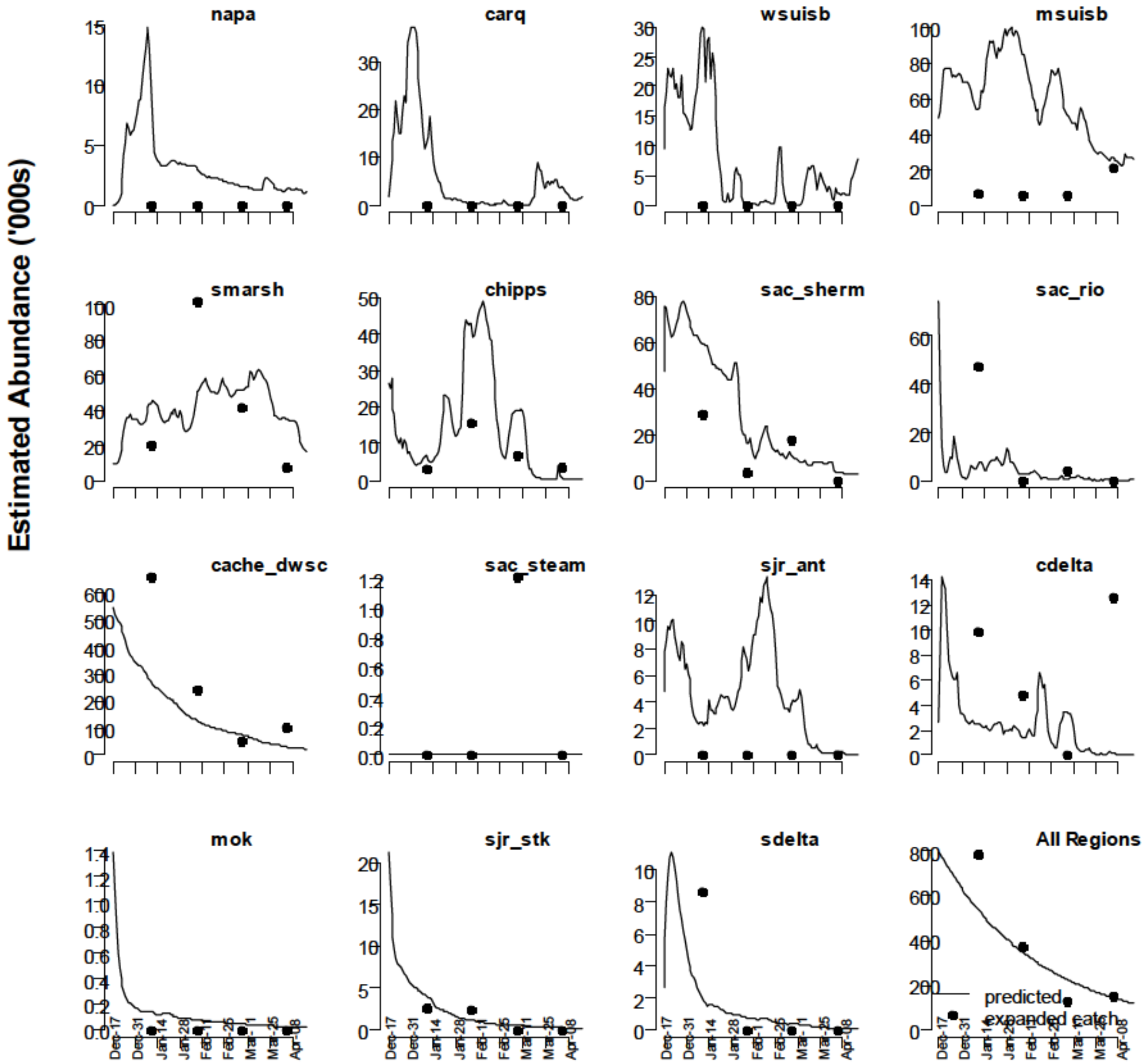

Figure 9. Con't. Abundance estimates by region and model day (lines) compared to estimates based on expanded catch (points).

d)

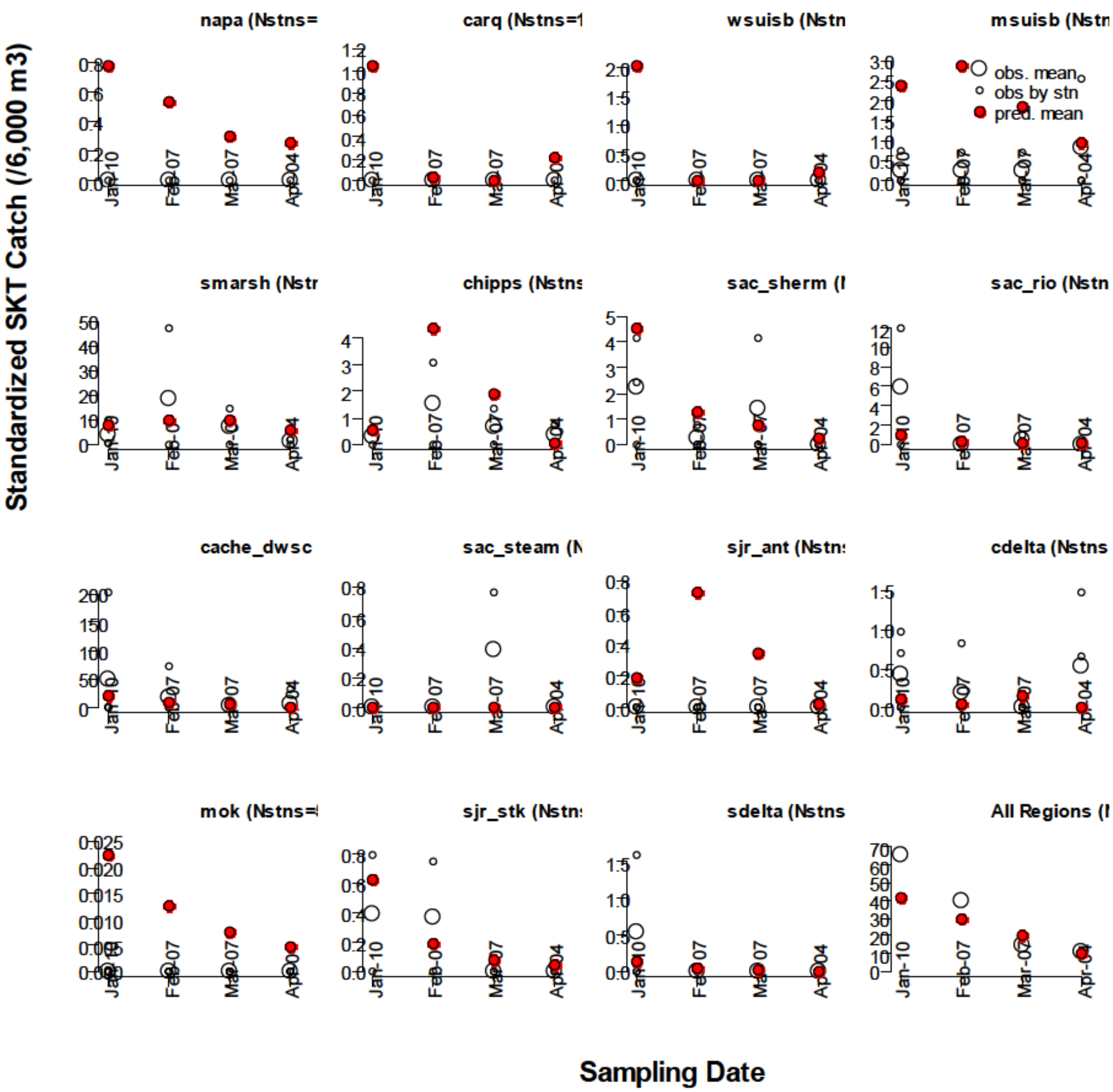

Figure 9. Con't. Comparison of predicted (red points) and mean observed (large open points) SKT catch by trip and region where catches are standardized by the approximate average tow volume. Also shown are the standardized station-specific standardized catches (small open points).

e)

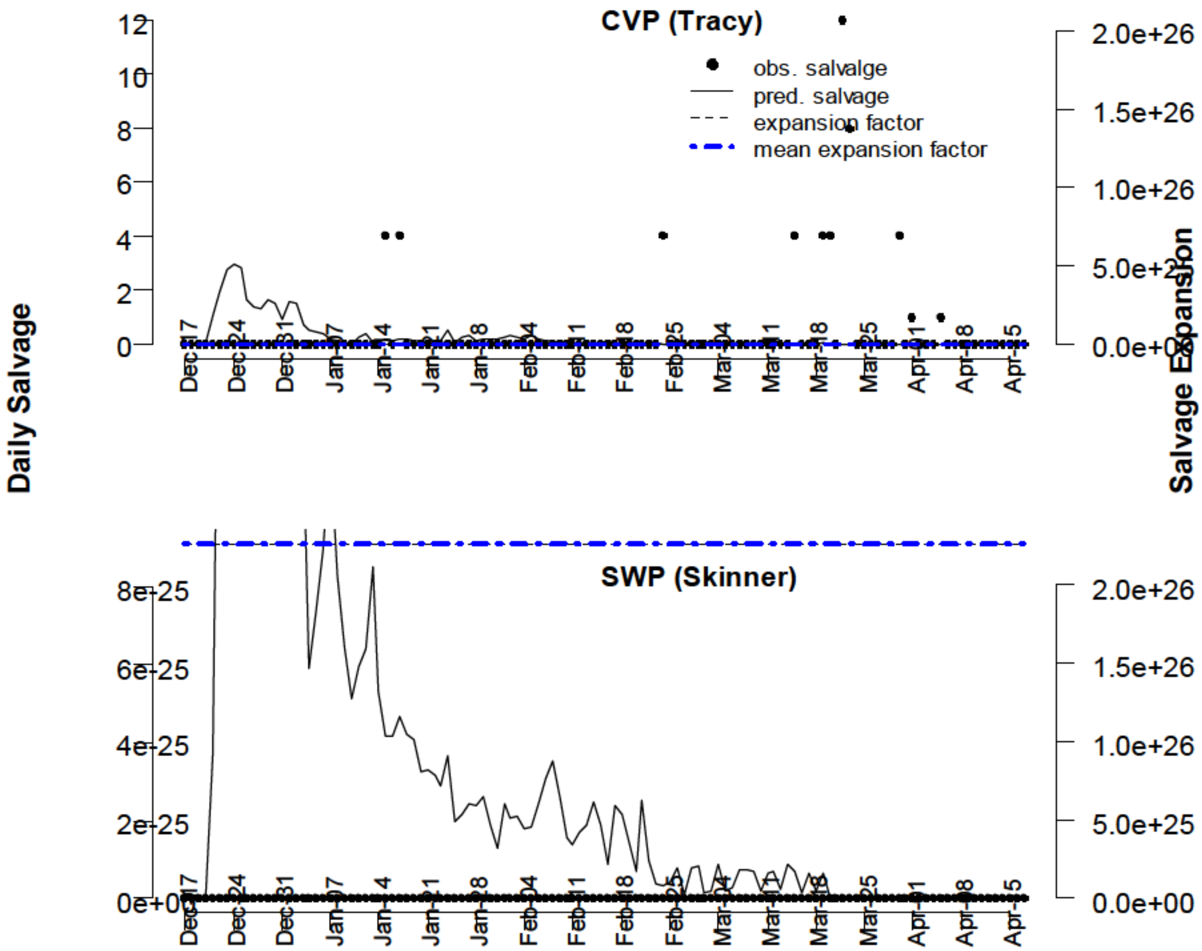

Figure 9. Con't. Predicted (solid line) and observed (points) daily salvage (left axis). Also shown are the daily salvage expansion factors ($1/\theta_S$, black dashed line right-hand axis) and the salvage-weighted average value across days (blue dashed line).

a)

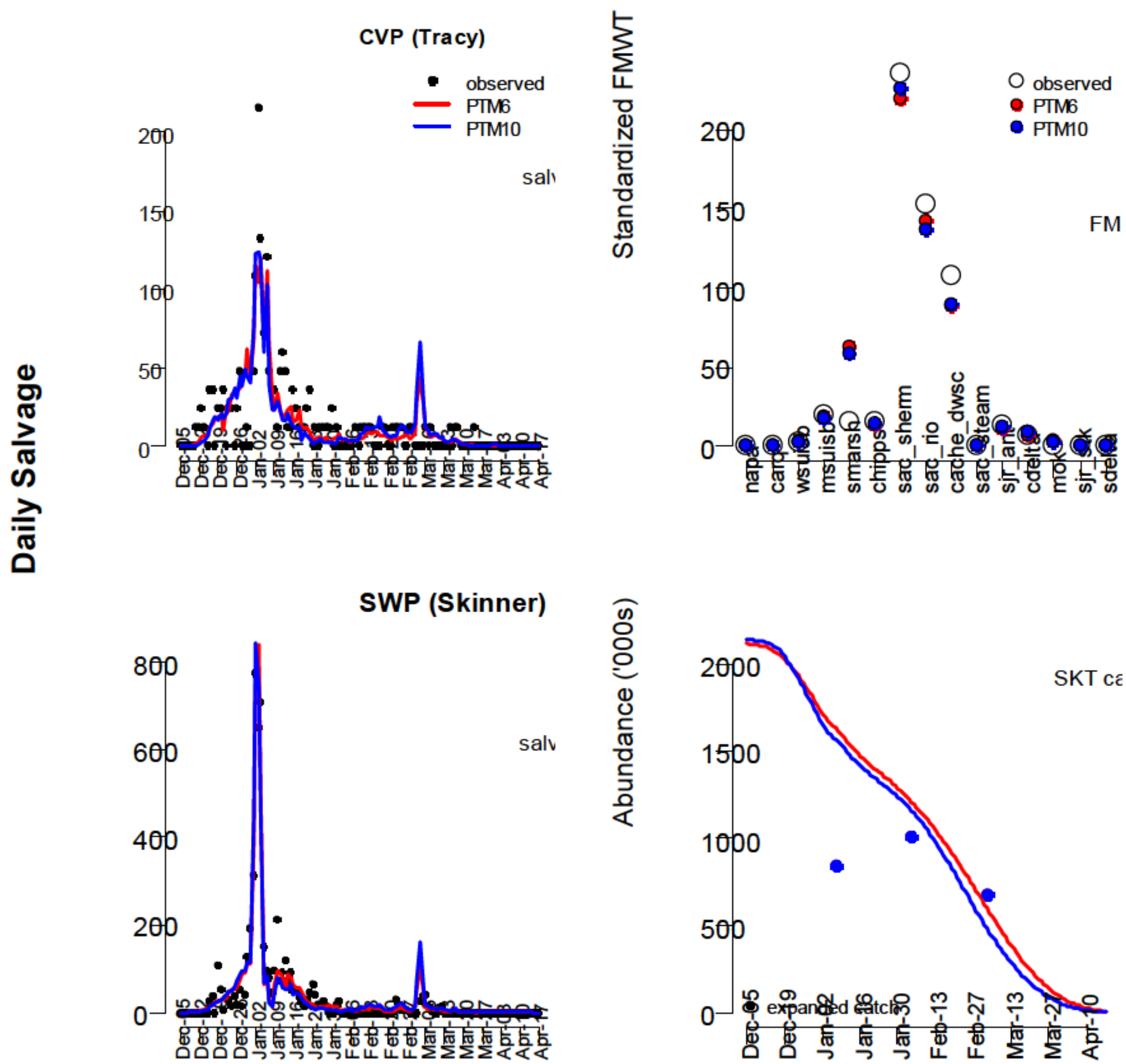

Figure 10. Comparison of fit 3D PTMs 6 (red, 1st ranked) and 10 (blue, 2nd-ranked) for water year 2002 assuming poisson (τ=1) error in SKT catch data. Results are based on population model 7 (Table 4) where daily survival rate is a smooth function of model day and salvage expansion factors depend on turbidity. a) shows the fit to salvage and FMWT data and to expanded estimates of abundance from SKT data. b) compares predicted and observed SKT catches.

b)

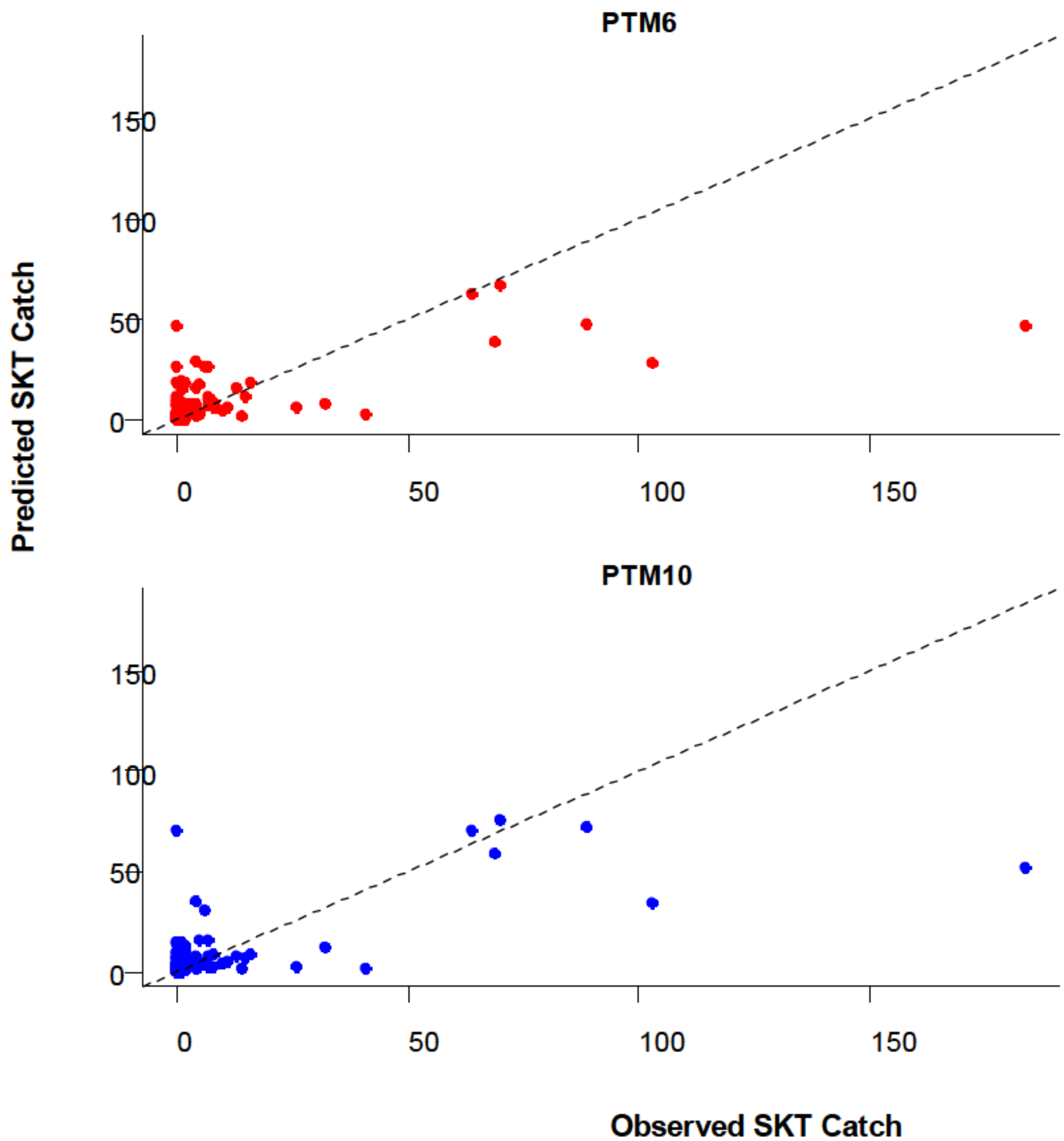

Figure 10. Con't.

a)

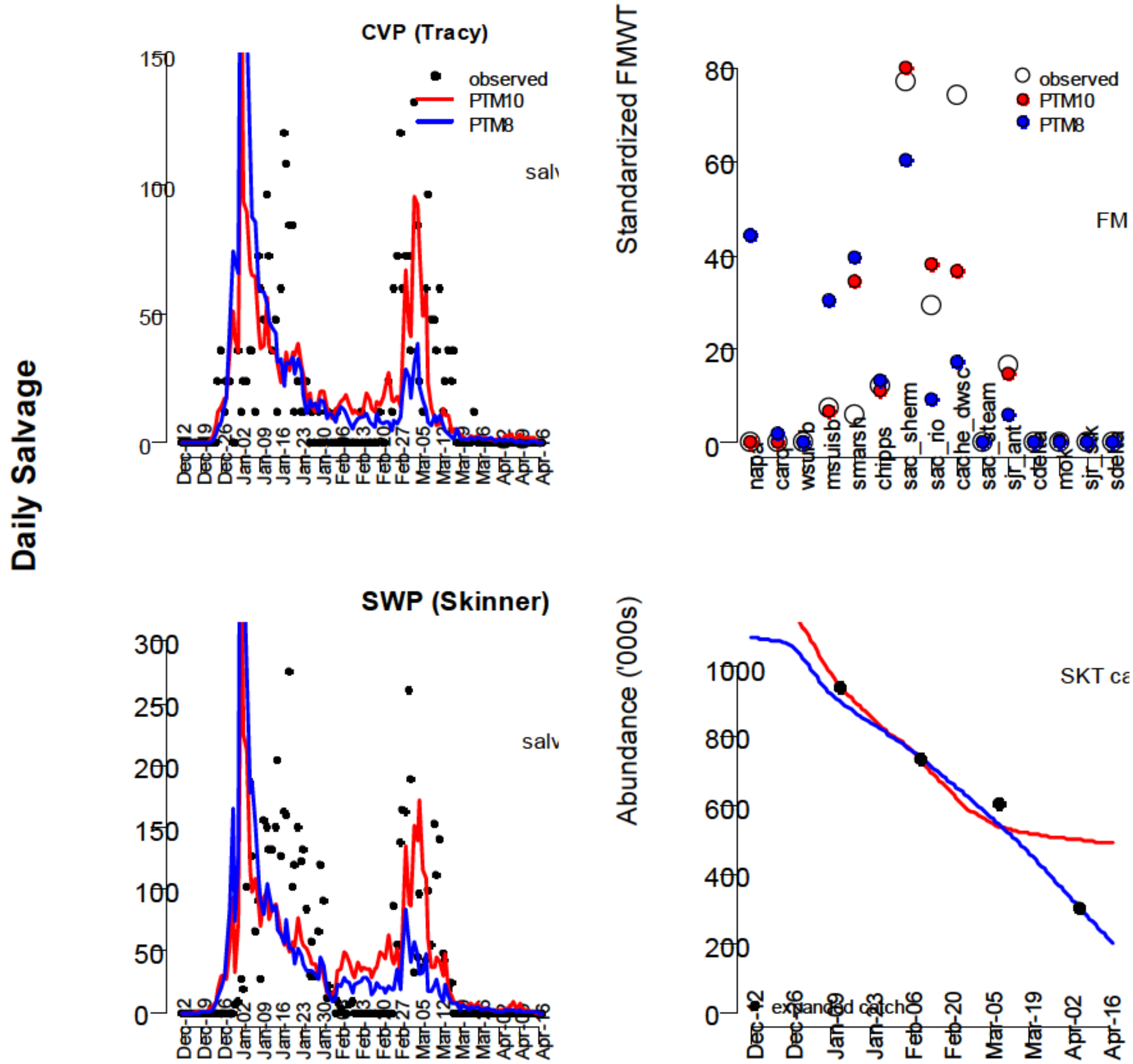

Figure 11. Comparison of fit 2D PTMs 10 (red, 1st ranked) and 8 (blue, 2nd-ranked) for water year 2004 assuming poisson (τ=1) error in SKT catch data. Results are based on population model 7 (Table 4) where daily survival rate is a smooth function of model day and salvage expansion factors depend on turbidity. a) shows the fit to salvage and FMWT data and to expanded estimates of abundance from SKT data. b) compares predicted and observed SKT catches.

b)

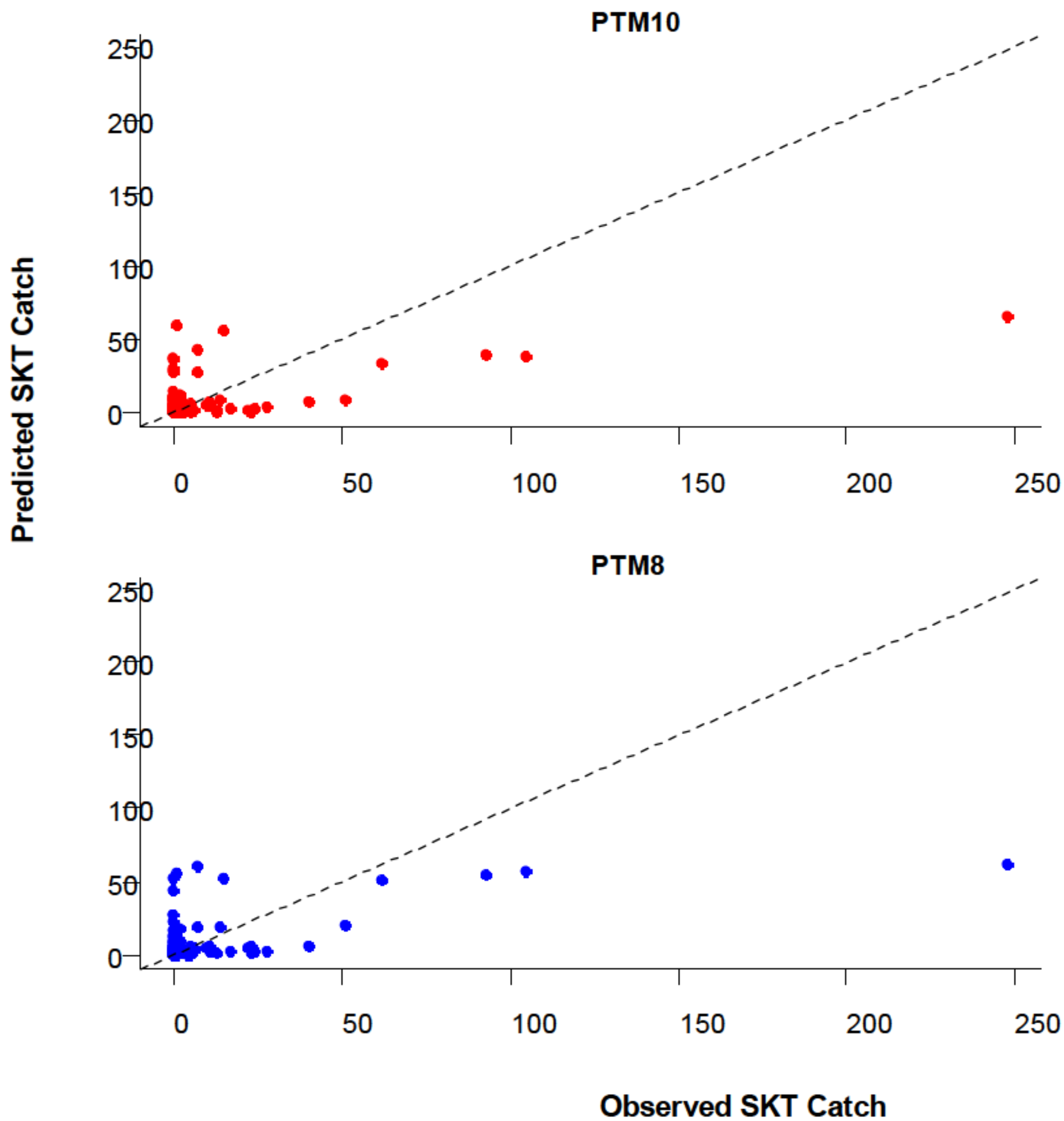

Figure 11. Con't.

Appendix A. Supplemental Tables

Table A1. Proportion of variability in observations explained by different combinations of particle tracking models (rows, see Table 2) and population dynamic models (columns) by water year and PTM type (2D or 3D), assuming poisson error in SKT catch data (variance-to-mean ratio of τ=1) or negative binomial error (τ=10). The table shows the square of the Pearson correlation coefficient quantifying the fit to the relative differences in Fall Midwater Trawl catch among regions (FMWT), the average Spring Kodiak Trawl catch by region and survey(SKT), and the daily expanded salvage at federal (CVP Salvage) and state (SWP salvage) fish collection facilities. #DIV/0! denote that r^2 values could not be computed because there were no salvage observations.

Table A1. Con't.

a) 3D WY 2002 Poisson error in SKT data (τ=1)

Population model number	1	2	3	4	5	6	7	8	9	10
Salvage efficiency structure	const	const	const	const	~turb	~turb	~turb	~turb	const	~turb
Natural survival structure	S_c	S_{SKT}	S_d	S_W	S_c	S_{SKT}	S_d	S_W	S_d	S_d
SKT efficiency structure ($\theta_{c\text{-}SKT}$)	=1	=1	=1	=1	=1	=1	=1	=1	~Secchi	~Secchi
FMWT relative catch across regions										
1) passive	0.74	0.74	0.74	0.74	0.81	0.81	0.81	0.81	0.77	0.85
2) turbidity seeking	0.88	0.88	0.86	0.89	0.89	0.89	0.89	0.89	0.98	0.98
3) tmd	0.62	0.62	0.62	0.62	0.69	0.69	0.69	0.69	0.63	0.85
4) ptmd_sal_gt_1	0.95	0.96	0.96	0.95	0.96	0.97	0.97	0.97	0.97	0.98
5) ptmd si pt 5	0.97	0.98	0.98	0.96	1.00	1.00	1.00	1.00	0.98	1.00
6) ptmd si pt 5 shallow ebb t gt 12	0.93	0.94	0.94	0.93	0.96	0.96	0.96	0.96	0.96	0.98
7) ptmd_sal_gt_1_si_pt_5	0.96	0.98	0.98	0.96	0.99	0.99	0.99	0.99	0.98	0.99
8) ptmd_sal_gt_1_h8_ebb_shallow_t_gt_18_acclim	0.91	0.91	0.91	0.91	0.94	0.95	0.94	0.94	0.91	0.95
9) tmd sal gt 1 ebb shallow t gt 18	0.97	0.97	0.97	0.97	0.99	0.99	0.98	0.99	0.98	0.99
10) tmd sal gt 1 ptmd prtmd sd pt 1 switch	0.97	0.97	0.97	0.97	0.97	0.97	0.97	0.97	0.98	0.98
SKT catch by survey and region										
1) passive	0.59	0.59	0.59	0.59	0.58	0.58	0.59	0.59	0.59	0.59
2) turbidity seeking	0.79	0.79	0.83	0.81	0.80	0.85	0.82	0.81	0.67	0.69
3) tmd	0.57	0.62	0.57	0.57	0.57	0.61	0.57	0.57	0.57	0.59
4) ptmd_sal_gt_1	0.60	0.67	0.64	0.62	0.63	0.69	0.66	0.64	0.68	0.69
5) ptmd_si_pt_5	0.37	0.48	0.45	0.41	0.40	0.51	0.47	0.44	0.51	0.54
6) ptmd si pt 5 shallow ebb t gt 12	0.71	0.77	0.78	0.75	0.73	0.81	0.79	0.76	0.79	0.80
7) ptmd sal gt 1 si pt 5	0.62	0.72	0.72	0.67	0.67	0.78	0.74	0.71	0.72	0.75
8) ptmd sal gt 1 h8 ebb shallow t gt 18 acclim	0.75	0.77	0.75	0.75	0.75	0.76	0.74	0.74	0.75	0.75
9) tmd_sal_gt_1_ebb_shallow_t_gt_18	0.76	0.80	0.76	0.76	0.76	0.79	0.76	0.76	0.76	0.76
10) tmd_sal_gt_1_ptmd_prtmd_sd_pt_1_switch	0.71	0.76	0.78	0.75	0.75	0.84	0.80	0.78	0.78	0.80
CVP Salvage										
1) passive	0.22	0.22	0.22	0.22	0.63	0.63	0.63	0.63	0.21	0.62
2) turbidity_seeking	0.06	0.07	0.07	0.06	0.52	0.53	0.53	0.52	0.09	0.50
3) tmd	0.02	0.02	0.02	0.02	0.67	0.67	0.67	0.67	0.02	0.66
4) ptmd sal gt 1	0.13	0.17	0.17	0.14	0.64	0.66	0.65	0.64	0.17	0.65
5) ptmd si pt 5	0.16	0.22	0.21	0.17	0.55	0.58	0.57	0.55	0.20	0.57
6) ptmd_si_pt_5_shallow_ebb_t_gt_12	0.23	0.28	0.27	0.24	0.63	0.64	0.63	0.63	0.27	0.63
7) ptmd_sal_gt_1_si_pt_5	0.13	0.18	0.17	0.14	0.59	0.62	0.60	0.59	0.17	0.61
8) ptmd sal gt 1 h8 ebb shallow t gt 18 acclim	0.09	0.09	0.09	0.09	0.65	0.65	0.66	0.66	0.09	0.66
9) tmd sal gt 1 ebb shallow t gt 18	0.10	0.10	0.10	0.10	0.57	0.57	0.57	0.57	0.10	0.57
10) tmd sal gt 1 ptmd prtmd sd pt 1 switch	0.14	0.19	0.18	0.15	0.63	0.66	0.64	0.63	0.18	0.64
SWP Salvage										
1) passive	0.26	0.26	0.27	0.26	0.90	0.90	0.90	0.90	0.26	0.90
2) turbidity seeking	0.01	0.01	0.01	0.01	0.66	0.67	0.66	0.66	0.02	0.69
3) tmd	0.02	0.02	0.02	0.02	0.75	0.75	0.75	0.75	0.02	0.76
4) ptmd_sal_gt_1	0.28	0.32	0.32	0.29	0.89	0.90	0.90	0.89	0.32	0.90
5) ptmd si pt 5	0.30	0.36	0.35	0.31	0.88	0.89	0.89	0.88	0.35	0.89
6) ptmd si pt 5 shallow ebb t gt 12	0.32	0.36	0.35	0.33	0.90	0.91	0.91	0.90	0.35	0.91
7) ptmd sal gt 1 si pt 5	0.29	0.35	0.34	0.30	0.87	0.89	0.88	0.87	0.34	0.88
8) ptmd_sal_gt_1_h8_ebb_shallow_t_gt_18_acclim	0.09	0.09	0.09	0.09	0.88	0.88	0.88	0.88	0.09	0.88
9) tmd_sal_gt_1_ebb_shallow_t_gt_18	0.12	0.12	0.12	0.12	0.88	0.88	0.88	0.88	0.12	0.88
10) tmd sal gt 1 ptmd prtmd sd pt 1 switch	0.22	0.27	0.26	0.22	0.88	0.89	0.89	0.88	0.26	0.88

Table A1. Con't.

b) 3D WY 2002 negative binomial error in SKT data (τ=10)

Population model number	**1**	**2**	**3**	**4**	**5**	**6**	**7**	**8**	**9**	**10**
Salvage efficiency structure	**const**	**const**	**const**	**const**	**~turb**	**~turb**	**~turb**	**~turb**	**const**	**~turb**
Natural survival structure	S_c	S_{SKT}	S_d	S_W	S_c	S_{SKT}	S_d	S_W	S_d	S_d
SKT efficiency structure ($\theta_{c\text{-}SKT}$)	**=1**	**=1**	**=1**	**=1**	**=1**	**=1**	**=1**	**=1**	**~Secchi**	**~Secchi**
FMWT relative catch across regions										
1) passive	0.92	0.92	0.92	0.92	0.99	0.99	0.99	0.99	0.92	0.99
2) turbidity_seeking	0.99	0.99	0.99	0.99	0.99	0.99	0.98	0.99	0.99	1.00
3) tmd	0.96	0.96	0.96	0.96	0.99	0.99	0.99	0.99	0.96	0.99
4) ptmd sal gt 1	0.95	0.96	0.95	0.95	1.00	1.00	1.00	1.00	0.95	1.00
5) ptmd si pt 5	0.93	0.94	0.95	0.93	1.00	1.00	1.00	1.00	0.95	1.00
6) ptmd_si_pt_5_shallow_ebb_t_gt_12	0.94	0.95	0.96	0.95	1.00	1.00	1.00	1.00	0.96	1.00
7) ptmd_sal_gt_1_si_pt_5	0.93	0.95	0.96	0.94	1.00	1.00	1.00	1.00	0.95	1.00
8) ptmd sal gt 1 h8 ebb shallow t gt 18 acclim	0.96	0.97	0.96	0.96	1.00	1.00	1.00	1.00	0.96	1.00
9) tmd sal gt 1 ebb shallow t gt 18	0.99	0.98	0.99	0.99	1.00	1.00	1.00	1.00	0.99	1.00
10) tmd sal gt 1 ptmd prtmd sd pt 1 switch	1.00	1.00	1.00	1.00	1.00	1.00	1.00	1.00	1.00	1.00
SKT catch by survey and region										
1) passive	0.06	0.05	0.06	0.06	0.04	0.04	0.04	0.04	0.06	0.06
2) turbidity seeking	0.56	0.28	0.58	0.34	0.75	0.68	0.78	0.78	0.43	0.64
3) tmd	0.07	0.07	0.07	0.07	0.06	0.06	0.06	0.06	0.22	0.06
4) ptmd_sal_gt_1	0.47	0.54	0.50	0.50	0.49	0.56	0.53	0.51	0.49	0.53
5) ptmd si pt 5	0.30	0.36	0.38	0.36	0.35	0.48	0.43	0.40	0.36	0.43
6) ptmd si pt 5 shallow ebb t gt 12	0.60	0.47	0.64	0.65	0.63	0.71	0.70	0.67	0.65	0.71
7) ptmd sal gt 1 si pt 5	0.49	0.57	0.58	0.56	0.55	0.69	0.64	0.61	0.55	0.64
8) ptmd_sal_gt_1_h8_ebb_shallow_t_gt_18_acclim	0.62	0.59	0.62	0.62	0.58	0.58	0.58	0.58	0.65	0.58
9) tmd_sal_gt_1_ebb_shallow_t_gt_18	0.75	0.54	0.76	0.75	0.73	0.69	0.73	0.70	0.73	0.71
10) tmd sal gt 1 ptmd prtmd sd pt 1 switch	0.55	0.46	0.58	0.61	0.59	0.70	0.66	0.65	0.57	0.66
CVP Salvage										
1) passive	0.21	0.21	0.21	0.21	0.63	0.63	0.63	0.63	0.21	0.63
2) turbidity_seeking	0.08	0.13	0.09	0.11	0.52	0.54	0.49	0.53	0.09	0.51
3) tmd	0.02	0.02	0.02	0.02	0.65	0.65	0.65	0.65	0.02	0.65
4) ptmd sal gt 1	0.14	0.18	0.18	0.14	0.63	0.66	0.64	0.63	0.18	0.64
5) ptmd_si_pt_5	0.18	0.25	0.24	0.18	0.56	0.60	0.59	0.56	0.24	0.59
6) ptmd_si_pt_5_shallow_ebb_t_gt_12	0.23	0.29	0.28	0.24	0.63	0.65	0.64	0.63	0.28	0.64
7) ptmd sal gt 1 si pt 5	0.14	0.21	0.20	0.15	0.61	0.64	0.63	0.60	0.20	0.63
8) ptmd sal gt 1 h8 ebb shallow t gt 18 acclim	0.09	0.09	0.09	0.09	0.66	0.66	0.66	0.66	0.09	0.66
9) tmd sal gt 1 ebb shallow t gt 18	0.10	0.10	0.10	0.10	0.57	0.56	0.57	0.57	0.10	0.57
10) tmd_sal_gt_1_ptmd_prtmd_sd_pt_1_switch	0.15	0.22	0.20	0.15	0.66	0.69	0.68	0.66	0.20	0.68
SWP Salvage										
1) passive	0.25	0.25	0.26	0.26	0.91	0.91	0.91	0.91	0.26	0.91
2) turbidity_seeking	0.02	0.03	0.02	0.02	0.67	0.67	0.67	0.67	0.02	0.70
3) tmd	0.02	0.02	0.02	0.02	0.75	0.75	0.75	0.75	0.02	0.75
4) ptmd sal gt 1	0.28	0.34	0.33	0.29	0.89	0.90	0.90	0.89	0.33	0.90
5) ptmd si pt 5	0.30	0.38	0.37	0.31	0.88	0.90	0.90	0.88	0.37	0.90
6) ptmd si pt 5 shallow ebb t gt 12	0.31	0.38	0.35	0.32	0.90	0.91	0.91	0.90	0.35	0.91
7) ptmd_sal_gt_1_si_pt_5	0.29	0.37	0.35	0.30	0.88	0.89	0.89	0.88	0.35	0.89
8) ptmd_sal_gt_1_h8_ebb_shallow_t_gt_18_acclim	0.08	0.08	0.08	0.08	0.88	0.88	0.88	0.88	0.08	0.88
9) tmd sal gt 1 ebb shallow t gt 18	0.12	0.12	0.12	0.12	0.88	0.88	0.88	0.88	0.12	0.88
10) tmd sal gt 1 ptmd prtmd sd pt 1 switch	0.20	0.28	0.26	0.21	0.88	0.90	0.89	0.88	0.26	0.89

Table A1. Con't.

c) 2D WY 2002 Poisson error in SKT data (τ=1)

Population model number	**1**	**2**	**3**	**4**	**5**	**6**	**7**	**8**	**9**	**10**
Salvage efficiency structure	**const**	**const**	**const**	**const**	**~turb**	**~turb**	**~turb**	**~turb**	**const**	**~turb**
Natural survival structure	S_c	S_{SKT}	S_d	S_W	S_c	S_{SKT}	S_d	S_W	S_d	S_d
SKT efficiency structure (θ_{c-SKT})	**=1**	**=1**	**=1**	**=1**	**=1**	**=1**	**=1**	**=1**	**~Secchi**	**~Secchi**
FMWT relative catch across regions										
1) passive	0.85	0.85	0.85	0.85	0.89	0.89	0.89	0.89	0.86	0.90
2) turbidity_seeking	0.81	0.81	0.81	0.81	0.81	0.81	0.81	0.81	0.90	0.90
3) tmd	0.33	0.31	0.32	0.32	0.51	0.51	0.52	0.51	0.42	0.69
4) ptmd sal gt 1	0.88	0.88	0.88	0.88	0.89	0.89	0.89	0.89	0.95	0.97
5) ptmd si pt 5	0.86	0.85	0.84	0.84	0.99	0.99	0.99	0.99	0.82	0.99
6) ptmd_si_pt_5_shallow_ebb_t_gt_12	0.66	0.67	0.69	0.66	0.73	0.74	0.73	0.73	0.74	0.80
7) ptmd_sal_gt_1_si_pt_5	0.88	0.87	0.85	0.86	0.99	0.99	0.99	0.99	0.83	0.99
8) ptmd sal gt 1 h8 ebb shallow t gt 18 acclim	0.93	0.93	0.94	0.93	0.97	0.96	0.97	0.97	0.95	0.98
9) tmd sal gt 1 ebb shallow t gt 18	0.99	0.99	0.99	0.99	0.99	1.00	0.99	0.99	1.00	1.00
10) tmd sal gt 1 ptmd prtmd sd pt 1 switch	0.88	0.87	0.88	0.88	0.85	0.85	0.86	0.85	0.96	0.96
SKT catch by survey and region										
1) passive	0.71	0.72	0.71	0.71	0.71	0.71	0.71	0.71	0.71	0.71
2) turbidity seeking	0.01	0.01	0.01	0.01	0.01	0.01	0.01	0.01	0.09	0.09
3) tmd	0.66	0.66	0.69	0.67	0.64	0.68	0.62	0.64	0.72	0.67
4) ptmd_sal_gt_1	0.06	0.08	0.07	0.06	0.06	0.09	0.08	0.07	0.40	0.41
5) ptmd si pt 5	0.24	0.26	0.24	0.24	0.26	0.29	0.27	0.27	0.51	0.53
6) ptmd si pt 5 shallow ebb t gt 12	0.52	0.52	0.57	0.55	0.53	0.60	0.58	0.56	0.57	0.58
7) ptmd sal gt 1 si pt 5	0.26	0.28	0.26	0.26	0.28	0.31	0.29	0.28	0.51	0.53
8) ptmd_sal_gt_1_h8_ebb_shallow_t_gt_18_acclim	0.76	0.72	0.82	0.79	0.79	0.83	0.82	0.80	0.82	0.82
9) tmd_sal_gt_1_ebb_shallow_t_gt_18	0.62	0.52	0.64	0.65	0.65	0.71	0.65	0.69	0.65	0.61
10) tmd sal gt 1 ptmd prtmd sd pt 1 switch	0.63	0.58	0.65	0.65	0.65	0.68	0.67	0.66	0.74	0.69
CVP Salvage										
1) passive	0.20	0.20	0.20	0.20	0.57	0.57	0.57	0.57	0.20	0.57
2) turbidity_seeking	0.00	0.00	0.00	0.00	0.00	0.00	0.00	0.00	0.00	0.01
3) tmd	0.16	0.17	0.17	0.16	0.68	0.68	0.68	0.68	0.17	0.68
4) ptmd sal gt 1	0.18	0.23	0.23	0.19	0.55	0.57	0.56	0.54	0.23	0.56
5) ptmd_si_pt_5	0.05	0.06	0.06	0.05	0.54	0.56	0.55	0.54	0.06	0.55
6) ptmd_si_pt_5_shallow_ebb_t_gt_12	0.20	0.25	0.24	0.21	0.67	0.68	0.68	0.67	0.24	0.68
7) ptmd sal gt 1 si pt 5	0.05	0.07	0.07	0.05	0.59	0.61	0.60	0.59	0.07	0.60
8) ptmd sal gt 1 h8 ebb shallow t gt 18 acclim	0.32	0.34	0.31	0.32	0.74	0.74	0.72	0.74	0.31	0.72
9) tmd sal gt 1 ebb shallow t gt 18	0.21	0.27	0.21	0.21	0.68	0.67	0.68	0.68	0.21	0.68
10) tmd_sal_gt_1_ptmd_prtmd_sd_pt_1_switch	0.33	0.36	0.34	0.33	0.67	0.66	0.67	0.67	0.33	0.68
SWP Salvage										
1) passive	0.32	0.32	0.32	0.32	0.93	0.93	0.93	0.93	0.32	0.93
2) turbidity_seeking	0.01	0.01	0.01	0.01	0.00	0.00	0.00	0.00	0.01	0.00
3) tmd	0.19	0.21	0.20	0.19	0.93	0.93	0.92	0.93	0.19	0.92
4) ptmd sal gt 1	0.24	0.30	0.30	0.25	0.91	0.91	0.91	0.91	0.30	0.91
5) ptmd si pt 5	0.08	0.11	0.11	0.09	0.91	0.92	0.92	0.91	0.11	0.92
6) ptmd si pt 5 shallow ebb t gt 12	0.27	0.34	0.31	0.28	0.92	0.92	0.92	0.92	0.31	0.92
7) ptmd_sal_gt_1_si_pt_5	0.10	0.12	0.12	0.10	0.89	0.90	0.90	0.89	0.12	0.89
8) ptmd_sal_gt_1_h8_ebb_shallow_t_gt_18_acclim	0.39	0.43	0.39	0.40	0.94	0.94	0.94	0.94	0.38	0.94
9) tmd sal gt 1 ebb shallow t gt 18	0.26	0.33	0.26	0.26	0.92	0.92	0.92	0.92	0.26	0.92
10) tmd sal gt 1 ptmd prtmd sd pt 1 switch	0.39	0.43	0.40	0.39	0.93	0.93	0.92	0.93	0.39	0.92

Table A1. Con't.

d) 2D WY 2002 negative binomial error in SKT data (τ=10)

Population model number	**1**	**2**	**3**	**4**	**5**	**6**	**7**	**8**	**9**	**10**
Salvage efficiency structure	**const**	**const**	**const**	**const**	**~turb**	**~turb**	**~turb**	**~turb**	**const**	**~turb**
Natural survival structure	S_c	S_{SKT}	S_d	S_W	S_c	S_{SKT}	S_d	S_W	S_d	S_d
SKT efficiency structure ($\theta_{c\text{-}SKT}$)	**=1**	**=1**	**=1**	**=1**	**=1**	**=1**	**=1**	**=1**	**~Secchi**	**~Secchi**
FMWT relative catch across regions										
1) passive	0.94	0.94	0.94	0.94	0.98	0.98	0.98	0.98	0.94	0.98
2) turbidity_seeking	0.99	0.99	0.99	0.99	0.99	0.99	0.99	0.99	0.99	0.99
3) tmd	0.80	0.73	0.77	0.81	0.98	0.98	0.98	0.98	0.78	0.98
4) ptmd sal gt 1	0.96	0.95	0.95	0.95	1.00	1.00	1.00	1.00	0.95	1.00
5) ptmd si pt 5	0.86	0.84	0.83	0.84	0.99	0.99	0.99	0.99	0.83	0.99
6) ptmd_si_pt_5_shallow_ebb_t_gt_12	0.88	0.88	0.90	0.88	0.99	0.99	1.00	0.99	0.90	1.00
7) ptmd_sal_gt_1_si_pt_5	0.87	0.84	0.83	0.84	0.99	0.98	0.98	0.99	0.83	0.98
8) ptmd sal gt 1 h8 ebb shallow t gt 18 acclim	0.94	0.94	0.95	0.95	1.00	1.00	1.00	1.00	0.96	1.00
9) tmd sal gt 1 ebb shallow t gt 18	0.95	0.94	0.96	0.98	1.00	1.00	1.00	1.00	0.96	1.00
10) tmd sal gt 1 ptmd prtmd sd pt 1 switch	1.00	1.00	1.00	1.00	1.00	1.00	1.00	1.00	1.00	1.00
SKT catch by survey and region										
1) passive	0.28	0.28	0.28	0.28	0.26	0.26	0.26	0.26	0.35	0.33
2) turbidity seeking	0.00	0.00	0.00	0.00	0.00	0.00	0.00	0.00	0.01	0.00
3) tmd	0.12	0.14	0.16	0.12	0.07	0.08	0.07	0.08	0.28	0.18
4) ptmd_sal_gt_1	0.03	0.04	0.03	0.03	0.04	0.05	0.04	0.04	0.13	0.04
5) ptmd si pt 5	0.23	0.23	0.22	0.23	0.25	0.27	0.25	0.20	0.33	0.25
6) ptmd si pt 5 shallow ebb t gt 12	0.18	0.07	0.17	0.20	0.18	0.16	0.19	0.20	0.26	0.27
7) ptmd sal gt 1 si pt 5	0.25	0.25	0.24	0.25	0.27	0.29	0.27	0.27	0.34	0.27
8) ptmd_sal_gt_1_h8_ebb_shallow_t_gt_18_acclim	0.65	0.31	0.65	0.69	0.72	0.55	0.71	0.74	0.66	0.69
9) tmd_sal_gt_1_ebb_shallow_t_gt_18	0.47	0.17	0.46	0.25	0.58	0.34	0.57	0.52	0.39	0.57
10) tmd sal gt 1 ptmd prtmd sd pt 1 switch	0.34	0.19	0.35	0.24	0.36	0.29	0.35	0.30	0.46	0.49
CVP Salvage										
1) passive	0.19	0.19	0.20	0.20	0.56	0.56	0.56	0.56	0.19	0.56
2) turbidity_seeking	0.00	0.00	0.00	0.00	0.00	0.00	0.00	0.00	0.00	0.00
3) tmd	0.15	0.17	0.15	0.15	0.67	0.67	0.68	0.67	0.15	0.68
4) ptmd sal gt 1	0.19	0.24	0.24	0.20	0.56	0.56	0.55	0.55	0.24	0.55
5) ptmd_si_pt_5	0.05	0.07	0.07	0.05	0.54	0.56	0.55	0.56	0.07	0.55
6) ptmd_si_pt_5_shallow_ebb_t_gt_12	0.18	0.25	0.23	0.19	0.67	0.68	0.68	0.67	0.23	0.68
7) ptmd sal gt 1 si pt 5	0.05	0.08	0.07	0.05	0.60	0.61	0.60	0.60	0.07	0.60
8) ptmd sal gt 1 h8 ebb shallow t gt 18 acclim	0.32	0.40	0.33	0.33	0.73	0.74	0.74	0.73	0.33	0.74
9) tmd sal gt 1 ebb shallow t gt 18	0.22	0.33	0.23	0.25	0.68	0.68	0.68	0.68	0.23	0.68
10) tmd_sal_gt_1_ptmd_prtmd_sd_pt_1_switch	0.33	0.37	0.34	0.35	0.66	0.65	0.66	0.66	0.34	0.66
SWP Salvage										
1) passive	0.32	0.32	0.32	0.32	0.93	0.93	0.93	0.93	0.32	0.93
2) turbidity_seeking	0.01	0.01	0.01	0.01	0.00	0.00	0.00	0.00	0.01	0.00
3) tmd	0.16	0.19	0.17	0.16	0.93	0.93	0.92	0.93	0.17	0.92
4) ptmd sal gt 1	0.25	0.31	0.31	0.26	0.91	0.91	0.91	0.91	0.31	0.91
5) ptmd si pt 5	0.09	0.12	0.11	0.09	0.91	0.93	0.92	0.92	0.11	0.92
6) ptmd si pt 5 shallow ebb t gt 12	0.24	0.34	0.30	0.26	0.92	0.92	0.92	0.92	0.30	0.92
7) ptmd_sal_gt_1_si_pt_5	0.10	0.13	0.12	0.10	0.89	0.90	0.90	0.89	0.12	0.90
8) ptmd_sal_gt_1_h8_ebb_shallow_t_gt_18_acclim	0.39	0.50	0.40	0.40	0.94	0.95	0.94	0.94	0.40	0.94
9) tmd sal gt 1 ebb shallow t gt 18	0.27	0.43	0.28	0.28	0.93	0.93	0.93	0.93	0.28	0.93
10) tmd sal gt 1 ptmd prtmd sd pt 1 switch	0.38	0.46	0.40	0.40	0.93	0.93	0.93	0.93	0.40	0.93

Table A1. Con't.

e) 2D WY 2004 Poisson error in SKT data (τ=1)

Population model number	1	2	3	4	5	6	7	8	9	10
Salvage efficiency structure	const	const	const	const	~turb	~turb	~turb	~turb	const	~turb
Natural survival structure	S_c	S_{SKT}	S_d	S_W	S_c	S_{SKT}	S_d	S_W	S_d	S_d
SKT efficiency structure ($\theta_{c\text{-}SKT}$)	=1	=1	=1	=1	=1	=1	=1	=1	~Secchi	~Secchi
FMWT relative catch across regions										
1) passive	0.50	0.50	0.50	0.50	0.53	0.53	0.52	0.52	0.53	0.56
2) turbidity_seeking	0.69	0.69	0.69	0.69	0.68	0.68	0.68	0.68	0.70	0.62
3) tmd	0.07	0.07	0.08	0.05	0.09	0.13	0.09	0.08	0.08	0.14
4) ptmd_sal_gt_1	0.80	0.80	0.81	0.81	0.70	0.69	0.70	0.70	0.75	0.64
5) ptmd_si_pt_5	0.81	0.81	0.81	0.81	0.45	0.44	0.45	0.45	0.81	0.47
6) ptmd_si_pt_5_shallow_ebb_t_gt_12	0.29	0.30	0.29	0.29	0.29	0.30	0.29	0.29	0.25	0.24
7) ptmd_sal_gt_1_si_pt_5	0.73	0.73	0.73	0.73	0.30	0.30	0.31	0.31	0.73	0.33
8) ptmd_sal_gt_1_h8_ebb_shallow_t_gt_18_acclim	0.44	0.39	0.37	0.45	0.39	0.31	0.41	0.29	0.34	0.26
9) tmd_sal_gt_1_ebb_shallow_t_gt_18	0.61	0.62	0.60	0.60	0.61	0.61	0.60	0.60	0.62	0.62
10) tmd_sal_gt_1_ptmd_prtmd_sd_pt_1_switch	0.74	0.73	0.74	0.74	0.76	0.74	0.76	0.75	0.68	0.69
SKT catch by survey and region										
1) passive	0.69	0.73	0.69	0.69	0.66	0.72	0.65	0.65	0.78	0.76
2) turbidity_seeking	0.00	0.00	0.00	0.00	0.00	0.00	0.00	0.00	0.00	0.00
3) tmd	0.57	0.70	0.55	0.66	0.63	0.70	0.73	0.71	0.77	0.77
4) ptmd_sal_gt_1	0.39	0.39	0.38	0.38	0.44	0.45	0.44	0.44	0.42	0.47
5) ptmd_si_pt_5	0.63	0.65	0.62	0.62	0.62	0.63	0.61	0.61	0.64	0.62
6) ptmd_si_pt_5_shallow_ebb_t_gt_12	0.70	0.75	0.69	0.69	0.71	0.75	0.70	0.70	0.76	0.77
7) ptmd_sal_gt_1_si_pt_5	0.68	0.70	0.67	0.67	0.68	0.69	0.67	0.67	0.69	0.69
8) ptmd_sal_gt_1_h8_ebb_shallow_t_gt_18_acclim	0.56	0.74	0.73	0.54	0.54	0.72	0.53	0.64	0.87	0.87
9) tmd_sal_gt_1_ebb_shallow_t_gt_18	0.74	0.82	0.72	0.72	0.74	0.82	0.72	0.72	0.87	0.87
10) tmd_sal_gt_1_ptmd_prtmd_sd_pt_1_switch	0.65	0.76	0.63	0.63	0.65	0.75	0.63	0.72	0.80	0.80
CVP Salvage										
1) passive	0.00	0.00	0.00	0.00	0.01	0.01	0.01	0.01	0.00	0.01
2) turbidity_seeking	0.00	0.00	0.00	0.00	0.00	0.00	0.00	0.00	0.00	0.00
3) tmd	0.02	0.02	0.02	0.02	0.14	0.15	0.14	0.13	0.02	0.15
4) ptmd_sal_gt_1	0.00	0.00	0.00	0.00	0.02	0.02	0.02	0.02	0.00	0.02
5) ptmd_si_pt_5	0.00	0.00	0.00	0.00	0.01	0.01	0.01	0.01	0.00	0.01
6) ptmd_si_pt_5_shallow_ebb_t_gt_12	0.01	0.02	0.01	0.01	0.06	0.06	0.06	0.06	0.01	0.06
7) ptmd_sal_gt_1_si_pt_5	0.00	0.00	0.00	0.00	0.02	0.02	0.02	0.02	0.00	0.02
8) ptmd_sal_gt_1_h8_ebb_shallow_t_gt_18_acclim	0.04	0.04	0.04	0.04	0.03	0.04	0.03	0.03	0.04	0.04
9) tmd_sal_gt_1_ebb_shallow_t_gt_18	0.02	0.03	0.02	0.02	0.10	0.10	0.10	0.10	0.02	0.10
10) tmd_sal_gt_1_ptmd_prtmd_sd_pt_1_switch	0.06	0.07	0.06	0.06	0.18	0.19	0.19	0.16	0.06	0.20
SWP Salvage										
1) passive	0.00	0.00	0.00	0.00	0.03	0.03	0.03	0.03	0.00	0.03
2) turbidity_seeking	0.02	0.02	0.02	0.02	0.00	0.00	0.00	0.00	0.02	0.00
3) tmd	0.04	0.04	0.04	0.03	0.08	0.09	0.08	0.08	0.04	0.09
4) ptmd_sal_gt_1	0.01	0.01	0.01	0.01	0.04	0.04	0.04	0.04	0.01	0.04
5) ptmd_si_pt_5	0.00	0.00	0.00	0.00	0.03	0.03	0.03	0.03	0.00	0.03
6) ptmd_si_pt_5_shallow_ebb_t_gt_12	0.04	0.04	0.04	0.04	0.06	0.06	0.06	0.06	0.04	0.06
7) ptmd_sal_gt_1_si_pt_5	0.00	0.00	0.00	0.00	0.03	0.03	0.03	0.03	0.00	0.03
8) ptmd_sal_gt_1_h8_ebb_shallow_t_gt_18_acclim	0.06	0.07	0.06	0.06	0.05	0.06	0.05	0.05	0.06	0.06
9) tmd_sal_gt_1_ebb_shallow_t_gt_18	0.15	0.15	0.14	0.14	0.16	0.16	0.17	0.17	0.14	0.17
10) tmd_sal_gt_1_ptmd_prtmd_sd_pt_1_switch	0.10	0.10	0.10	0.10	0.16	0.17	0.17	0.15	0.10	0.17

Table A1. Con't.

f) 2D WY 2004 negative binomial error in SKT data (τ=10)

Population model number	**1**	**2**	**3**	**4**	**5**	**6**	**7**	**8**	**9**	**10**
Salvage efficiency structure	**const**	**const**	**const**	**const**	**~turb**	**~turb**	**~turb**	**~turb**	**const**	**~turb**
Natural survival structure	S_c	S_{SKT}	S_d	S_W	S_c	S_{SKT}	S_d	S_W	S_d	S_d
SKT efficiency structure ($\theta_{c\text{-}SKT}$)	=1	=1	=1	=1	=1	=1	=1	=1	**~Secchi**	**~Secchi**
FMWT relative catch across regions										
1) passive	0.91	0.91	0.91	0.91	0.90	0.90	0.90	0.90	0.92	0.90
2) turbidity_seeking	0.96	0.96	0.96	0.96	0.94	0.93	0.95	0.95	0.98	0.94
3) tmd	0.57	0.49	0.59	0.59	0.40	0.40	0.42	0.42	0.57	0.42
4) ptmd sal gt 1	0.94	0.94	0.94	0.94	0.89	0.89	0.89	0.89	0.94	0.89
5) ptmd si pt 5	0.87	0.87	0.87	0.87	0.42	0.42	0.42	0.42	0.88	0.42
6) ptmd_si_pt_5_shallow_ebb_t_gt_12	0.83	0.80	0.85	0.85	0.65	0.64	0.67	0.67	0.84	0.67
7) ptmd_sal_gt_1_si_pt_5	0.76	0.76	0.77	0.77	0.25	0.25	0.26	0.26	0.77	0.26
8) ptmd sal gt 1 h8 ebb shallow t gt 18 acclim	0.61	0.53	0.65	0.65	0.15	0.15	0.17	0.17	0.63	0.42
9) tmd sal gt 1 ebb shallow t gt 18	0.95	0.95	0.95	0.95	0.82	0.82	0.85	0.85	0.95	0.84
10) tmd sal gt 1 ptmd prtmd sd pt 1 switch	0.99	0.99	0.99	0.99	1.00	0.99	1.00	1.00	0.99	1.00
SKT catch by survey and region										
1) passive	0.15	0.15	0.14	0.14	0.13	0.13	0.12	0.12	0.27	0.12
2) turbidity seeking	0.00	0.00	0.00	0.00	0.00	0.00	0.00	0.00	0.00	0.00
3) tmd	0.03	0.02	0.03	0.03	0.07	0.07	0.06	0.06	0.07	0.06
4) ptmd_sal_gt_1	0.17	0.17	0.17	0.17	0.18	0.18	0.18	0.18	0.14	0.18
5) ptmd si pt 5	0.62	0.62	0.61	0.61	0.61	0.61	0.60	0.60	0.62	0.60
6) ptmd si pt 5 shallow ebb t gt 12	0.14	0.16	0.13	0.13	0.17	0.17	0.16	0.16	0.19	0.17
7) ptmd sal gt 1 si pt 5	0.69	0.69	0.68	0.68	0.68	0.68	0.67	0.67	0.68	0.69
8) ptmd_sal_gt_1_h8_ebb_shallow_t_gt_18_acclim	0.29	0.39	0.27	0.27	0.19	0.23	0.18	0.18	0.52	0.50
9) tmd_sal_gt_1_ebb_shallow_t_gt_18	0.63	0.67	0.62	0.62	0.53	0.53	0.52	0.52	0.77	0.56
10) tmd sal gt 1 ptmd prtmd sd pt 1 switch	0.39	0.43	0.38	0.38	0.36	0.38	0.35	0.35	0.45	0.42
CVP Salvage										
1) passive	0.00	0.00	0.00	0.00	0.03	0.03	0.03	0.03	0.00	0.03
2) turbidity_seeking	0.00	0.00	0.00	0.00	0.00	0.00	0.00	0.00	0.00	0.00
3) tmd	0.02	0.04	0.02	0.02	0.21	0.22	0.21	0.21	0.02	0.21
4) ptmd sal gt 1	0.00	0.00	0.00	0.00	0.03	0.03	0.03	0.03	0.00	0.03
5) ptmd_si_pt_5	0.00	0.00	0.00	0.00	0.02	0.02	0.03	0.03	0.00	0.03
6) ptmd_si_pt_5_shallow_ebb_t_gt_12	0.01	0.01	0.01	0.01	0.08	0.08	0.09	0.09	0.01	0.09
7) ptmd sal gt 1 si pt 5	0.00	0.00	0.00	0.00	0.03	0.03	0.04	0.04	0.00	0.04
8) ptmd sal gt 1 h8 ebb shallow t gt 18 acclim	0.03	0.04	0.03	0.03	0.10	0.10	0.10	0.10	0.03	0.04
9) tmd sal gt 1 ebb shallow t gt 18	0.02	0.03	0.02	0.02	0.18	0.18	0.19	0.19	0.02	0.19
10) tmd_sal_gt_1_ptmd_prtmd_sd_pt_1_switch	0.06	0.07	0.06	0.06	0.19	0.19	0.19	0.19	0.06	0.20
SWP Salvage										
1) passive	0.00	0.00	0.00	0.00	0.07	0.07	0.07	0.07	0.00	0.07
2) turbidity_seeking	0.02	0.02	0.02	0.02	0.00	0.00	0.00	0.00	0.02	0.00
3) tmd	0.06	0.08	0.06	0.06	0.32	0.33	0.32	0.32	0.06	0.32
4) ptmd sal gt 1	0.01	0.01	0.01	0.01	0.07	0.07	0.08	0.08	0.01	0.08
5) ptmd si pt 5	0.00	0.00	0.00	0.00	0.07	0.07	0.07	0.07	0.00	0.07
6) ptmd si pt 5 shallow ebb t gt 12	0.03	0.03	0.03	0.03	0.19	0.19	0.19	0.19	0.03	0.19
7) ptmd_sal_gt_1_si_pt_5	0.00	0.00	0.00	0.00	0.07	0.07	0.07	0.07	0.00	0.07
8) ptmd_sal_gt_1_h8_ebb_shallow_t_gt_18_acclim	0.06	0.07	0.06	0.06	0.27	0.28	0.27	0.27	0.06	0.07
9) tmd sal gt 1 ebb shallow t gt 18	0.14	0.14	0.14	0.14	0.35	0.35	0.36	0.36	0.14	0.36
10) tmd sal gt 1 ptmd prtmd sd pt 1 switch	0.10	0.10	0.10	0.10	0.17	0.17	0.17	0.17	0.10	0.17

Table A1. Con't.

g) 2D WY 2005 Poisson error in SKT data (τ=1)

Population model number	1	2	3	4	5	6	7	8	9	10
Salvage efficiency structure	const	const	const	const	~turb	~turb	~turb	~turb	const	~turb
Natural survival structure	S_c	S_{SKT}	S_d	S_W	S_c	S_{SKT}	S_d	S_W	S_d	S_d
SKT efficiency structure ($\theta_{c\text{-}SKT}$)	=1	=1	=1	=1	=1	=1	=1	=1	~Secchi	~Secchi
FMWT relative catch across regions										
1) passive	0.85	0.85	0.85	0.84	0.85	0.85	0.85	0.84	0.89	0.89
2) turbidity_seeking	1.00	1.00	1.00	1.00	1.00	1.00	1.00	1.00	0.96	0.96
3) tmd	0.32	0.38	0.35	0.36	0.31	0.37	0.34	0.35	0.29	0.28
4) ptmd sal gt 1	0.99	0.99	0.99	0.99	0.99	0.99	0.99	0.99	0.99	0.99
5) ptmd si pt 5	1.00	1.00	1.00	1.00	1.00	1.00	1.00	1.00	1.00	1.00
6) ptmd_si_pt_5_shallow_ebb_t_gt_12	0.75	0.77	0.76	0.76	0.75	0.77	0.76	0.76	0.92	0.92
7) ptmd_sal_gt_1_si_pt_5	1.00	1.00	1.00	1.00	1.00	1.00	1.00	1.00	1.00	1.00
8) ptmd sal gt 1 h8 ebb shallow t gt 18 acclim	0.91	0.95	0.93	0.93	0.92	0.95	0.94	0.93	0.94	0.94
9) tmd sal gt 1 ebb shallow t gt 18	1.00	1.00	1.00	1.00	1.00	1.00	1.00	1.00	1.00	1.00
10) tmd sal gt 1 ptmd prtmd sd pt 1 switch	0.86	0.87	0.86	0.86	0.85	0.86	0.85	0.85	0.95	0.94
SKT catch by survey and region										
1) passive	0.48	0.59	0.41	0.54	0.49	0.59	0.41	0.54	0.44	0.64
2) turbidity seeking	0.22	0.22	0.22	0.22	0.22	0.22	0.22	0.22	0.32	0.32
3) tmd	0.51	0.51	0.55	0.57	0.54	0.63	0.60	0.62	0.60	0.65
4) ptmd_sal_gt_1	0.50	0.62	0.59	0.57	0.51	0.62	0.59	0.57	0.69	0.69
5) ptmd si pt 5	0.70	0.84	0.79	0.79	0.71	0.84	0.79	0.79	0.80	0.80
6) ptmd si pt 5 shallow ebb t gt 12	0.58	0.67	0.64	0.62	0.59	0.68	0.65	0.63	0.77	0.77
7) ptmd sal gt 1 si pt 5	0.71	0.84	0.79	0.80	0.71	0.84	0.79	0.80	0.80	0.80
8) ptmd_sal_gt_1_h8_ebb_shallow_t_gt_18_acclim	0.66	0.79	0.74	0.73	0.65	0.79	0.74	0.73	0.81	0.81
9) tmd_sal_gt_1_ebb_shallow_t_gt_18	0.60	0.63	0.64	0.66	0.62	0.73	0.68	0.67	0.76	0.80
10) tmd sal gt 1 ptmd prtmd sd pt 1 switch	0.57	0.62	0.61	0.63	0.59	0.70	0.65	0.65	0.67	0.69
CVP Salvage										
1) passive	0.00	0.00	0.00	0.00	0.03	0.03	0.03	0.03	0.00	0.03
2) turbidity_seeking	0.01	0.00	0.00	0.01	0.01	0.00	0.01	0.00	0.01	0.01
3) tmd	0.05	0.05	0.04	0.03	0.17	0.15	0.16	0.16	0.05	0.17
4) ptmd sal gt 1	0.00	0.00	0.00	0.00	0.03	0.03	0.03	0.03	0.00	0.03
5) ptmd_si_pt_5	0.00	0.00	0.00	0.00	0.02	0.03	0.03	0.03	0.00	0.03
6) ptmd_si_pt_5_shallow_ebb_t_gt_12	0.03	0.05	0.05	0.04	0.06	0.09	0.08	0.07	0.04	0.08
7) ptmd sal gt 1 si pt 5	0.00	0.00	0.00	0.00	0.01	0.01	0.01	0.01	0.00	0.01
8) ptmd sal gt 1 h8 ebb shallow t gt 18 acclim	0.15	0.18	0.18	0.17	0.15	0.19	0.18	0.18	0.18	0.18
9) tmd sal gt 1 ebb shallow t gt 18	0.14	0.16	0.16	0.15	0.26	0.28	0.29	0.29	0.16	0.29
10) tmd_sal_gt_1_ptmd_prtmd_sd_pt_1_switch	0.09	0.12	0.11	0.11	0.14	0.16	0.16	0.16	0.11	0.16
SWP Salvage										
1) passive	0.01	0.02	0.02	0.01	0.04	0.05	0.05	0.04	0.02	0.05
2) turbidity_seeking	0.01	0.01	0.01	0.01	0.01	0.01	0.01	0.01	0.01	0.01
3) tmd	0.14	0.17	0.13	0.12	0.28	0.30	0.29	0.29	0.15	0.30
4) ptmd sal gt 1	0.01	0.02	0.02	0.01	0.04	0.05	0.04	0.04	0.02	0.05
5) ptmd si pt 5	0.01	0.02	0.01	0.01	0.02	0.03	0.03	0.03	0.01	0.03
6) ptmd si pt 5 shallow ebb t gt 12	0.08	0.14	0.12	0.11	0.11	0.17	0.16	0.14	0.12	0.15
7) ptmd_sal_gt_1_si_pt_5	0.01	0.02	0.02	0.02	0.03	0.04	0.04	0.04	0.02	0.04
8) ptmd_sal_gt_1_h8_ebb_shallow_t_gt_18_acclim	0.41	0.50	0.48	0.47	0.42	0.50	0.48	0.48	0.47	0.47
9) tmd sal gt 1 ebb shallow t gt 18	0.33	0.40	0.37	0.37	0.44	0.50	0.49	0.49	0.37	0.49
10) tmd sal gt 1 ptmd prtmd sd pt 1 switch	0.27	0.37	0.34	0.33	0.32	0.37	0.36	0.36	0.34	0.37

Table A1. Con't.

h) 2D WY 2005 negative binomial error in SKT data (τ=10)

Population model number	1	2	3	4	5	6	7	8	9	10
Salvage efficiency structure	const	const	const	const	~turb	~turb	~turb	~turb	const	~turb
Natural survival structure	S_c	S_{SKT}	S_d	S_W	S_c	S_{SKT}	S_d	S_W	S_d	S_d
SKT efficiency structure ($\theta_{c\text{-}SKT}$)	=1	=1	=1	=1	=1	=1	=1	=1	~Secchi	~Secchi
FMWT relative catch across regions										
1) passive	0.98	0.98	0.98	0.98	0.98	0.98	0.98	0.98	0.97	0.97
2) turbidity_seeking	1.00	1.00	1.00	1.00	1.00	1.00	1.00	1.00	1.00	1.00
3) tmd	0.79	0.78	0.80	0.79	0.84	0.81	0.87	0.88	0.80	0.87
4) ptmd_sal_gt_1	0.99	0.99	0.99	0.99	0.99	0.99	0.99	0.99	0.99	0.99
5) ptmd_si_pt_5	1.00	1.00	1.00	1.00	1.00	1.00	1.00	1.00	1.00	1.00
6) ptmd_si_pt_5_shallow_ebb_t_gt_12	1.00	1.00	1.00	1.00	1.00	1.00	1.00	1.00	1.00	1.00
7) ptmd_sal_gt_1_si_pt_5	1.00	1.00	1.00	1.00	1.00	1.00	1.00	1.00	1.00	1.00
8) ptmd_sal_gt_1_h8_ebb_shallow_t_gt_18_acclim	1.00	1.00	1.00	1.00	1.00	1.00	1.00	1.00	1.00	1.00
9) tmd_sal_gt_1_ebb_shallow_t_gt_18	1.00	1.00	1.00	1.00	0.99	0.99	1.00	1.00	1.00	0.99
10) tmd_sal_gt_1_ptmd_prtmd_sd_pt_1_switch	1.00	1.00	1.00	1.00	1.00	1.00	1.00	1.00	1.00	1.00
SKT catch by survey and region										
1) passive	0.12	0.16	0.12	0.12	0.12	0.16	0.12	0.12	0.12	0.12
2) turbidity_seeking	0.22	0.22	0.22	0.22	0.22	0.22	0.22	0.22	0.22	0.25
3) tmd	0.12	0.06	0.13	0.13	0.14	0.07	0.16	0.17	0.15	0.16
4) ptmd_sal_gt_1	0.41	0.56	0.39	0.39	0.41	0.56	0.39	0.39	0.39	0.37
5) ptmd_si_pt_5	0.60	0.81	0.59	0.59	0.60	0.81	0.59	0.59	0.53	0.53
6) ptmd_si_pt_5_shallow_ebb_t_gt_12	0.20	0.28	0.27	0.27	0.19	0.31	0.27	0.26	0.27	0.32
7) ptmd_sal_gt_1_si_pt_5	0.60	0.81	0.58	0.58	0.60	0.81	0.58	0.58	0.53	0.53
8) ptmd_sal_gt_1_h8_ebb_shallow_t_gt_18_acclim	0.42	0.56	0.51	0.52	0.42	0.55	0.32	0.52	0.51	0.51
9) tmd_sal_gt_1_ebb_shallow_t_gt_18	0.60	0.37	0.61	0.61	0.63	0.47	0.67	0.68	0.65	0.68
10) tmd_sal_gt_1_ptmd_prtmd_sd_pt_1_switch	0.18	0.13	0.19	0.20	0.19	0.17	0.21	0.22	0.25	0.21
CVP Salvage										
1) passive	0.00	0.00	0.00	0.00	0.03	0.03	0.03	0.03	0.00	0.03
2) turbidity_seeking	0.01	0.01	0.01	0.01	0.01	0.01	0.00	0.01	0.01	0.01
3) tmd	0.06	0.22	0.06	0.06	0.17	0.26	0.17	0.17	0.06	0.17
4) ptmd_sal_gt_1	0.00	0.00	0.00	0.00	0.03	0.03	0.03	0.03	0.00	0.03
5) ptmd_si_pt_5	0.00	0.00	0.00	0.00	0.03	0.03	0.03	0.03	0.00	0.03
6) ptmd_si_pt_5_shallow_ebb_t_gt_12	0.04	0.05	0.05	0.04	0.09	0.09	0.08	0.08	0.05	0.08
7) ptmd_sal_gt_1_si_pt_5	0.00	0.00	0.00	0.00	0.02	0.01	0.02	0.02	0.00	0.02
8) ptmd_sal_gt_1_h8_ebb_shallow_t_gt_18_acclim	0.17	0.18	0.18	0.18	0.18	0.18	0.18	0.18	0.18	0.18
9) tmd_sal_gt_1_ebb_shallow_t_gt_18	0.15	0.26	0.16	0.16	0.28	0.33	0.29	0.29	0.16	0.29
10) tmd_sal_gt_1_ptmd_prtmd_sd_pt_1_switch	0.09	0.15	0.11	0.11	0.14	0.17	0.16	0.16	0.11	0.16
SWP Salvage										
1) passive	0.02	0.02	0.02	0.02	0.05	0.05	0.05	0.05	0.02	0.05
2) turbidity_seeking	0.01	0.01	0.01	0.01	0.01	0.00	0.01	0.01	0.01	0.01
3) tmd	0.16	0.44	0.17	0.16	0.27	0.38	0.28	0.28	0.17	0.28
4) ptmd_sal_gt_1	0.02	0.02	0.02	0.02	0.05	0.05	0.05	0.05	0.02	0.05
5) ptmd_si_pt_5	0.01	0.01	0.02	0.02	0.03	0.03	0.03	0.03	0.02	0.03
6) ptmd_si_pt_5_shallow_ebb_t_gt_12	0.12	0.13	0.13	0.12	0.17	0.17	0.16	0.15	0.13	0.16
7) ptmd_sal_gt_1_si_pt_5	0.02	0.02	0.02	0.02	0.04	0.04	0.05	0.05	0.02	0.05
8) ptmd_sal_gt_1_h8_ebb_shallow_t_gt_18_acclim	0.46	0.49	0.48	0.47	0.47	0.49	0.49	0.48	0.48	0.49
9) tmd_sal_gt_1_ebb_shallow_t_gt_18	0.34	0.50	0.36	0.36	0.48	0.54	0.49	0.49	0.36	0.49
10) tmd_sal_gt_1_ptmd_prtmd_sd_pt_1_switch	0.29	0.43	0.34	0.34	0.34	0.41	0.36	0.37	0.34	0.36

Table A1. Con't.

i) 2D WY 2011 Poisson error in SKT data (τ=1)

Population model number	**1**	**2**	**3**	**4**	**5**	**6**	**7**	**8**	**9**	**10**
Salvage efficiency structure	**const**	**const**	**const**	**const**	**~turb**	**~turb**	**~turb**	**~turb**	**const**	**~turb**
Natural survival structure	S_c	S_{SKT}	S_d	S_W	S_c	S_{SKT}	S_d	S_W	S_d	S_d
SKT efficiency structure ($\theta_{c\text{-}SKT}$)	**=1**	**=1**	**=1**	**=1**	**=1**	**=1**	**=1**	**=1**	**~Secchi**	**~Secchi**
FMWT relative catch across regions										
1) passive	0.98	0.98	0.98	0.98	0.98	0.98	0.98	0.98	0.96	0.96
2) turbidity_seeking	0.73	0.73	0.73	0.73	0.73	0.73	0.73	0.73	0.72	0.72
3) tmd	0.82	0.82	0.83	0.83	0.82	0.82	0.83	0.83	0.80	0.80
4) ptmd sal gt 1	0.64	0.65	0.65	0.65	0.64	0.65	0.65	0.65	0.64	0.64
5) ptmd si pt 5	0.63	0.63	0.63	0.63	0.63	0.63	0.63	0.63	0.64	0.64
6) ptmd_si_pt_5_shallow_ebb_t_gt_12	0.66	0.66	0.66	0.66	0.66	0.66	0.66	0.66	0.64	0.64
7) ptmd_sal_gt_1_si_pt_5	0.62	0.62	0.62	0.62	0.62	0.62	0.62	0.62	0.63	0.63
8) ptmd sal gt 1 h8 ebb shallow t gt 18 acclim	0.65	0.65	0.65	0.65	0.65	0.65	0.65	0.65	0.63	0.63
9) tmd sal gt 1 ebb shallow t gt 18	0.63	0.63	0.63	0.63	0.63	0.63	0.63	0.63	0.63	0.63
10) tmd sal gt 1 ptmd prtmd sd pt 1 switch	0.63	0.63	0.63	0.63	0.63	0.63	0.64	0.63	0.63	0.63
SKT catch by survey and region										
1) passive	0.70	0.73	0.71	0.70	0.70	0.73	0.71	0.70	0.66	0.66
2) turbidity seeking	0.02	0.02	0.02	0.02	0.02	0.02	0.02	0.02	0.02	0.02
3) tmd	0.69	0.71	0.68	0.68	0.69	0.71	0.68	0.68	0.68	0.68
4) ptmd_sal_gt_1	0.18	0.20	0.19	0.19	0.18	0.20	0.19	0.19	0.18	0.18
5) ptmd si pt 5	0.34	0.33	0.31	0.31	0.34	0.33	0.31	0.31	0.38	0.38
6) ptmd si pt 5 shallow ebb t gt 12	0.77	0.79	0.76	0.76	0.77	0.79	0.76	0.76	0.75	0.75
7) ptmd sal gt 1 si pt 5	0.34	0.33	0.30	0.31	0.34	0.33	0.30	0.31	0.37	0.37
8) ptmd_sal_gt_1_h8_ebb_shallow_t_gt_18_acclim	0.67	0.71	0.67	0.67	0.67	0.71	0.67	0.67	0.64	0.64
9) tmd_sal_gt_1_ebb_shallow_t_gt_18	0.17	0.19	0.17	0.17	0.17	0.19	0.17	0.17	0.17	0.17
10) tmd sal gt 1 ptmd prtmd sd pt 1 switch	0.33	0.32	0.31	0.31	0.33	0.32	0.31	0.31	0.34	0.34
CVP Salvage										
1) passive	0.01	0.01	0.01	0.01	0.01	0.01	0.01	0.01	0.01	0.01
2) turbidity_seeking	0.03	0.03	0.03	0.03	0.03	0.03	0.03	0.03	0.03	0.03
3) tmd	0.03	0.03	0.03	0.03	0.03	0.03	0.03	0.03	0.03	0.03
4) ptmd sal gt 1	0.01	0.01	0.01	0.01	0.01	0.01	0.01	0.00	0.01	0.00
5) ptmd_si_pt_5	0.01	0.01	0.01	0.01	0.01	0.01	0.01	0.01	0.01	0.01
6) ptmd_si_pt_5_shallow_ebb_t_gt_12	0.01	0.01	0.01	0.01	0.01	0.01	0.01	0.01	0.01	0.01
7) ptmd sal gt 1 si pt 5	0.01	0.01	0.01	0.01	0.01	0.01	0.00	0.01	0.01	0.00
8) ptmd sal gt 1 h8 ebb shallow t gt 18 acclim	0.01	0.01	0.01	0.01	0.01	0.01	0.01	0.01	0.01	0.01
9) tmd sal gt 1 ebb shallow t gt 18	0.01	0.01	0.01	0.01	0.01	0.01	0.01	0.01	0.01	0.01
10) tmd_sal_gt_1_ptmd_prtmd_sd_pt_1_switch	0.01	0.01	0.01	0.01	0.02	0.02	0.02	0.02	0.01	0.02
SWP Salvage										
1) passive	#DIV/0!	#DIV/0!	#DIV/0!	#DIV/0!	#DIV/0!	#DIV/0!	#DIV/0!	#DIV/0!	#DIV/0!	#DIV/0!
2) turbidity_seeking	#DIV/0!	#DIV/0!	#DIV/0!	#DIV/0!	#DIV/0!	#DIV/0!	#DIV/0!	#DIV/0!	#DIV/0!	#DIV/0!
3) tmd	#DIV/0!	#DIV/0!	#DIV/0!	#DIV/0!	#DIV/0!	#DIV/0!	#DIV/0!	#DIV/0!	#DIV/0!	#DIV/0!
4) ptmd sal gt 1	#DIV/0!	#DIV/0!	#DIV/0!	#DIV/0!	#DIV/0!	#DIV/0!	#DIV/0!	#DIV/0!	#DIV/0!	#DIV/0!
5) ptmd si pt 5	#DIV/0!	#DIV/0!	#DIV/0!	#DIV/0!	#DIV/0!	#DIV/0!	#DIV/0!	#DIV/0!	#DIV/0!	#DIV/0!
6) ptmd si pt 5 shallow ebb t gt 12	#DIV/0!	#DIV/0!	#DIV/0!	#DIV/0!	#DIV/0!	#DIV/0!	#DIV/0!	#DIV/0!	#DIV/0!	#DIV/0!
7) ptmd_sal_gt_1_si_pt_5	#DIV/0!	#DIV/0!	#DIV/0!	#DIV/0!	#DIV/0!	#DIV/0!	#DIV/0!	#DIV/0!	#DIV/0!	#DIV/0!
8) ptmd_sal_gt_1_h8_ebb_shallow_t_gt_18_acclim	#DIV/0!	#DIV/0!	#DIV/0!	#DIV/0!	#DIV/0!	#DIV/0!	#DIV/0!	#DIV/0!	#DIV/0!	#DIV/0!
9) tmd sal gt 1 ebb shallow t gt 18	#DIV/0!	#DIV/0!	#DIV/0!	#DIV/0!	#DIV/0!	#DIV/0!	#DIV/0!	#DIV/0!	#DIV/0!	#DIV/0!
10) tmd sal gt 1 ptmd prtmd sd pt 1 switch	#DIV/0!	#DIV/0!	#DIV/0!	#DIV/0!	#DIV/0!	#DIV/0!	#DIV/0!	#DIV/0!	#DIV/0!	#DIV/0!

Table A1. Con't.

j) 2D WY 2011 negative binomial error in SKT data (τ=10)

Population model number	**1**	**2**	**3**	**4**	**5**	**6**	**7**	**8**	**9**	**10**
Salvage efficiency structure	**const**	**const**	**const**	**const**	**~turb**	**~turb**	**~turb**	**~turb**	**const**	**~turb**
Natural survival structure	S_c	S_{SKT}	S_d	S_W	S_c	S_{SKT}	S_d	S_W	S_d	S_d
SKT efficiency structure ($\theta_{c\text{-}SKT}$)	=1	=1	=1	=1	=1	=1	=1	=1	~Secchi	~Secchi
FMWT relative catch across regions										
1) passive	0.95	0.95	0.95	0.95	0.95	0.95	0.95	0.95	0.94	0.92
2) turbidity_seeking	0.90	0.90	0.90	0.90	0.90	0.90	0.90	0.90	0.87	0.86
3) tmd	0.97	0.97	1.00	0.97	0.97	0.97	0.97	0.97	0.97	0.97
4) ptmd sal gt 1	0.86	0.87	0.87	0.87	0.86	0.87	0.87	0.87	0.86	0.86
5) ptmd si pt 5	0.87	0.87	0.87	0.87	0.87	0.87	0.87	0.87	0.89	0.89
6) ptmd_si_pt_5_shallow_ebb_t_gt_12	0.90	0.90	0.90	0.90	0.90	0.91	0.99	0.91	0.91	0.90
7) ptmd_sal_gt_1_si_pt_5	0.84	0.84	0.84	0.85	0.84	0.84	0.84	0.84	0.83	0.87
8) ptmd sal gt 1 h8 ebb shallow t gt 18 acclim	0.91	0.91	0.91	0.91	0.91	0.91	0.91	0.91	0.92	0.92
9) tmd sal gt 1 ebb shallow t gt 18	0.84	0.84	0.84	0.84	0.84	0.84	0.84	0.84	0.84	0.90
10) tmd sal gt 1 ptmd prtmd sd pt 1 switch	0.94	0.94	0.97	0.94	0.94	0.94	0.94	0.94	0.94	0.94
SKT catch by survey and region										
1) passive	0.63	0.63	0.62	0.62	0.63	0.63	0.62	0.62	0.57	0.61
2) turbidity seeking	0.00	0.00	0.00	0.00	0.00	0.00	0.00	0.00	0.00	0.00
3) tmd	0.41	0.41	#DIV/0!	0.41	0.41	0.41	0.37	0.41	0.37	0.37
4) ptmd_sal_gt_1	0.07	0.08	0.07	0.07	0.07	0.08	0.07	0.07	0.07	0.07
5) ptmd si pt 5	0.23	0.23	0.23	0.23	0.23	0.23	0.23	0.23	0.19	0.21
6) ptmd si pt 5 shallow ebb t gt 12	0.39	0.40	0.40	0.39	0.39	0.40	0.23	0.40	0.34	0.32
7) ptmd sal gt 1 si pt 5	0.23	0.23	0.23	0.20	0.23	0.23	0.23	0.23	0.18	0.18
8) ptmd_sal_gt_1_h8_ebb_shallow_t_gt_18_acclim	0.30	0.32	0.30	0.30	0.30	0.32	0.30	0.30	0.30	0.30
9) tmd_sal_gt_1_ebb_shallow_t_gt_18	0.07	0.07	0.07	0.07	0.07	0.07	0.07	0.07	0.07	0.06
10) tmd sal gt 1 ptmd prtmd sd pt 1 switch	0.21	0.19	0.04	0.20	0.21	0.19	0.20	0.19	0.21	0.21
CVP Salvage										
1) passive	0.01	0.01	0.01	0.01	0.01	0.01	0.01	0.01	0.01	0.01
2) turbidity_seeking	0.03	0.03	0.03	0.03	0.03	0.03	0.03	0.03	0.03	0.03
3) tmd	0.02	0.02	0.00	0.02	0.02	0.02	0.02	0.02	0.02	0.02
4) ptmd sal gt 1	0.01	0.01	0.01	0.01	0.01	0.01	0.00	0.00	0.01	0.00
5) ptmd_si_pt_5	0.01	0.01	0.01	0.01	0.01	0.01	0.01	0.01	0.01	0.01
6) ptmd_si_pt_5_shallow_ebb_t_gt_12	0.01	0.01	0.01	0.01	0.01	0.01	0.01	0.01	0.01	0.01
7) ptmd sal gt 1 si pt 5	0.01	0.01	0.01	0.01	0.01	0.01	0.01	0.01	0.01	0.01
8) ptmd sal gt 1 h8 ebb shallow t gt 18 acclim	0.01	0.01	0.01	0.01	0.01	0.01	0.01	0.01	0.01	0.01
9) tmd sal gt 1 ebb shallow t gt 18	0.01	0.01	0.01	0.01	0.01	0.01	0.01	0.01	0.01	0.00
10) tmd_sal_gt_1_ptmd_prtmd_sd_pt_1_switch	0.01	0.01	0.01	0.01	0.01	0.01	0.01	0.01	0.01	0.01
SWP Salvage										
1) passive	#DIV/0!	#DIV/0!	#DIV/0!	#DIV/0!	#DIV/0!	#DIV/0!	#DIV/0!	#DIV/0!	#DIV/0!	#DIV/0!
2) turbidity_seeking	#DIV/0!	#DIV/0!	#DIV/0!	#DIV/0!	#DIV/0!	#DIV/0!	#DIV/0!	#DIV/0!	#DIV/0!	#DIV/0!
3) tmd	#DIV/0!	#DIV/0!	#DIV/0!	#DIV/0!	#DIV/0!	#DIV/0!	#DIV/0!	#DIV/0!	#DIV/0!	#DIV/0!
4) ptmd sal gt 1	#DIV/0!	#DIV/0!	#DIV/0!	#DIV/0!	#DIV/0!	#DIV/0!	#DIV/0!	#DIV/0!	#DIV/0!	#DIV/0!
5) ptmd si pt 5	#DIV/0!	#DIV/0!	#DIV/0!	#DIV/0!	#DIV/0!	#DIV/0!	#DIV/0!	#DIV/0!	#DIV/0!	#DIV/0!
6) ptmd si pt 5 shallow ebb t gt 12	#DIV/0!	#DIV/0!	#DIV/0!	#DIV/0!	#DIV/0!	#DIV/0!	#DIV/0!	#DIV/0!	#DIV/0!	#DIV/0!
7) ptmd_sal_gt_1_si_pt_5	#DIV/0!	#DIV/0!	#DIV/0!	#DIV/0!	#DIV/0!	#DIV/0!	#DIV/0!	#DIV/0!	#DIV/0!	#DIV/0!
8) ptmd_sal_gt_1_h8_ebb_shallow_t_gt_18_acclim	#DIV/0!	#DIV/0!	#DIV/0!	#DIV/0!	#DIV/0!	#DIV/0!	#DIV/0!	#DIV/0!	#DIV/0!	#DIV/0!
9) tmd sal gt 1 ebb shallow t gt 18	#DIV/0!	#DIV/0!	#DIV/0!	#DIV/0!	#DIV/0!	#DIV/0!	#DIV/0!	#DIV/0!	#DIV/0!	#DIV/0!
10) tmd sal gt 1 ptmd prtmd sd pt 1 switch	#DIV/0!	#DIV/0!	#DIV/0!	#DIV/0!	#DIV/0!	#DIV/0!	#DIV/0!	#DIV/0!	#DIV/0!	#DIV/0!